STRASSFELD, MOSES J.

FLUCTUATION STUDIES OF ELECTROLYTE SOLUTIONS AND LIPOSOME SUSPENSIONS

City University of New York PH.D. 1980

PLEASE NOTE:

In all cases this material has been filmed in the best possible way from the available copy. Problems encountered with this document have been identified here with a check mark ✓.

1. Glossy photographs _____
2. Colored illustrations _____
3. Photographs with dark background ✓
4. Illustrations are poor copy ✓
5. Print shows through as there is text on both sides of page _____
6. Indistinct, broken or small print on several pages ✓ throughout _____
7. Tightly bound copy with print lost in spine _____
8. Computer printout pages with indistinct print ✓
9. Page(s) _____ lacking when material received, and not available from school or author _____
10. Page(s) _____ seem to be missing in numbering only as text follows _____
11. Poor carbon copy _____
12. Not original copy, several pages with blurred type _____
13. Appendix pages are poor copy _____
14. Original copy with light type _____
15. Curling and wrinkled pages _____
16. Other _____

Fluctuation Studies of Electrolyte Solutions and Liposome Suspensions

by

Moses J. Strassfeld

A dissertation submitted to the
Graduate Faculty in Chemistry
in partial fulfillment of the
requirements for the degree of
Doctor of Philosophy

The City University of New York

1980

This manuscript has been read and accepted for the Graduate Faculty in Chemistry satisfaction of the dissertation requirement for the degree of Doctor of Philosophy.

May 21, 1980
date

Chairman of Examining Committee

May 21, 1980
date

David C. Lorke
Executive Officer

Ezra Shaw

Thomas R. Haines

Supervisory Committee

The City University of New York

ABSTRACT

Fluctuation Studies of Electrolyte Solutions and Liposome Suspensions

by

Moses J. Strassfeld

Adviser: Professor Michael E. Green

A method for determining relaxation times associated with ion transport through liposome membranes, using ion concentration fluctuation spectroscopy (adapting a technique of Feher and Weissman (*Proc. Natl. Acad. Sci. (USA)*, **1973**, *70*,870)), is presented. To be measurable, fluctuations in a very small volume are required; this is achieved by use of a 250μm thick ruby with an approximately 10 μm diameter minimum aperture. The method is now suitable for the determination of relaxation times in the 10 *ms* to 10 μs range, and this range can be extended.

The method has been applied to a gramicidin-D doped soy-lecithin in 0.149 M KCl vesicle preparation. Two relaxation phenomena have been observed. The first, a -2 slope in the region 20 to 150 Hz, is attributed to the high frequency portion of the known gramicidin relaxation. The second, at 152±46 Hz (one standard deviation), is shown to be characteristic of the vesicles themselves.

Additionally, noise spectra of potassium chloride solutions with concentrations 0.005 M and 0.149 M were measured, as were spectra of sodium chloride with concentrations $9.9 \cdot 10^{-4}$ M to 0.149 M. At NaCl concentrations of $6 \cdot 10^{-3}$ M and above, and for 0.149 M KCl, the spectrum is 1/f in the measured range, 30 Hz to 10 kHz, when the current is 5 μa or 7 μa; it is usually steeper at 12 μa. For four concentrations showing 1/f noise the ratio of spectral intensities for the 7 μa to the 5 μa spectra is 2.14±0.33 (one standard deviation), in agreement with the expectation of proportionality to I^2.

The flow rate through the ruby aperture was measured by applying a hydrostatic pressure and determining the resulting current. The Onsager Reciprocal relations were used to determine the mass flow accompanying the electrical current. The mass flow was calculated to be 0.01 ms^{-1} on average; and 0.5 ms^{-1} at the 10 μm minimum diameter opening.

לשרה, יעקב,
ברכה, וצבי

Acknowledgements

I wish to thank the many individuals that have generously given of their time and effort to enable me to bring this work to successful fruition. First and foremost among them is Professor Michael E. Green, who guided and encouraged my project from its inception.

I am very grateful to George Kleiner, Hugo R. Schimatz, Gerard Cannella, and Robert Cope, for their technical assistance and the many hours of helpful discussion they provided.

I extend special thanks to William D. Crozier for his assistance in compiling data during his summer internship and to Robert Koestler of the American Museum of Natural History - N.Y. for taking the electron micrographs of the rubies.

Finally, I would like to thank Professor Melvin Lax for providing me with the opportunity to use his typesetter and Harvey L. Berezin for typing the bibliography.

TABLE OF CONTENTS

LIST OF TABLES

LIST OF FIGURES

INTRODUCTION

The mechanisms responsible for the regulatory functions of the cell membrane are a subject of intense interest and study. Cell membranes are highly sophisticated and specialized structures. It is desirable to seek out and to study the properties of simpler systems which have some of the properties of natural membranes, with the hope that inferences can be drawn.

Early attempts to produce a model membrane included the use of polar oils(*1,2*), collodion films(*3*), and cellophane(*4*). The late 1950's saw the introduction of the planar black lipid membrane (BLM)(*5*), which was a superior model, in that the thickness and other properties of the membrane more closely resembled those of real membranes(*6*). Most notably, ion selectivity can be imparted to the membranes by the addition of certain proteins (e.g. gramicidin, valinomycin). BLM have been produced from a wide variety of lipids (with or without organic solvents) and from an assortment of biological extracts. Asymmetric (i.e. each layer containing a different lipid) BLM have also been produced.

A still better model is the liposome. As with the BLM, it can be produced from a wide variety of materials, and ion transport across its bilayer may be facilitated by the addition of the same proteins. The outward resemblance to the cell membrane, in terms of structure and molecular dimensions, is striking. However, in order to study the electrical properties of the membrane one normally uses electrodes on both sides. Inserting an electrode into the interior of a liposome presents much more serious problems than trying to insert it into many living cells including, for example, the squid giant axon.

The purpose of this work is to demonstrate the use of a direct non-invasive technique, electrical fluctuation spectroscopy, as a means of determining relaxation times of ion transport in liposomes. The technique is a modified version of the one used by Feher and Weissman(*7*) to measure the

rate constants associated with the aqueous $BeSO_4$ equilibrium. The technique is modified so as to permit the study of membrane transport. It is hoped that this will make possible the study of those membrane transport systems, derived from biologically important membranes, which have been or may be reconstituted into liposomes (*17*). It is further believed that neuron-derived systems will prove to be of particular interest.

Additionally, the central component of the technique presented is a pore (approximately 250 μm long and approximately 10 μm in diameter) which is within a ruby. The small volume of the pore is used to maximize the relative size of the concentration fluctuations in the liposome preparation under study and thereby make them measurable. Flow within the pore may also prove to be a model for a system of biological interest, as will be discussed in a later chapter.

Chapter One

NOISE AS A PROBE OF MOLECULAR PROCESSES.

Sources of Noise - an Historical Perspective.

Classically, researchers in planning their experiments have tried to maximize the signal to noise ratio of their system. The noise has traditionally been considered to be a nuisance (*8*), whose unwanted interference, if not removed, could obstruct the measurement (i.e. information) of interest. However, a close examination of the sources of the noise in a particular system may yield important physical parameters. A liability may be turned into an asset, producing results otherwise unattainable.

Initial studies of noise (i.e. fluctuations from a mean) were carried out on electrical circuits containing vacuum tubes (*9*), resistors, and aqueous solutions (*10*). These sources produced noise which was white; i.e., the square of the fluctations in voltage for a given bandwidth were independent of frequency. The resistor and solution noise sources were and are thought to be due to the random motion of the atoms and molecules; their thermal power expressed as (*11*):

$$(\delta V)^2 = 4kTR\delta f \qquad (1.1)$$

where,

$(\delta V)^2$ = Thermal power

k = Boltzmann's constant

T = Absolute Temperature

R = resistance of the medium

δf = frequency bandwidth

The vacuum tube noise was designated "shot effect", caused by random emission of electrons at the cathode (*12*) imparting a grainy nature to the current and expressed as:

$$\textit{Shot noise power} = (\delta V)^2 = \frac{e<I>}{(1+\omega^2\tau_c^2)} \tag{1.2}$$

where,

$<I>$ = mean current

$\omega = 2\pi f$

e = electronic charge

τ_c = time constant

For a noise generating diode, $\tau_c = 3 \cdot 10^{-10}$ (*165*); so that for frequencies less than 500 MHz $(\delta V)^2$ reduces to $e<I>$ (which is frequency independent, hence, White noise).

Subsequently, Johnson (*13*) encountered another large noise source in vacuum tubes. The noise was frequency dependent, but had a different current dependence than shot noise. Schottky, who named this phenomenon the Flicker Effect, attributed the effect to a relaxation time with a 0 to -2 slope dependence on a log-log plot of power versus frequency[1]. Physical sources were thought to be the movement of oxide atoms on filaments and the adsorbed gases on tungsten filaments (*14*). Others (*15,16*) claimed that Johnson's data could be better explained by f^{-1} dependence; Kingston and McWhorter(*18*) contended that this frequency dependence is due to a distribution of relaxation times. f^{-1} (commonly referred to as "one over f") noise has been found in numerous systems. It has been observed in semiconductors. Hooge (*19,20,21,22,23*) has shown that

$$\frac{(\delta V)^2}{V^2} = \alpha \frac{\delta f}{Nf} \tag{1.3}$$

where,

$(\delta V)^2$ = magnitude of the voltage fluctuation

V^2 = applied voltage squared

δf = bandwidth

N = number of mobile charge carriers

$\alpha = 2.1 \cdot 10^{-3}$ in semiconductors.

Furthermore, this empirical relation has been found to be obeyed by concentration cells and thermodynamic EMF cells (*180*). Hooge and Gaal (*24*) have shown that for aqueous solutions α is a function of concentration with a value of approximately 10 for 1 Molar solutions. Microelectrodes (*25*) and, under certain circumstances of ionic composition and concentration, anion exchange membranes (*26,34*), have shown f^{-1} noise; the anion exchange noise source has been attributed to the boundary between the membrane and the aqueous depletion layers. f^{-1} noise has been shown to be associated with bulk phenomena of various systems (*20,21,22*). Although it has been studied extensively (*27*), there is no satisfactory explanation for f^{-1} noise; it has been theoretically linked to the following independent processes, among others: the cascade range of the turbulence spectrum (*28,29,30,31*), a continuous spectrum of relaxation times (*18*), and the diffusion polarization effect in channel doped membranes (*32*). Since f^{-1} noise has been observed in so many varied systems, it is unlikely that there is only one physical source for it.

Noise slopes less than one have been observed in glass electrodes (*25*). Van Vliet, et al., measured Lorentzian spectra[2] in photoconductors (CdS crystals) and attributed the break frequency to a relaxation time associated with generation-recombination of electrons and holes in the photoconductors (*35*). The relaxation of chemical systems typically produces Lorentzian spectra. This was found by Feher and Weissman (*7*), who determined the rate constants for the association-dissociation equilibrium of $BeSO_4$ in water by analyzing the resistance (i.e. concentration) fluctations of aqueous $BeSO_4$ solutions in a glass capillary. Weissman (*36*) has used fluctuation analysis to measure the molecular weight of DNA by utilizing the equation:

$$M.W. = \bar{C}\left[\frac{\delta C}{\bar{C}}\right]^2 \nu A \qquad (1.4)$$

---

1 Noise spectra are typically plotted as log power versus log frequency. The slopes are then the frequency dependence of power.

2 Lorentzian spectra are power spectra which are characterized by a region of zero slope at low frequencies, followed immediately at higher frequencies by a region where the spectrum has a slope of f^{-2}. The frequency (-3 dB point) where the slope transition takes place is referred to as the corner or break frequency.

where,

M.W. = molecular weight

$\bar{C}$ = average concentration ($\frac{weight}{volume}$)

$\left[\frac{\delta C}{\bar{C}}\right]$ = standard deviation

(i.e. fluctuations)

of the concentration

ν = volume

A = Avogadro's number

The DNA concentration fluctuations were obtained by measuring the fluorescense intensity fluctuations of an added dye (ethidium bromide).

There have been numerous studies of noise accompanying ion transport to and across membranes. Among the systems studied were ion exchange membranes. Yafuso and Green (*37*), and Stern and Green (*38*), found approximate -3 slopes at low frequencies and -5 slopes at high frequencies for cation exchange membranes; they attributed these slopes to turbulence. As mentioned above, anion membranes exhibited 1/f behavior.

Sokol (*39*), and Sokol and Green (*169*), studied ion transport through *n*-butanol membranes (i.e. *n*-butanol separating two aqueous phases). Steep slopes at low frequencies were attributed to mechanical vibrations of the butanol/water interfaces. Above 80 Hz, aqueous NaCl/*n*-butanol systems exhibited -1 slopes at low frequencies and -2 slopes at higher frequencies.

Studies conducted on etched mica sheets (*40*), and Nuclepore® membranes (*41,42*) have shown $f^{-1.5}$ noise; the noise was attributed to diffusion. Lax (*33*) has theoretically linked $f^{-1.5}$ to diffusion. f^{-1} noise found with Mylar® films and collodion films (*40*) has been attributed to diffusion through paths of varying lengths (*41*).

Biological Sources of Noise.

A). Biological Membrane Structure and Functions.

Before proceeding further with the history of noise, a digression will be made to the history of the steps leading up to and the motivation for the use of fluctuation analysis in biological systems. Included in this digression is a brief history of two important model systems for biological membranes; the bimolecular (or black) lipid membrane (BLM) and the liposome. Biological membranes differ from those that were discussed above by their capability of exhibiting high selectivity towards the ions passing through them and their capacity to serve as sites for energy conversion systems.

i) Membrane Structure.

The prevailing model of a biological membrane, the Fluid Mosaic model (*79*), is that of two layers of lipids, with each layer's hydrocarbon moieties in opposition to the other's (see Figure 1.1). The polar moieties of each layer are in contact with a hydrophilic environment. The lipid composition varies from species to species; and within a species, between cell types. The variations in functionality of cell types are principally accounted for by the presence of other molecules, particularly proteins. The proteins may be characterized (by the laboratory extraction procedure used to isolate them) as integral (detergent extracted) or peripheral (salt extracted). Integral proteins may have one of the following alternative properties: 1) they may span the membrane and provide a high dielectric passageway for ions traveling from one hydrophilic surface to the other through the hydrophobic interior; or 2) they may be largely embedded within the hydrophobic portion of the membrane. Peripheral proteins are located at the hydrophilic surfaces of the membrane; they are held in place by electrostatic forces. Both types of protein may serve as energy conversion sites. The constituents of each layer are generally free to move laterally within their own layer.

The Fluid Mosaic model is only the most recent refinement of several membrane models to evolve from Overton's 1895 (*43*) model. Overton established the lipid nature of the cell membrane through studies which showed

that biological membranes are permeable to lipids. In 1925, Gorter and Grendel (*44*) postulated the bileaflet nature of biological membranes from monolayer studies of the lipid extracts of the cell membranes of erythrocytes; the cells were derived from various mammals. They found the ratio of the area formed by the monolayers to the surface area of the original cells (the sources of the lipid extracts) to be approximately two. However, measured values of the surface tension of various cell membranes appeared to be approximately two orders of magnitude too low (*182*). Danielli and Davson (*45*) explained these depressed values as being due to proteins absorbed onto the polar surfaces of a bilayer. Electron microscopy (*46*) studies have generally confirmed the features of the Gorter-Grendel model. Freeze-fracture studies demonstrated conclusively the Gorter-Grendel bilayer and freeze f racture in conjunction with freeze-etch studies (*47*) have, additionally, shown the presence of globular proteins imbedded within cell membranes. Studies of spin labeled lipids incorporated into BLM (*48*) have shown that the lipids in each layer of both synthetic bilayers and biological membranes diffuse laterally.

ii) Membrane Functions.

Membranes have a selectivity feature, which controls the admission of nutrients to and the discharge of waste products from the interior of biological cells. It would not be unreasonable to state that life, as we know it, could not exist without this selectivity capability. A viable organism of more than a few cells would require communication between the various cells and would therefore be limited by the diffusion time, or, at least flow, of molecular messenger species from one intercellular site to another. To overcome this limitation in animals, it may reasonably be suggested that the nerve cell (neuron) has evolved. It is an electrical transmission system which uses the transport of cations across the cell membrane in a sequential manner to communicate electrical signals.

The physical appearance of one type of a neuron is that of a bulbous cell (cell body) having a dense system of protruding short roots (dendrites); also, there is a comparatively long fiber (axon) protruding from the cell which itself terminates in a root system. The axon's membrane is charged due to cationic

concentration differences between the aqueous phase in its interior and the aqueous phase on its exterior.

It is now believed, for the reasons elucidated below, that the electrical transmission along the axon is a consequence of ion flows across the axon; these flows result from the opening and closing of highly specific ion channels, which are proteins, within the axon membrane. Two principal ion flows result, one of sodium, and the other of potassium, driven by concentration differences between the aqueous phases. An energy pump (Na,K ATPase) in the membrane restores the concentration differences across the membrane. In a non-myelinated axon, a local voltage change on the membrane occurs due to these events and then triggers the same set of events at an adjoining site. The sequence of events is repeated down the length of the membrane until it reaches a synapse[3]. The net effect is that of an electrical pulse propagating down the length of the axon. The pulse, which is illustrated in Figure 1.2, is known as an action potential. The sequential transmission of information in this manner is extremely fast, in comparison to diffusion times. However, although this is sufficient for long distance signal transmission, coordination of the parts of a living system requires interneuron communication. This is accomplished by the release of the contents of liposome-like structures containing messenger compounds (neurotransmitters) at the terminal root portion of the axon (i.e. presynaptic membrane). The release of these compounds is preceded by an influx of calcium ions from the exterior of the cell, via a calcium selective pathway. The neurotransmitters diffuse across the synapse (aqueous space) to the postsynaptic membrane. There are numerous types of neurotransmitters. In order for them to elicit a response, they must interact with very specific sites (receptors) on the postsynaptic membrane. The neurotransmitter may be specific for more than one type of receptor. In response to this interaction, the neuron cell body will generate as many as seven different ion current flows, via channels, resulting in the transmission of

3 A synapse is a region of space separating the terminal portion of an axon from a dendrite (or a neuromuscular junction). The membrane of the axon in this region is referred to as the presynaptic membrane and the membrane of the adjoining dendrite as the postsynaptic membrane.

pulses to its own axon.

The channels thus far mentioned may be characterized as "gated-channels"; they open in response to external stimuli, which may be electrical or chemical in origin. In response to a particular voltage level, the conformation of the channel protein may change by the swinging aside of a polar group in the interior of the channel, in much the same fashion that a dipole will align itself in response to an electric field. The combination of a neurotransmitter and a receptor protein may cause a conformation change in the protein moiety which will open a high-dielectric passageway through the membrane.

The knowledge that some animals possess tissues of an electrical nature dates to early civilization (*49*). However, studies of the electrical behavior of tissues did not begin in earnest until the nineteenth century. In 1902 the following explanation for the electrical behavior of cells was formulated by Jules Bernstein (according to Jain (*50*)) :

1) Living cells have an electrolytic interior and exterior.
2) In the resting state the cell membrane is permeable to potassium ions only, which gives rise to a diffusion potential.
3) During excitation the resting potential changes to a relatively lower value by permitting the passage of ions.

An important experimental advance came with J.Z. Young's (*51*) perfection of a technique to isolate squid axons, which maintained their electrical behavior for as long as 12 hours. In 1936 measurements by Cole and Curtis (*52*) of the resistance and capacitance of a single squid axon showed the capacitance of the membrane to be approximately $1\frac{\mu F}{cm^2}$. This value appears to be a ubiquitous feature of all biological membranes. Despite the resistance changes which accompanied depolarizations, the capacitance value remained constant. This implied that the thickness of the membrane did not change; to do so would require a major reorientation of the structural organization of the lipids, which constituted the supporting framework of the membrane. If the

membrane framework did not change, then the changes of resistance might be accounted for by localized pathways for ions in the membrane.

iii) Hodgkin-Huxley Model:

Major insight into the electrical behavior of the axon came from the work of Hodgkin and Huxley (HH) in 1952. In a set of papers (*53,54,55,56*) they described an empirical set of equations, derived from their own voltage-clamp data and Cole's (*76*) voltage–clamp data, which explained the form and behavior of the action potential. Voltage-clamping is a technique, originated by Cole (*52*), by which the axon membrane potential may be held constant, at different voltage levels, spatially and temporally. The spatial fixation is accomplished by placing electrodes, which are as long as the axon, alongside the exterior and into the interior of the axon membrane. The electrodes serve to apply a spatially uniform electric field and to sense currents flowing through the axon. The temporal fixation is accomplished by the use of electronic feedback circuitry to maintain a desired voltage. The time course of the current is followed at each applied voltage (see Figure 1.3).

HH's analysis of the current-time curves showed that the current could be described by the summation of four current flows (see Figure 1.3).

$$I=I_C+I_L+I_{Na}+I_K \tag{1.5}$$

The first, (I_C), which is very fast and has a small amplitude when compared to I_{Na} and I_K, was attributed to a capacitative transient of two parts (an early and a late part). The early large part represented the charging or discharging of the membrane capacity through the equivalent series resistance of the membrane and the small later part was ascribed to the slow movement of charged species within the membrane.

$$I_C=C_M\left(\frac{dE_M}{dt}\right) \tag{1.6}$$

where,

C_M = membrane capacitance

E_M = membrane voltage

The second, the leakage current (I_L), which is essentially ohmic, immediately follows the first. It is a fast transient and its amplitude is negligible when compared to the next two components.

$$I_L = g_L (E_M - E_L) \tag{1.7}$$

where

g_L = leakage current conductivity

E_L = reversal leakage potential

The third current, I_{Na}, is carried by sodium ions flowing down their ionic gradient[4], from the exterior of the axon into its interior, and is observed as a downward dip in current.

$$I_{Na} = g_{Na} m^3 h (E_M - E_{Na}) \tag{1.8}$$

where,

g_{Na} = *Na* channel conductance

E_{Na} = *Na* reversal potential

m, h = probabalistic independent variables in the region $0 \leqslant m, h \leqslant 1$

The fourth component, I_K, is carried by potassium ions flowing down their ionic gradient[4]; the peak of this current follows immediately on that of the third current. The flow is from the interior of the membrane to the exterior and is expressed as:

$$I = g_K n^4 (E_M - E_K) \tag{1.9}$$

where,

g_K = K channel conductivity

E_K = K reversal potential

n = probabalistically independent variable in the region $0 \leqslant n \leqslant 1$

Of the three dimensionless parameters n,m and h HH described n and m as activation parameters, and h as an inactivation parameter. They were further described by HH as following three first order differential equations of the form:

$$\frac{dP}{dt} = \alpha_P(1-P) - \beta_P P \tag{1.10}$$

where,

P = m or n or h

The α_P s and β_P s are empirically derived rate constants for each parameter and are functions of applied voltage.

Since their formulation, the HH equations have been the focal point of experimental studies and theoretical treatments directed at explaining nerve potentials in terms of detailed molecular mechanisms. It must be stressed that the HH equations are the results of an exercise in curve fitting and that the curves they fit may be incomplete descriptions of the true current-time profiles; the inadequacies are due to inherent instrumental limitations of HH's apparatus. Improved instrumentation and technique has, in fact, resolved features not observed by HH (see below). Although the equations do not neccessarily give a correct representation of the underlying mechanisms, certain important generalizations have been made: The potassium current depends on

---

4 Although the word "gradient" is frequently used in the literature in this manner, strictly speaking it fails to accurately describe the actual conditions present. It would be more appropriate to describe the environment that the ion, traveling through the membrane, encounters, as a concentration discontinuity, rather than as a concentration gradient.

the occurrence of four sequential events (n^4 dependence); for example, four molecules may line up to form a pathway through the membrane. The sodium current depends on the occurence of three sequential events (m^3 dependence); there appears to be a single event which inactivates it (h dependence). The current of each ionic species travels via a different pathway. Nearly thirty years later, the molecular interpretation for the mechanism is still a matter of intense study and speculation.

Attempts to establish the existence and characteristics of the postulated distinct pathways followed. Hodgkin and Keynes (*57*) proposed, on the basis of their studies of the variation in the flux of radioactively labeled potassium with potassium concentration, the movement of potassium ions in a single file procession through the membrane via a narrow passageway.

The argument for spatially independent pathways was strengthened when it was found that certain compounds could selectively reduce or eliminate individual components of the total membrane current (*58,59,60*).

When tetrodotoxin (TTX) or saxitoxin (STX), which are neurotoxins of biological origin, were added to the outside of the axon, the third component I_{Na} was eliminated. The addition of TTX and STX to the interior had no effect on the current. Addition of tetraethyl ammonium ion (TEA) (*61*) to the interior of the axon blocked the fourth current component I_K.

Having established the existence of pathways, the next step was to characterize the diameter of the channels, assuming they were channels. The evidence up to this point could be attributed to a mechanism based on a carrier molecule. That is, a carrier molecule could form a complex with an ion at a membrane-solution interface; the molecule could envelope the ion and, in its complexed conformation, exhibit a hydrophobic exterior. The complex might then shuttle across the hydrophobic interior of the membrane and dissociate, releasing the ion at the other membrane-solution interface. The carrier mechanism was ruled out on the basis of theoretical calculations of required transport rates (*62*) and energy barrier considerations (*63,64,65,66*).

On the basis of his studies of the permeability of axon membranes to various cations injected into the interior of the axon, Hille (*67,68*) concluded that the narrowest portion of the sodium channel was three to five Angstroms

in diameter. He labeled this constriction the 'selectivity filter'. Of the ions he studied, guanidinium was the largest which was capable of traversing the sodium channel. Woodhull (*69*) has given evidence, based on sodium channel conductance vs pH, that the selectivity filter incorporates a carboxyl group near the exterior portion of the axon. The reduction of sodium current by hydrogen ion was found to be voltage dependent. Membranes treated with materials which normally alter carboxyl groups (*70,71*) showed elimination of the sodium current and the reduction of TTX binding.

The sodium inactivation process was found to be destroyed by perfusing[5] the interior of squid axons with electrolytic solutions of pronase, a mixture of proteolytic enzymes. This led to the conclusion that a protein near the interior side of the axon was intimately associated with sodium inactivation (*72,73*).

Permeability studies of the potassium channel indicated a selectivity filter of three Angstroms in diameter (*74*) located near the outside of the membrane (*75*). pH vs conductance studies indicated the presence of an ionizable group in the channel (*74*).

Although they did not observe them, HH predicted the existence of very small and brief "gating-currents". These gating currents were supposed to be a consequence of the movement of charged species in response to changes of the membrane polarization, which unblocked the ionic pathways. These gating currents were finally observed (*77,78*) by "poisoning" the sodium and potassium channels and utilizing sophisticated signal averaging techniques; the current values were of the order of 30 $\mu a \cdot cm^{-2}$ at their peak.

B) Model Membrane Systems.

5 Perfusion, in the particular case being considered here, is a technique in which the interior contents of an axon are extruded and replaced with a solution of interest.

i) Black Lipid Membrane.

In the late 1950s the direct assault on biological systems had begun to be paralleled by the study of a new model membrane system, the planar bimolecular lipid membrane (BLM) of Mueller and Rudin (*5*). As mentioned in the introduction, these membranes had properties closely resembling those of biological origin.

The BLM is typically produced by injecting or brushing a solution containing lipids, of synthetic or biological origin, onto an aperture which is in a partition separating two aqueous compartments. The lipids are dissolved in an organic solvent such as decane. The organic solvent diffuses away from the aperture and the lipids form a highly ordered bilayer structure (see Figure 1.4), representing an energetic minimum. As the progression of the thinning process is observed with a microscope (the membranes are generally not greater than 1 mm^2 in area) bands of moving colors appear. The bands of color are present because the membrane has reached a thickness which is of the order of the wavelength of light and reflection from its two membrane-solution interfaces cause the destructive interference of light. Subsequently, black (actually grey) regions appear and grow in area until all the bands of color dissappear; at this point the membrane has reached a thickness of 50 to 100 Angstroms.

The membrane thickness has been found to be voltage dependent due to the reversible formation of solvent lenses in the membrane interior, which are a response to the compressive force of an applied electric field (*80*). The BLM thickness is also affected by the length of the aliphatic solvent used. Hexadecane forms relatively solventless membranes by this technique (*81*).

A second technique for producing BLM was developed by Mueller and Montal (*82*). Two aqueous compartments are separated by a partition containing an aperture (see Figure 1.5). Lipid monolayers are carefully spread onto the top of each; the solution level of each compartment is then raised. As the level of the solutions reaches the aperture, the hydrophobic tails of each monolayer begin to attract the tails of the other monolayer. The two monolayers " zip " together to form a bilayer in the aperture. It was believed that this process formed truly solventless membranes, as the lipids were not applied dissolved in organic solvents. However, it has been shown that the aperture

must be prepared by coating it with an organic material (e.g. petroleum jelly) (*167*). It cannot be stated with certainty that this organic preparatative material does not diffuse through the structure of the membrane and thereby affect its composition.

If two monolayers of different lipid composition are used, asymmetric membranes may be prepared. Asymmetric distribution of lipids in biological membranes appears common, if not the rule (*83*).

The bilayers produced by either technique are accessible to electrical study by the placement of electrodes on both sides of the membrane.

ii) Liposomes.

Another important model system is the liposome or vesicle (see Figure 1.6). It was found that dispersions of lipids in water would form closed concentric structures after agitation (*84*). These structures were shown to be bounded by lipid bilayers. Each structure (i.e. liposome) enclosed an aqueous phase; if there was more than one shell (i.e. multilamellar system), each shell was separated from the others by an aqueous phase.

Liposomes and BLM are similar in several important aspects. They each have a bilayer, they can each be formed from a wide variety of synthetic lipids or lipid extracts (albeit, not necessarily the same molecules in every instance) and each may be made permeable by the same transport promoting agents (*85*).

The structure of liposomes and the conditions which are conducive to their formation has led to the speculation (*86*) that liposomes are the evolutionary precursors of the biological cell. The plausibility of this speculation is reinforced by the observation of the presence of liposome-like vesicles as functioning sub-units of living cells. In the case of the neuron, vesicles are used to transport materials required for the maintenance and functioning of the membrane away from their point of manufacture in the cell body. Vesicles (lysosomes) are used by the neuron to degrade and transport away waste products from the synaptic terminals. And as previously mentioned, vesicles are used by the neuron to contain and mediate the release of neurotransmitters in the presynaptic region.

With few exceptions (*87,88*), the lipid extracts of biological membranes are composed primarily of glycerolipids or sphingolipids, containing two fatty acid carbon chains. However, the 'proto-cell' is most likely to have been formed with much simpler molecules (liposomes have been made from dilute dispersions of simple C8 to C18 single chain amphiphiles (*89*)); in the course of its evolution the 'proto-cell' has incorporated more complex molecules and complex substructures. In recent years it has been possible to reconstitute such interesting biological processes as ion pumps, mitochondrial oxidative phosphorylation systems (*17,90*) and voltage dependent anion channels (VDAC) into liposomes (*92,93*). However, attempts to incorporate the first two of these processes into BLM have failed. VDAC is isolated from the outer mitochondrial membrane. It has been reported by one worker that sodium channels have been incorporated into liposomes (*94*).

C) Induced Electrical Excitability in Artificial Membranes.

Initial studies of BLM (*5*) made from biological lipid extracts showed very large resistances. It was therefore concluded that something within biological membranes (e.g. proteins) imparted their low resistance and the lipid bilayer functioned in a support role. It was later found (*162*) that certain materials (e.g. EIM - a proteinaceous material derived from aged eggs) when added to BLM produced sharp resistance drops, which were in some instances also voltage dependent. It has been shown that these materials accomplished this by either forming channels through the membrane or by acting as carrier molecules.

i) Channel formers.

The electrical behavior of single channels has been observed by adding trace quantities of channel formers (e.g. gramicidin - see below) to BLM and examining the current versus time behavior induced by applying a voltage to the membrane. The current-time recordings exhibit discrete current steps of one fixed value or integral multiples thereof. The presence of a current step of fixed value is a consequence of a single channel opening and then closing, in

the process permitting one or more ions to traverse the membrane. The ion transit time being a function of the environment (e.g. electrical, solution mobility, tortuosity) in the interior of the channel.

The current-time recordings of some channel formers (e.g. alamethicin - see below) exhibit current steps of several discrete values (or linear combinations of these values); the values are characteristic of the particular channel former. The presence of the different step values indicates that the channel has more than one conductance state. The multiple conductance states may be the result of different conformational states assumed by the channel molecule(s), each state providing ion pathways with different internal environments. Alternatively, the multiple conductance states may be a consequence of the opening and closing of parallel interacting pathways, either within the channel former complex itself or by the incorporation of additional channel former type molecules into the initial channel complex.

Channel conductances in BLM range from 1 pS to 1 nS (*95*). Although the conductance of a particular state is unaffected by the applied electrical field, the field does have an effect on the probability of occurrence of such a state. Interestingly, the voltage dependent openings manifest themselves in opposite ways for different channel formers. Whereas, a particular voltage level will result in the closing of all the channels in one variety of channel former, the same voltage level will maximize the opening of the channels of another variety of channel former. The conductance values of a particular channel type in membranes of differing lipid composition tend to be invariant (*96*). The lipid composition does, however, affect the relaxation time of the conductance transitions, which is a measure of channel opening and closing times and of gating motions. Depending on the channel and the lipid composition, the relaxation times for conductance transitions vary from 10^{-3} to 10 seconds (*95*).

Examples of two structurally different archetypical channel former types, alamethicin and gramicidin:

a) Alamethicin.

It is believed that alamethicin, a cyclic peptide (M.W. - 1691 D.) derived from the fungus *Trichoderma viride*, forms a channel incorporating up to 9 monomeric units (*97*). A ninth order concentration dependence of the current has been observed (*98*). The molecules are believed to form a transmembrane pore by arranging themselves as the staves of a water barrel (*99*). Alamethicin exhibits nine different conductance states; in 0.5 M NaCl the conductance states range from 0.6 nS to 10 nS. Although the conductance levels are independent of the membrane thickness, the frequency of opening and the average lifetime of the channels are dependent on it. Alamethicin pores show a lack of selectivity towards both cations and anions, whether uni- or di-valent. The conductance ratios of univalent cations are near those in aqueous solutions. Single channel studies have shown that transitions between the lowest conductance state and the higher ones are voltage dependent; transitions between the higher conductance states show little if any voltage dependence.

b) Gramicidin.

The gramicidin channel, which spans the bilayer, is formed as the result of the dimerization of two gramicidin molecules in a head to head conformation (*100*). Gramicidin is a linear hydrophobic pentadecapeptide, derived from *Bacillus brevis*, and when dimerized it is approximately 28 Angstroms in length. The channel, which is cation selective, will pass single dehydrated ions up to approximately four angstroms in diameter. Gramicidin's interaction with BLM has been well characterized through studies which include: statistical and kinetic analysis (*65,101*), water and ion permeability studies (*102,103,104*) and the use of substituted gramicidins (*105,106*). The conductance of a single gramicidin channel has been measured to be 40 pS in 1.0 Molar KCl solution (*108*). At an applied potential of 100 mv, this corresponds to the transport of $3 \cdot 10^7$ K^+ ions/sec through the channel (*65*). The macroscopic conductance is proportional to the square of the concentration of the gramicidin monomer

(*108*). Voltage clamp relaxation studies (i.e. voltage jump) measurements have been used to confirm the dimeric nature of the channel (*65*). It was found that the relaxation of current followed a simple exponential decay, with a time constant which was itself a function of gramicidin concentration. Examination of single channel studies (*101,108*) of gramicidin doped BLM showed the distribution of the occurrence of two or more simultaneous channel openings to be Poissonian. This would indicate that the underlying mechanism involves statistically indpendent unitary steps. At constant ionic composition the conductance change was independent of membrane thickness or of temperature; however, the exponential distribution of the channel's lifetimes was dependent on them.

An electrostatic model (*102*) has indicated the presence of a potential well close to each end of the channel. This suggests that the conductance is partially limited by the rate of the ion going from bulk solution into the well.

ii) Carriers.

Despite the lack of any evidence to support a carrier mechanism in biological systems other than as antibiotics, this mechanism has been observed in BLM. Since antibiotics need only destroy cell selectivity, there is no need to postulate an additional biological role for the antibiotics, though such an additional role is not ruled out.

Carriers exhibit high selectivity towards the ions they transport; the transported ion (and possibly a hydration shell) must fit exactly (in terms of physical dimensions and spatial orientation) into a cavity formed by the carrier molecule in its hydrophobic conformation. A well studied carrier is the antibiotic valinomycin, which is a cyclic dodecadepsipeptide (M.W. 1100 D). It is made up of successively alternating amino- and hydroxy-acids. Its potassium ion complex is stabilized by intramolecular hydrogen bonding between its amide hydrogens. Its six carbonyl groups, which are in the interior of the complex conformation, act in such a manner as to displace the potassium ion's hydration shell and lock the potassium ion into a cavity of approximately three Angstroms in diameter (*110,111*).

Theoretical treatments of carrier mechanisms include Nernst-Planck (*112,113,114*) and Eyring rate theory approaches (*115,116*). These treatments derive the carrier complex membrane behavior in terms of the carrier-ion equilibrium constants, carrier concentration, applied voltage and the ionic strength of the aqueous phases. Experimental findings have been consistent with these models (*117*).

D) Noise from Biological Membranes and BLM.

Having laid the historical foundation for the interest in biological channels and having detailed some of the important experiments using traditional methods, the discussion returns to the examination of noise[6] as a probe and discriminator of molecular processes, especially those associated with the transmission of nerve pulses.

C.F. Stevens (*118*) has divided the noise to be expected from a nerve membrane into four categories[7]. Each category is potentially capable of yielding a different piece of information concerning the membrane as each is the result of a different physical source. First, the passive membrane impedance may be obtained from the thermal noise spectrum (equation 1.1). Second, if experimentally measurable, the shot noise spectrum (equation 1.2) will give information concerning the average motion of single ions traversing the membrane. The movement of an ion through a membrane is analogous to the movement of an electron through the space separating an anode and a cathode in a vacuum tube. The third category of noise comprises 1/f noise, the physical meaning of which will be discussed further below. Steven's fourth category of noise is the noise derived from the conductance fluctuations caused by channels opening and closing.

---

6 Note: the single channel studies previously mentioned can be considered to come under the heading of fluctuation analysis, despite the fact that the fluctuations they consider are not about a mean value (i.e. the discrete steps are all in one direction). To avoid confusion, in all further discussions 'noise analysis' or 'fluctuation analysis' will be understood to refer to autocorrelation analysis (see chapter 2) or the use of its fourier transform (the power spectrum) on systems which are both stationary and ergodic.

7 This categorization may also be applied, in part or whole, to other biological membranes and doped artificial membranes.

As two or more categories of noise sources may be present at the same time, the noise spectrum of a particular category may be obscured in the total spectrum. Noise sources add according to:

$$E_t = \sqrt{\sum_i E_i^2} \tag{1.11}$$

where,

E_t = total rms voltage

E_i = mean value of the i^{th} noise source

To sort out each noise contribution it becomes necessary to experimentally sequester one or more of the contributing noise sources. As will be shown below, this is not always a trivial exercise, and the sequestering of a particular noise source may lead to unexpected results.

The ability to discriminate between different noise sources in biological membranes has been aided by fluctuation studies of doped BLM. For the very same reasons that BLM have provided a controlled situation for the determination of biological membrane structure and biological mechanism parameters using classical methods (e.g. electrical, optical), BLM have provided a controlled situation for the incorporation and measurement of noise from known transport promoting mechanisms within a membrane. This has permitted the qualitative and quantitative comparison of theoretical noise models (*118*) with experimental data.

A nonlinear phenomenon, not categorized by Stevens, is that of burst noise. The phenomenon manifests itself as randomly occuring bursts of excess noise in the current-time recordings of some membranes. It was first observed in frog node of Ranvier during large hyperpolarizations (*119,120*) and then later in undoped BLM (*121*). As a result of the BLM studies, burst noise has been attributed to localized dielectric breakdowns of the membrane (*122*).

i) Noise from BLM.

The behavior of at least three of the four categories of noise described by Stevens has been observed in BLM and in each case the behavior has been consistent with that expected from theoretical considerations.

Valinomycin doped BLM (*123*) exhibited frequency independent (i.e. 'white') behavior, as would be expected from a carrier transport model based on Nyquist's theorem[8].

The conductance fluctuations of channel doped membranes has been examined in several studies (*124,125,126,127,128*). A comparison of fluctuation analysis with single channel studies for the determination of average channel lifetime (i.e. the inverse of the rate dissociation constant) and unit channel conductance is illustrated in Figure 1.7, which is taken from Neher, et al. (*128*). The inset of Figure 1.7a represents a current-time recording of a dioleoyl-L-α-phosphatidylcholine (*n*-decane/ 1 M KCL) BLM doped with gramicidin A. The average channel lifetime obtained from the correlation function was 0.78 ± 0.05 sec, which is consistent with the value (0.76 ± 0.03 sec) obtained by manual measurement of the same 300 recorded single events. The value for the channel lifetime obtained by fluctuation analysis remains the same (within 10 percent) up to a current level due to the superimposition of $3 \cdot 10^4$ channels ($2 \cdot 10^7$ channels/cm^2). Neher, et al., suggest that the reason the value for the channel lifetime changes (see Figure 1.7b) at the higher channel concentrations is associated with channel-channel interactions.

The ability of fluctuation analysis to resolve experimental parameters at larger than trace quantities of channels is a demonstration of its superiority to single channel techniques. In addition, correlation analysis, complemented by varying the gramicidin concentration, yields rate constants of channel formation (*125*).

1/f noise is exhibited up to frequencies of several kHz (*129*) by diphytanoyl lecithin membranes doped with malonyl bis-desformyl gramicidin. Malonyl bis-desformyl gramicidin is known to form long lived channels[9]; the

8 Nyquist's theorem relates the spectral intensity (i.e. power spectrum) of a material to the admittance of that material.

dimerization is essentially permanent on the relevant time scale. Hooge's relationship (equation 1.3) in terms of current was obeyed, with N equal to the number of channels and α equal to $1.0 \cdot 10^2$.

ii) Noise from biological tissues.

Fluctation analysis as a probe of biological tissues has been the subject of several comparatively recent reviews (*122,130,131,132,175*). Noise studies of biological tissues include frog node of Ranvier (*119,133,134*), squid giant axon (*135,136,137,138,139,140*), isolated patches of lobster axon (*141,142*), the apical membrane of the outer stratum granulosum of frog skin (*143*), and denervated frog muscle fibers (*144*).

Early studies of the (frog) node of Ranvier (*119,134*) and lobster axon (*141,142*) exhibited 1/f behavior; the amplitude of the 1/f component was found to be a function of the driving force of the potassium ion flow. Fishman observed (*139,145*) in the power spectra of small patches of squid axon a 1/f component and a Lorentzian component. The amplitude of the 1/f was found to be dependent on the potassium ion driving force. Furthermore, the Lorentzian feature disappeared after reduction of the outward potassium current by internal perfusion of the axon with solutions containing TEA^+,Cs^+ or reduction of the internal potassium concentration. The Lorentzian feature was insensitive to the addition of sodium blocking agents. Power spectra of large areas of squid axon have also shown 1/f + Lorentzian behavior (*135,146,147*).

Subsequent studies (*148,149*) of the node of Ranvier also showed a relaxation component in its power spectrum. The relaxation components have been attributed to the mechanisms controlling the potassium ion flow (*133,140,145*), specifically the opening and closing of channels. 1/f is considered to be inconsistent, on the basis of studies of charge carrier flows in solid state materials (*151*) and a theoretical treatment based on the HH equations (*152*), with the noise expected from that of the opening and closing

9 The mean channel lifetime for unmodified gramicidin is 0.1 to 1 seconds. Malonyl bis-desformyl gramicidin has a mean channel lifetime of the order of 2 minutes.

of the ion channels postulated by HH treatment of squid axon. Complementary evidence from noise studies of channel doped BLM (*125,153,154*) have shown only a relaxation time. This has further indicated that the source of the 1/f component in the biological tissues is not associated with the opening and closing of channels. As mentioned, 1/f is a ubiquitous feature and is generated by different physical sources and in this instance has been strongly associated with the restrictive diffusive movement of ions through pores (biological and non-biological) (*32,40,41,42,151,155*). 1/f noise as associated with membranes has been recently reviewed by Neumcke (*156*). It has been suggested by Holden and Rubio (*157*) that 1/f noise may be produced by the interaction of adjacent ionic channels via a membrane wave; they supported their suggestion with a one dimensional model calculation involving only three channels. The channel interactions would be the result of a conformational change in a channel forming protein(s), which would result in a local disturbance in the spatial orientation of the neighboring lipid molecules. The disturbance would propagate, altering the fluidity of any region it passes through and thereby constrain the freedom of movement (conformational movement) of any other channel protein it might encounter. An experimental study (*158*) which has claimed to have measured such an interaction has determined the Young's modulus of egg-lecithin/*n*-decane BLM as a function of gramicidin A concentration. The results have been interpreted as showing an interaction between the channels, over a distance of 900 Angstroms, via the elastic membrane. However, the data are not convincing. It may also be noted that the results of a light scattering study (*159*) (i.e. optical mixing spectroscopy) of the squid giant axon showed spectra which were the sum of a 1/f term and a Lorentzian term. The light scattering technique uses laser light to detect the fluctuations of membrane macromolecules (i.e. fluctuations in the membrane surface topography) which are associated with conductance fluctuations. The conductance is a function of the channel-protein conformation. The amplitude of the spectra was found to increase when the membrane was depolarized and it decreased on hyperpolarization. The similar appearance of the noise spectrum and the light scattering spectrum of the squid axon membrane would seem, at the least, to indicate a coupling of membrane

fluidity to channel noise. The question of channel-channel interaction as a noise source is thus left open to further inquiry. The light scattering data was shown to be consistent with a damped second order system. It was further shown that the fluctuations due to the HH n-parameter are identical to the experimental voltage fluctuations.

Measurements by Fishman, et al. (*138*) of isolated patches of squid axon, in the frequency range 1 to 1000 Hz, were accomplished through the use of a pair of concentric glass pipettes. Electrical contact to a patch was made via the inner pipette, which was filled with seawater. The outer pipette was used to isolate the patch by flowing sucrose solution over the annulus surrounding the membrane area underlying the inner pipette. The sucrose isolated areas were usable for a maximum period of one-half of an hour. Total access resistance (i.e. electrode plus series membrane resistance) was estimated to be approximately 100kΩ, which corresponds to a membrane resistivity of 7 ohm·cm^2. Patch capacitance ranged from 10 to 100 pF, suggesting areas of 10^{-4} to 10^{-5} cm^2 and resting patch resistances of 10 to 100 MΩ. The shunt resistance (i.e. the resistance through the interstitial space exposed to sucrose solution which isolates the patch) ranged from one to two MΩ.

As mentioned earlier, Fishman, et al. (*145*), found that the addition of TEA ion eliminated a Lorentzian feature associated with potassium conduction. However, the reduction of the low frequency Lorentzian component was accompanied by an unexpected intensification of the high frequency portion of the spectrum. This was also observed for the potassium conduction blocker triethyldecyl ammonium ion (TEDA), a close analog of TEA. The intensification was unexpected, because macroscopic current studies have shown a diminuation of K^+ flow upon the addition of TEA (*58,59,60*). Moore, et al. (*160*), suggest that the induced noise arises from the modulation of the K^+ conductance due to the blocking and unblocking of the potassium channel. Moore, et al., further suggest a model which explains their data in terms of a 2 step sequential pseudo-unimolecular reaction where TEA binds during an open conductance state. A unit channel conductance of 2 pS is also estimated from their TEA and TEDA data.

Fishman, et al. (*145*), were able to resolve a sodium dependent spectrum feature in squid axon patches. They perfused the interior of the axon with a solution of low potassium concentration (50 mM) and measured the power spectrum, under this condition, at a voltage clamp of -20 mv. This was repeated at a voltage clamp of 35 mv. Taking the difference of the latter minus the former, they found the sodium feature to manifest itself as a small high frequency bump on top of a 1/f spectrum in the frequency region where TEA appears to induce excess noise. The intensity of the sodium feature was also an order of magnitude smaller than the normal potassium concentration noise in that region. External treatment of six axons with TTX (1uM) applied to the patch resulted in the disappearance of the sodium bump.

In a later work, Fishman (*161*) observed an unambiguous TTX sensitive sodium noise source. This was accomplished by internally perfusing the axon with either CsF or tetramethylammonium fluoride (TMAF). The cations are channel impermeant and do not generate excess noise. The fluoride ion is a known blocker of active transport (*132*). Difference spectra obtained under these conditions appeared to resemble, though not closely fit, a single Lorentzian and the corner frequency appeared to shift to a lower frequency on depolarization. The frequency shift was attributed to an incomplete inactivation (HH h process) of the sodium conductance. A larger than normal inward current, one that is significant when compared to the steady state current of a TTX treated axon under normal ionic conditions, was observed.

It may be noted that the sodium related spectral features were resolved from patches of axon which were at non-physiological potassium concentrations. A sodium related spectral feature has been resolved from large area noise studies of squid axon, under physiological ionic concentration conditions (*122,135,147*), with the aid of blocking agents (e.g. TTX and TEA). Fishman, et al. (*132*), are critical of the interpretation of these large area results. They point out that a TTX sensitive spectral feature is not observable in small patch measurements at normal potassium concentration, as its intensity is masked by that of the potassium noise. The component identified in the large area difference spectra (i.e. before and after the application of TTX) as a sodium feature is the same as that induced by TEA (*145*). They are

also critical of the description of the sodium feature as a single Lorentzian and its attribution to the sodium activation process (HH m process), which, they argue, is inconsistent with the view of the sodium process as being at least a second order system. Fishman, et al., are further critical of large area measurements on technical grounds. They question the uniformity of the applied potential in large area measurements (0.1 cm^2 to 0.3 cm^2) , as compared to that obtained in small patches, before and after the application of TTX. Using the lowest resistance current electrode the potential variation may be as large as ten millivolts over a length of 1.2 cm (*163*). Fishman, et al. (*132*), conclude that the large effective capacitance of the large area measurement will interact with the amplifier in such a way as to produce excess noise in the region of the sodium sensitive spectral component.

The foregoing paragraphs would indicate that the selection of blocking agents for use in fluctuation analysis requires care, as they may produce results inconsistent with extrapolations from macroscopic observations. This does not neccessarily negate the value of blocking agents which induce noise (e.g. TEA and TEDA), as a knowledge of their behavior may under appropriate conditions permit their use as probes of noise sources.

F) Summary.

In summary, fluctuation analysis of currents in nerve membranes, with the aid of channel blocking agents, has proven to be a valuable tool in the understanding of the nature of nerve excitation. Isolation of the various physical sources of noise has further been aided by noise measurements on BLM, which has permitted the incorporation of known transport promoting mechanisms (i.e. carrier- or channel-forming molecules) into well characterized (composition, structure, etc.) membranes. However, BLM studies suffer from certain experimental difficulties. In order to reach frequencies above 1 kHz a very small membrane is required to avoid impedance limitations; measurments to 10 kHz are very difficult. Further, there is the question of solvent, which is present in appreciable quantity in membranes prepared by the Mueller-Rudin technique. Even Montal-Muller (*164*) membranes, which are nearly solvent free, require the surface of the Teflon®

support to be prepared (e.g. by coating with petroleum jelly). An additional difficulty with BLM is the inability, up to the present at least, to reconstitute many interesting channels into them. Reconstitution has been found to be much more easily accomplished with liposomes.

A principal reason for the reconstitution of channels into BLM is for electrical studies; until this present work electrical studies were not possible on liposomes.

Additionally, because of its strong physical resemblance to functioning cellular sub-units the liposome is a much better experimental model (if not an actual reconstruction in some instances) of biological structures than BLM.

It is proposed that, by applying the noise measurement technique demonstrated in this work, to a model liposome system into which sodium channels have been incorporated, kinetic parameters of the sodium channel and of the sodium gating current may be obtained. This would yield an understanding of the not yet completely understood intimate relationship between sodium conduction and gating. Study of this system would circumvent the limitations encountered in *in situ* studies of the sodium channel. The liposome's aqueous phases may easily be prepared at physiological composition and concentration and the sodium system noise will not suffer competition from potassium channel noise sources or other complications.

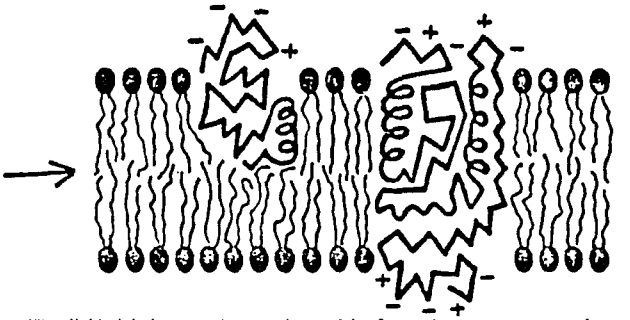

The lipid-globular protein mosaic model of membrane structure: schematic cross-sectional view. The phospholipids are depicted as in Fig. 1, and are arranged as a discontinuous bilayer with their ionic and polar heads in contact with water. Some lipid may be structurally differentiated from the bulk of the lipid (see text), but this is not explicitly shown in the figure. The integral proteins, with the heavy lines representing the folded polypeptide chains, are shown as globular molecules partially embedded in, and partially protruding from, the membrane. The protruding parts have on their surfaces the ionic residues (− and +) of the protein, while the nonpolar residues are largely in the embedded parts; accordingly, the protein molecules are amphipathic. The degree to which the integral proteins are embedded and, in particular, whether they span the entire membrane thickness depend on the size and structure of the molecules. The arrow marks the plane of cleavage to be expected in freeze-etching experiments.

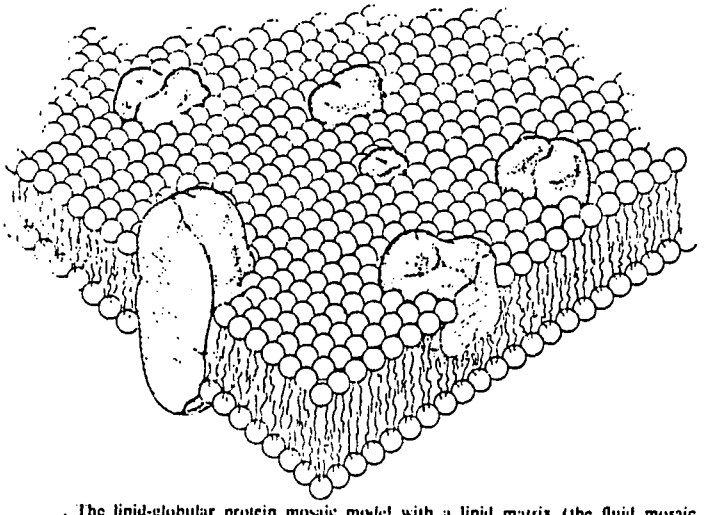

The lipid-globular protein mosaic model with a lipid matrix (the fluid mosaic model): schematic three-dimensional and cross-sectional views. The solid bodies with stippled surfaces represent the globular integral proteins, which at long range are randomly distributed in the plane of the membrane. At short range, some may form specific aggregates, as shown.

Reprinted from Singer and Nicholson (*79*)

Figure 1.1

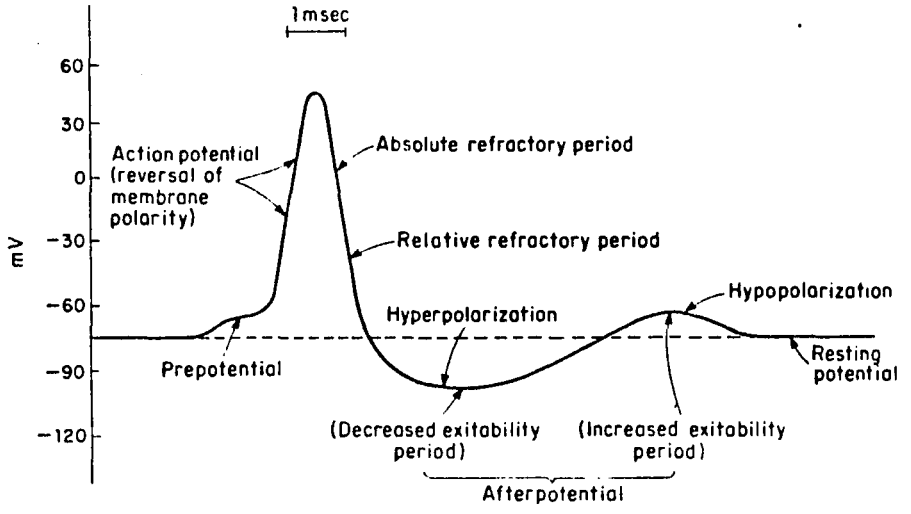

Fig. 8-1. Some of the characteristics of the different phases of an action potential recorded intracellularly from an axon.

Reprinted from Jain (*50*)

Figure 1.2

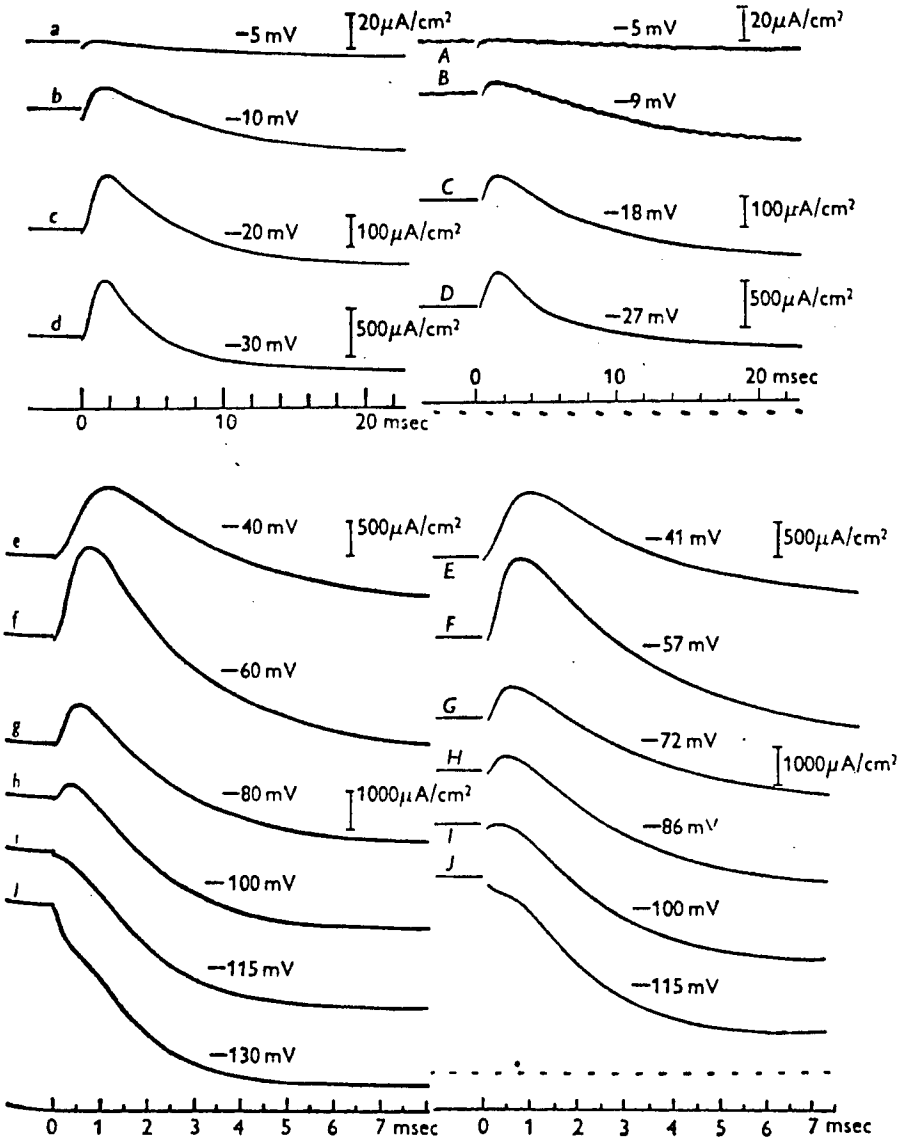

Left-hand column: time course of membrane current during voltage clamp, calculated for temperature of 4° C from eqn. 1.5 and subsidiaries and plotted on the same scale as the experimental curves in the right-hand column. Right-hand column: observed time course of membrane currents during voltage clamp. Axon 31 at 4° C; compensated feedback. The time scale changes between *d*, *D* and *e*, *E*. The current scale changes after *b*, *B*; *c*, *C*; *d*, *D* and *f*, *F*.

Reprinted from Hodgkin and Huxley (*56*)

Figure 1.3

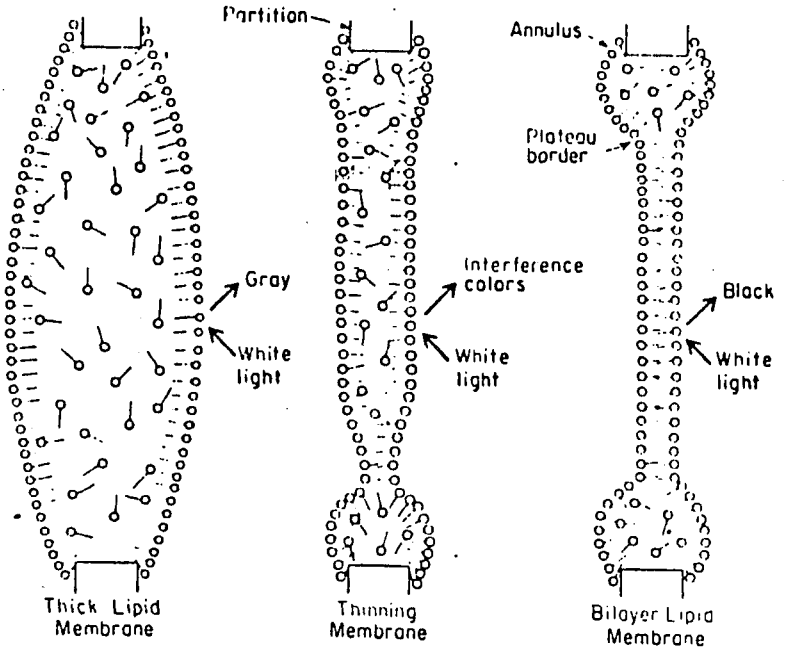

Diagram illustrating the three stages observed during thinning of a lipid membrane in aqueous media, and indicating the patterns of reflected light.

Reprinted from Howard and Burton (*181*)

Figure 1.4

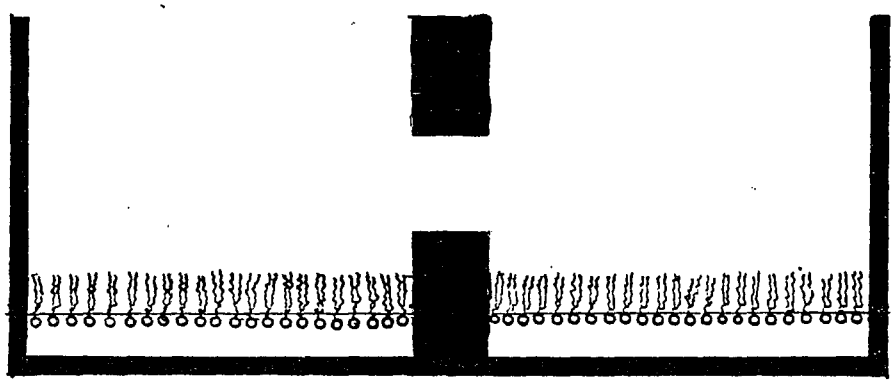

A

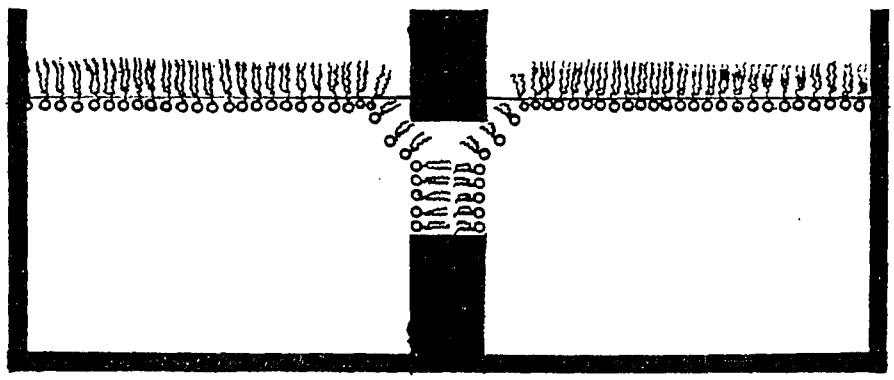

B

A) A lipid Monolayer is formed at the air-water interface of each of the two compartments.

B) The solution level of each compartment has been raised forming a a lipid bilayer in the partition aperture which separates the two compartments.

Figure 1.5

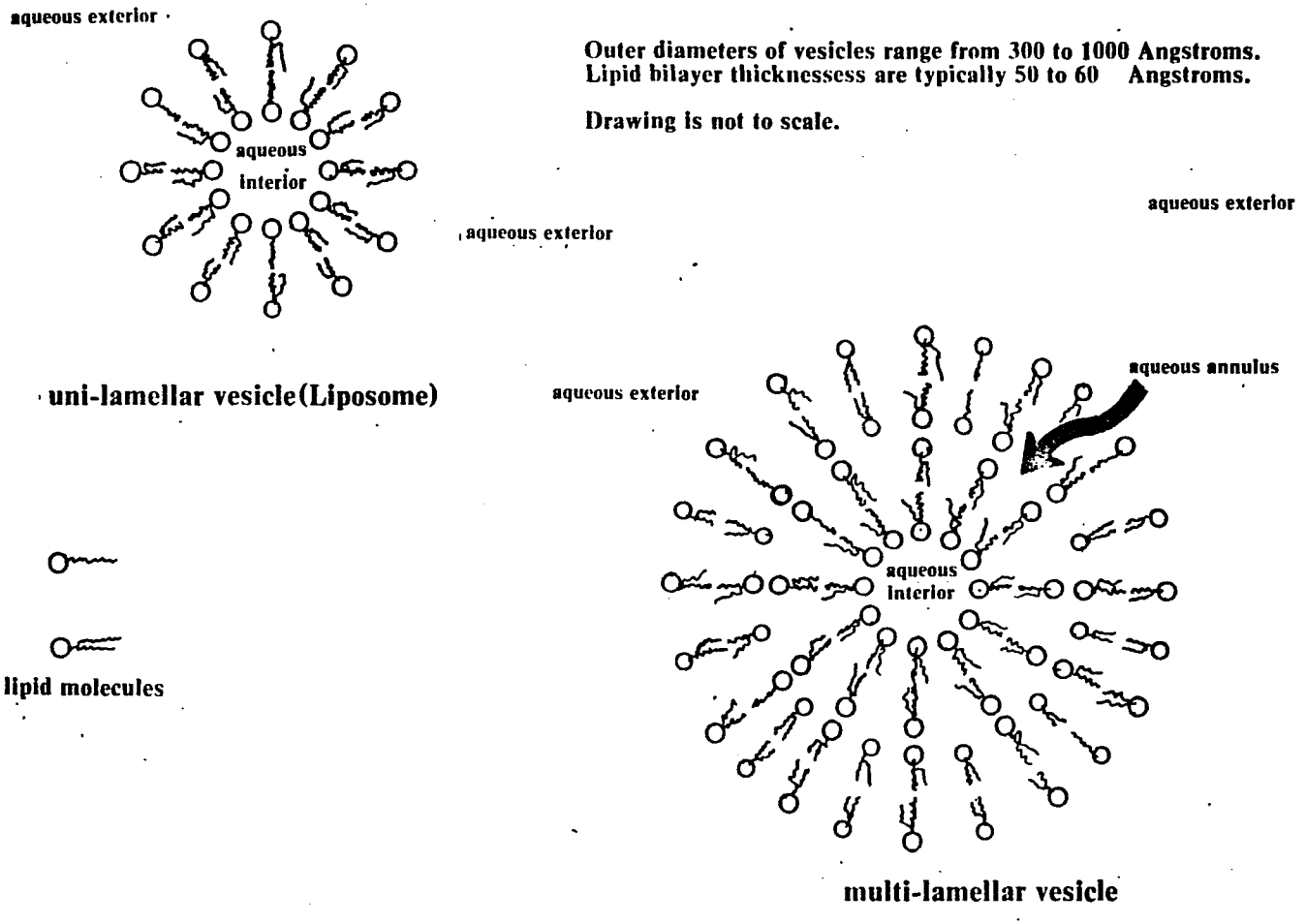

Simplified drawing of uni- and multi-lameller vesicles.

Figure 1.6

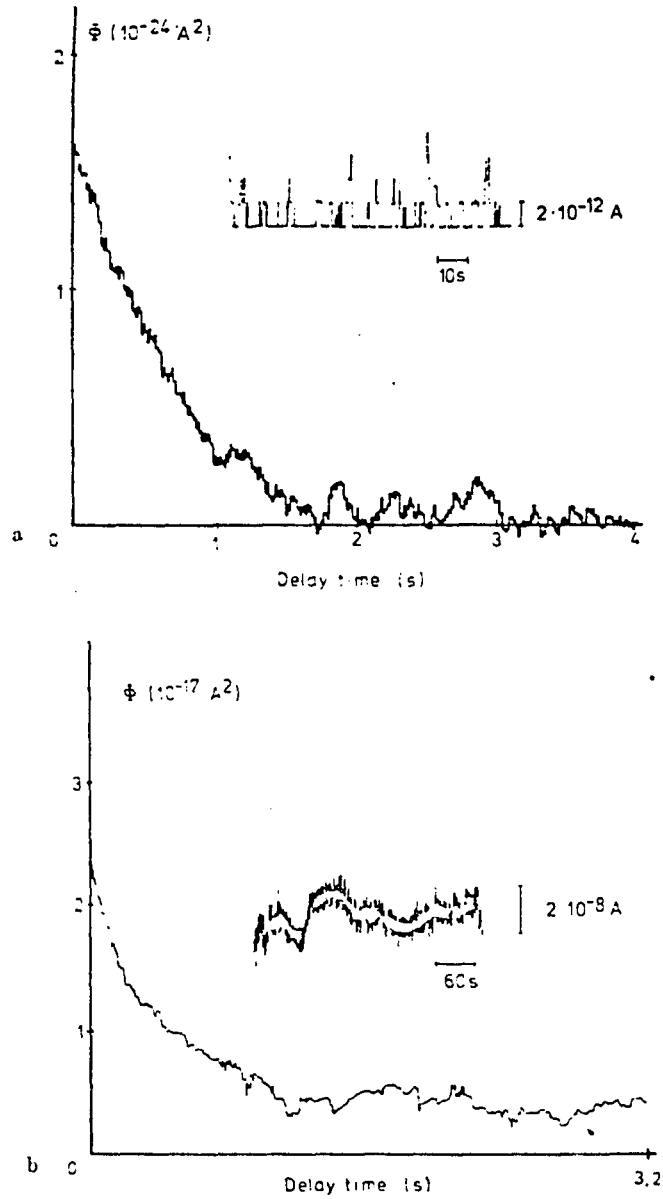

Fig. 1. (a) Autocorrelation function obtained at the unit channel conductance level. Single ion channels were produced by small amounts of gramicidin A in black lipid membranes formed from solutions of dioleoyl-L-α-lecithin in *n*-decance at 1 M KCl. Insert: Direct recording of a few current fluctuations. The autocorrelation function was obtained from approx. 300 single events. Membrane area approx. $2 \cdot 10^{-3}$ cm². (b) Autocorrelation function obtained at a high conductivity level (approx. $1.5 \cdot 10^{10}$ channels per cm²). Insert: Recording of the current noise signal (ac-component only) from which the autocorrelation function was calculated. Membrane area approx. $2 \cdot 10^{-3}$ cm²

Reprinted from Neher and Zingsheim (*128*)

Figure 1.7

Chapter Two

FLUCTUATION THEORY.

If one observes a small volume containing molecules, and the molecules are free to react and/or to move in and out of the volume, it will be found that the number of molecules fluctuates about some mean value. Although the fluctuations are random, they must obey well defined physical laws. It can be shown, via the fluctuation-dissipation theorem(*165*), that the relaxation of a fluctuation to the mean (i.e. steady state value) is governed by the same laws which apply to macroscopic perturbations.

To extract meaningful information from fluctuations we will first let V(t) be the value of an extensive thermodynamic variable (e.g. concentration), which is experimentally measureable at any time t. If V(ss) represents the steady state value of this variable, then we may define the deviation from the steady state $\delta V(t)$ at time t as:

$$\delta V(t)=V(t)-V(ss) \tag{2.1}$$

Furthermore, we require that the time average of the fluctuations be zero:

$$<\delta V(t)>=0 \tag{2.2}$$

If $\delta V(t)$ is measured at some time t and then again at some later time (t + T), then the ensemble averaged product will be:

$$C(T,t)=<\delta V(t)\delta V(t+T)> \tag{2.3}$$

C(T,t) is referred to as the correlation function. If the thermodynamic parameters do not vary with time (which defines a stationary system), the correlation function reduces to:

$$C(T)=<\delta V(0)\delta V(T)> \tag{2.4}$$

We will also assume that the process is ergodic and Markovian. Ergodic means that we may take the time and ensemble averages to be equal to each other. The statistics of the process may be deduced by either examining one member of the process over a long time or examining each and every member of the process once. Markovian systems are systems for which knowledge of δV at a time t gives as much information as it is possible to have concerning the distribution of fluctuations at a future time, without making reference to the past history of δV.

Kinetic information concerning a chemical reaction will be found in equation (2.4). Theoretically, the information produced by (2.4) will be qualitatively better than that produced by traditional relaxation methods as the reaction of interest is not disturbed during the measurement process. We need only measure the fluctuations of the process, which are a direct measure of particle interactions. Traditional methods make the assumption, which may not always be valid, that the applied perturbation does not alter the mechanism under study. The effects of a perturbation on a system must be examined by independent means before traditional relaxation methods may be used. Traditional relaxation methods' dual requirements, that a suitable experimental means of perturbing the system be available and that the perturbation itself not alter the system, places traditional methods at a disadvantage with respect to correlation analysis. However, despite these constraints, where relaxation methods work they are generally as good as correlation techniques and are sometimes more accurate and easier to interpret. Correlation techniques are, then, best used in situations where an appropriate means of perturbing the system is unavailable or experimentally difficult (e.g. kinetics associated with ion transport through a biological membrane).

It may be shown, via the Wiener - Khintchine theorem(*12*), that the correlation function and the power spectrum are equivalent quantities. They are each others Fourier cosine transform:

$$G(f) = 2\mathrm{Re}\int C(T)e^{i2\pi ft}dt \qquad (2.5)$$

$$= 4\int C(T)\cos(2\pi ft)dt$$

If a power spectrum of a process can be measured, its correlation function is then known and we can recover the same kinetic information.

Chapter Three

KINETICS.

Determination of the kinetics of a system containing one relaxation time.

Consider the reaction

$$AB \underset{k_{-1}}{\overset{k_1}{\rightleftharpoons}} A + B \qquad (3.1)$$

which may, among other things, represent the generation-recombination process of an electron and a hole, the dimerization of 2 molecules to form a membrane channel, the complexation of an ion with a carrier molecule, or the dissociation of a weak electrolyte.

If $c-x$ is the total concentration of AB and x is the concentration of A (or B), then the rate equation for the above process may be expressed as:

$$\frac{dA}{dt}=k_1(c-x)-k_{-1}x^2 \qquad (3.2)$$

assuming steady state conditions, i.e. $\frac{dA}{dt}=0$.

$$k_1(c-x)=k_{-1}x^2 \qquad (3.3)$$

Further, if we represent deviations from equilibrium (assumed to be small) as $\alpha=x-x_{eq}$ then we may write equation (3.2) as(*166*):

$$\frac{d\alpha}{dt}=-k_1\alpha-k_{-1}\alpha^2-2k_{-1}x_{eq}\alpha \qquad (3.4)$$

If we linearize (3.3) by ignoring all alpha squared terms, then:

$$\frac{d\alpha}{\alpha}=-(k_1+2k_{-1}x_{eq})dt \qquad (3.5)$$

Upon integration of (3.5),we find:

$$\ln\left[\frac{\alpha(t=0)}{\alpha(t)}\right]=(k_1+2k_{-1}x_{eq})t \tag{3.6}$$

The relaxation time, τ, is then defined as the time when(*166*):

$$\frac{\alpha(t=0)}{\alpha(t)}=e \tag{3.7}$$

or

$$\tau=(k_1+2k_{-1}x_{eq})^{-1} \tag{3.8}$$

then from (3.5) and (3.7):

$$\alpha(t)=\alpha(0)e^{\frac{-t}{\tau}} \tag{3.9}$$

substituting α(t) from equation (3.9) into the correlation function (2.4), the power spectrum (2.5) becomes:

$$G(f)=4<\alpha^2(0)>\left[\frac{\tau}{1+(2\pi f)^2\tau^2}\right] \tag{3.10}$$

A plot of G(f) (in units of 10 dB) vs log frequency will exhibit Lorentzian behavior (see Figure 3.1) with the break frequency equal to:

$$f_{break}=\frac{1}{2\pi\tau} \tag{3.11}$$

Therefore, a knowledge of the equilibrium constant $K=\frac{k_1}{k_{-1}}$ and break frequency (3.11) will permit the determination of the rate constants via equation 3.8 .

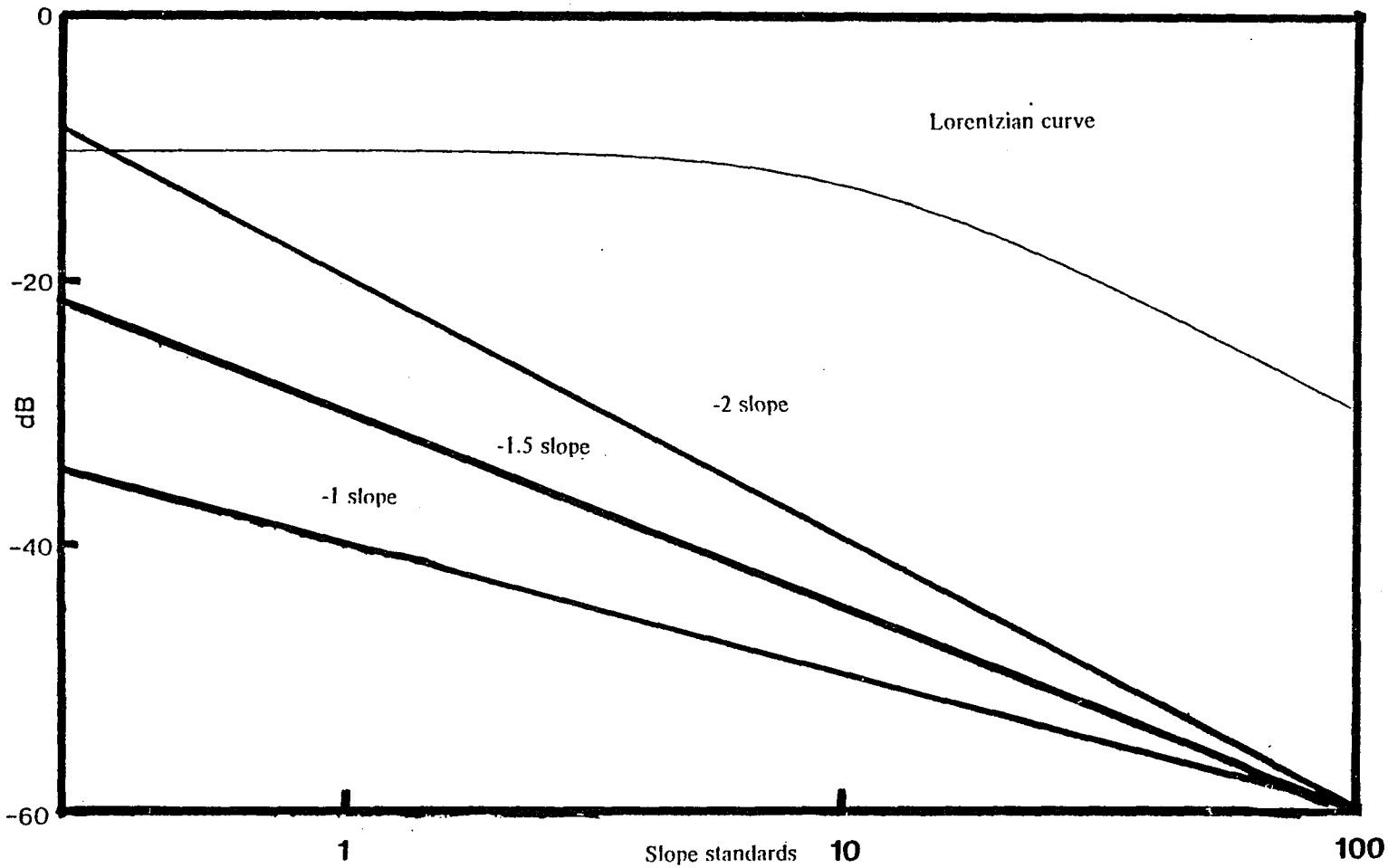
0
-20
-40
-60
dB
Lorentzian curve
-2 slope
-1.5 slope
-1 slope
1
Slope standards
10
100

Figure 3.1

Chapter Four

NOISE SOURCES.

Experimental Requirements for Fluctuation Analysis.

The experimental isolation of the desired fluctuating quantity is not always an easy task. The theory for the measurement of concentration fluctuations is detailed below.

The resistance of a material is a function of its dimensions(*168*).

$$R=\frac{(\rho l)}{A} \tag{4.1}$$

ρ = resistivity of the material
l = length of the material
A = cross-sectional area

and

$$\rho=K^{-1} \tag{4.2}$$

$$=(\sum_i C_i z_i e u_i)^{-1}$$

K = conductivity of the material
C_i = concentration of charge carriers of species i per unit volume
z_i e = absolute value of the charge per i^{th} carrier
u_i = mobility of the i^{th} carrier

from (4.1) and (4.2):

$$R=(\sum_i C_i z_i e u_i)^{-1}(\frac{l}{A}) \tag{4.3}$$

Or, to the approximation that $u_i=u$ =constant, $z_i=z$ =constant,

$$R \propto (\sum_i C_i)^{-1} \tag{4.4}$$

This means that if we measure the fluctuations in R, we will then know how the concentration fluctuates. Furthermore, from Ohm's law we know that:

$$I=\frac{V}{R} \tag{4.5}$$

If we clamp the current I (or the voltage V), R may be determined by measuring V (or I). The voltage autocorrelation function at fixed current may then be written as

$$C(T)=<\delta V(0)\delta V(T)> \tag{4.6}$$

$$=I^2_{clamped}<\delta R(0)\delta R(T)>$$

It is advantageous to measure voltage noise, as opposed to current noise, because current noise folds in the velocity of the carriers.

The magnitute of the concentration fluctuations ($\frac{weight}{volume}$) is given by(*32*):

$$\frac{\delta C}{\bar{C}} \tag{4.7}$$

and is related to the fluctuations in the number of molecules by:

$$\overline{\left[\frac{\delta N}{\bar{N}}\right]^2}=\overline{\left[\frac{\delta C}{\bar{C}}\right]^2} \tag{4.8}$$

$$=\frac{1}{\bar{N}}$$

Where,

N = total number of molecules

and the bars indicate time or ensemble averages.

If the fluctuations in magnitude of a particular extensive variable are small it may be experimentally difficult to measure the fluctuations. To improve the

signal to noise ratio, the relative size of the fluctations (4.7) may be maximized by minimizing the number of charge carriers (4.8). This may be done by using a very small volume of material, for example, a solution contained in a microscopic pore.

In order to measure chemical reaction noise it is further necessary that:

$$G(f)_{experimental} > 4kTR\delta f \tag{4.9}$$

i.e. experimental (excess) noise must be greater than thermal noise. Aside from chemical relaxation noise, the experimental noise may include noise from other sources (et. alia. diffusion, flow). By selecting appropriate dimensions of the volume under study, it may be possible to eliminate certain undesirable noise sources (e.g. diffusion). Note: A and l may be varied, yet keeping R within required limits. In this work, this was done by varying the material used as a pore(*170*); for example, hand drawn glass capillaries of varied diameter and length, Nuclepore® membranes, fritted glass disks (of various coarseness) ground to various thicknesses, or a pore in a ruby. The Nuclepore® membranes have multiple pathways which are parallel and of the same length, while the glass frits have multiple pathways of various lengths and tortuosities.

Chapter Five

INDUCED MASS FLOW DETERMINATION.

A knowledge of mass flow (J_M) through a pore induced by an applied current (I) is required for the evaluation of the noise spectra obtained in this work. Irreversible thermodynamics can be used to determine the interaction of these two (i.e. J_M and I) or, for that matter, any two or more coupled processes within a steady state system. The relationships between the coupled processes may be derived from Onsager's work(*171,172*), which states that the forces and fluxes within a dynamic system may be chosen to fit:

$$\frac{d_{irrev}S}{dT}=\sum_i J_i X_i \qquad (5.1)$$

where,

$\frac{d_{irrev}S}{dT}$ = rate of entropy production due to irreversible processes within the system

J_i = flux of i^{th} irreversible process

X_i = conjugate force of J_i

The conjugate forces X may be expressed as the gradients of generalized potentials. Equation (5.1) linearly relates each flux present to each force present. If L_{ik} is the phenomenonological coefficient relating the k^{th} force to the i^{th} flux, then the form of the i^{th} flux is expressed as :

$$J_i=\sum_i L_{ik} X_k \qquad (5.2)$$

Onsager has shown under general conditions, that by a proper choice of fluxes and forces the relation

$$L_{ik}=L_{ki} \qquad (5.3)$$

will always hold. Equation (5.3) is referred to as the "Onsager Reciprocal Relation". Onsager's derivation assumes that the principle of microscopic reversibility holds and that the conditions are close to equilibrium. Onsager's reciprocal relation has been found to be valid under a wide variety of conditions departing significantly from equilibrium.

In the specific situation of a porous diaphragm (or a microscopic pore in a ruby) separating two reservoirs of liquid, with an electrical pathway connecting the two reservoirs, the interrelationships between mass flow and electrical flow for the system are expressed as (using equation (5.2):

$$J_M = L_{11}\Delta P + L_{12}E \tag{5.4a}$$

$$I = L_{21}\Delta P + L_{22}E \tag{5.4b}$$

ΔP = pressure head between the reservoirs

E = applied e.m.f.

Experimentally, the coupling coefficient (L_{21}) for expressing values of mass flow in terms of electric field was obtained by varying the pressure head between the two reservoirs and recording the induced current at zero potential. In other words, if $E=0$, then from equation (5.4b):

$$I = L_{21}\Delta P \tag{5.5}$$

and

$$L_{21} = \frac{I}{\Delta P} \quad AN^{-1}m^2 \tag{5.6}$$

During the recording of noise spectra the pressure head was zero, $\Delta P=0$, so that from equation (5.4a):

$$J_M = L_{12}E \tag{5.7}$$

and using equation (5.3) and the coupling coefficient derived from equation (5.6),

$$J_M = \frac{IE}{\Delta P} \quad m^3 sec^{-1} \tag{5.8}$$

which is the relationship describing the mass flow through the pore induced by an applied current.

Chapter Six

EXPERIMENTAL METHODS.

A) NOISE MEASURING APPARATUS

Figure 6.1 is an overall representation of the experimental configuration used to measure voltage noise. Several cells were used in the course of this work; however, they are all conceptually similar. Two aqueous compartments are connected to each other via a noise source, for example, a microscopic pore in a ruby.

The two outer electrodes provide a current from a battery pack via a swamping resistor (Figure 6.2), generally 4.5 MΩ in this work. If the value of the resistor is much greater than that of the cell resistance, the circuit current will be determined by the resistor. The battery pack consists of several dry cells wired together in series. The positive terminal of each battery has a pin-tip socket soldered to it. The voltage is selected by plugging a pin-tip plug into one of these sockets. An additional socket, soldered to the swamping resistor, was used to connect the two outer electrodes to each other (via the swamping resistor) during the recording of system background spectra (i.e. no current applied to the cell). This method of varying applied current was chosen to avoid the use of mechanical switches, which are inherently noisy.

The inner electrode pair serves to sense the voltage fluctuations due to the noise source. One electrode runs via a shorting plug to ground. The shorting plug is replaced with a white noise source during system bandwidth response measurements. The other electrode runs to the input of a two stage preamplifier (Figure 6.3), total gain 60 dB.

The preamplifier consisted of 2 Teledyne - Philbrick model 1321

operational amplifiers connected in series. The TP1321s were selected from our own stock for the lowest output noise with the amplifier input grounded. The first stage was AC coupled through a high pass RC filter ($R = 4\ M\Omega$, $C = 0.1\ \mu F$, giving a 3dB down frequency of 0.4 Hz) and was used as a voltage follower with 40 dB gain. The second stage had 20 dB gain and was DC coupled to the first amplifier. Both TP1321s and their supporting circuitry were mounted on a fiberglass breadboard and inserted, with their power supply, into a 7.5 cm by 8.0 cm by 10 cm aluminum box. The TP1321s were powered by two 12.6 volt mercury cells (Mallory Purcell TR289); the mercury cell voltages were measured before each day's runs.

The cell, preamplifier, and battery supplies were all enclosed in a magnetically shielded (two layers of annealed iron shielding; Magnashield S ---- G.L. Industries; Westvale, N.J.) 18.5 cm by 25.0 cm by 32.0 cm aluminum box. The box had two hinged doors to provide access.

The output of the preamplifier was amplified with a Hewlett-Packard model 400F AC voltmeter/amplifier, with a low frequency cut off of approximately 10 Hz (3 dB down); this set the low frequency limit of the system. The high frequency limit was set by the preamplifiers at approximately 30 kHz.

The output of the HP400F was connected to the input of a Tektronix D11 oscilloscope, equipped with a 5A23N amplifier plug-in, and to a Nicolet Scientific Model 444a Ubiquitous Fast Fourier Transform (FFT) spectrum analyzer.

The Nicolet analyzer had an input sensitivity range of 50 dB, with an additional 30 dB of gain available internally. The analyzer has a frequency resolution of 400 points on each of its frequency ranges. All spectra recorded were subject to the following three conditions: One, each was the average of 256 statistically independent FFT spectra (512 averages setting on the analyzer). Two, the display annotation and the internally generated graticle were not displayed when spectra were taken. This resulted in shorter acquisition time for each spectrum average, as the analyzer's cpu did not have to spend time updating the analyzer display. Three, the weighting window switch was set to auto.

Before and after taking spectra at each concentration, the potential and resistance between the sensing electrodes was measured. The current in the cell power supply circuit was measured at each applied voltage.

Before recording any spectra, the signal originating from the cell was observed on the Tektronix oscilloscope and on the time display of the Nicolet analyzer. The amplification setting of the HP400F and the input sensitivity switch of the Nicolet analyzer were chosen in such a manner as to maximize the noise signal presented to the FFT analyzer, without saturating the FFT analyzer input amplifiers. The HP400F amplification ranges were -50 dB to +80 dB, in increments of 10 dB; ranges -20 dB to +50 dB were typically used. During the period of time in which the spectra were acquired, the oscilloscope was monitored to insure that the noise pattern was essentially the same. In addition to measuring the noise spectrum of the signal provided to its input, the FFT analyzer computes the total RMS voltage of the spectrum.

The frequency response of the system was determined by removing the shorting plug and replacing it with a coaxial cable leading to a General Radio 1390B white noise generator. The white noise spectrum, as modified by the system impedance, was then recorded in the same manner as previously, except that the sensitivity of the HP400F amplifier was typically decreased by 20 dB. The change in the sensitivity setting insured that the white noise injected into the system overwhelmed the noise due to the chemical relaxation. Essentially, no difference was found between current on and current off results (unless cell noise with current on was very large at low frequencies, thus contributing measurable excess noise) so that the impedance was independent of current. Correction for impedance in the 20 Hz to 20 kHz range was very small.

Spectra were taken under four possible electrical conditions: 1) current on; 2) current off -- i.e. system background; 3) current on + white noise injected into the system; 4) current off + white noise injected into the system. Spectra were typically recorded on the 1 -, 10 - and 100 - thousand Hz frequency ranges for each set of experimental conditions (e.g. concentration, temperature).

Spectra were recorded for storage by using the analog output of the Nicolet analyzer to plot the data with a Varian F80A X-Y recorder (set for a 6 inch (power - dB) by 10 inch (log frequency) plot) or by transmitting the data

directly to a DEC MINC-11 minicomputer for storage on a "floppy" disk. Five categories of plots were recorded for storage: i) cell current on; ii) cell current off; iii) subtracted[1]; iv) system frequency response with the cell current on; and v) system frequency response with the cell current off.

An Ealing (model 224493) air piston table was used to isolate the cell from building (9 Hz) and other vibrations. The Ealing table was modified by placing lead ingots, having a total weight of 300 pounds, topped by a half-inch thick virgin rubber mat, between the steel support plate (33.0 inch long by 20.25 inch wide by 0.75 inch thick) and the honeycomb construction optical table top. It was found convenient to support the air pistons with nitrogen gas from a tank, rather than air. The air table was leveled by the placement of brass weights at suitable points on the optical table top. The unmodified table is rated, by its manufacturer, to attenuate vibrations above 4 Hz.

Secondary vibration-isolation precautions taken included: placing the shielded box, which contained the cell and an 0.75 inch aluminum baseplate, onto a 0.5 inch thick virgin rubber mat. The mat in turn was placed on a 12 inch long by 12 inch wide by 0.75 inch thick aluminum plate, which in turn was supported by three 3.0 inch diameter brass pistons arranged in triangular fashion. The piston chambers contained a compressible plastic medium. The pistons in turn were supported by a C.R.C. vibration-isolation platform, which is a 22 inch long by 18 inch by 2.5 inch composite slab. The slab in turn rested on the Ealing air table top .

---

1 The Nicolet analyzer has the ability to perform the operations of addition, subtraction, multiplication and division of two different spectra stored in its memory. The resultant spectrum is available at any one of its outputs. In these experiments, subtracted is current on minus current off.

B) DATA STORAGE.

All spectra acquired were stored as files on eight inch diameter " floppy " disks. The files were of two forms: a) digitized files and b) Nicolet ASCII files.

i) Digitized Data Link.

A digitized file was produced by placing one of the Varian F80A X-Y plots onto a Summagraphics Bitpad and tracing the curve with the Bitpad's cursor. The Bitpad generates a coordinate pair (resolution 0.005 inches) representative of the cursor location on the Bitpad's active surface. The optimum data transfer rate from the Bitpad to the MINC-11 was 9600 Baud at 20 coordinate conversion pairs per second. This conversion limitation was set by the software " overhead " of the MINC-11. Two hundred coordinate pairs were typically used to reproduce a spectrum. The fidelity of the data transfer was checked by directing, under program control (see appendix A for data transfer program), digitized files to a digital plotter (Hewlett-Packard 7202A graphic plotter). The HP-plots were then superimposed, on top of a light box, over their source analog plots. The superimposed plots showed very good agreement (± 1 *mm*) with each other despite the following two errors that were introduced in the digitizing process: i) 200 points at equal intervals, rather than 400 points spaced logarithmically, were used to represent the spectrum; and ii) operator hand jitter and parallax error that occurred while moving the cursor across the analog plot.

ii) Direct Data Link

A RS-232c link between the Nicolet analyzer and the MINC-11 was implemented during the latter portion of the experimental work. The Nicolet analyzer transmits, on request, ASCII code containing information to reconstruct a 400 point noise spectrum plus details of the analyzer front panel settings. As a precaution, spectra were also recorded on the analog plotter.

C) ANALYSIS OF NOISE SPECTRA.

A program (appendix B) was used to correct spectra for frequency response. This involves subtracting the appropriate white noise spectrum from a "subtracted" spectrum on a point by point basis. Corrected spectra were plotted on the digital plotter and compared, using a light box, with standard spectra (lines of known slope and a Lorentzian).

The program (appendix B) permitted the determination of RMS voltages between specified frequency limits.

D) EXPERIMENTAL CELLS.

i) Cell used for soy lecithin vesicles and salt solutions.

The cell is illustrated in Figure 6.4 . Total volume is approximately six ml.

The upper and lower compartments of the cell are separated by a 250 μm thick ruby containing an aperture. The appearance of the hole (Figure 6.5) was determined from scanning electron micrographs, taken at the American Museum of Natural History, N.Y.. The aperture is round and has a diameter of 10 μm ($\pm$10%) at one end. The other end is elliptical with a major axis of 150 μm ($\pm$10%) and a minor axis of 100 μm ($\pm$10%). The ruby was sealed into glass at its circumference with its narrower opening facing upwards. The aperture was produced with a laser pulse by Precision Aperture -- Ft. Wayne, Ind.

The electron micrographs were taken by mounting the ruby on an electron beam target with Scotch® Brand tape and setting the electron microscope to 2 kV. The ruby was not sputtered with gold, as this would have destroyed the insulating quality of the ruby. The magnification values are $\pm$10 percent.

For flow studies the upper glass piece, which contains the ruby sealed into glass, was equipped with a side arm terminating in a ground glass ball joint (Figure 6.6). The calibrated barrel of a glass pipet Pyrex® #7060 - 10in1/10ml) plus a reservoir was then connected via the ball joint, making it possible to determine the pressure head from the pipet reading.

Ag | AgCl on platinum electrodes were used.

ii) Cell used for NaCl studies.

The cell is illustrated in Figure 6.7 and was made by sealing a ruby containing an aperture between two 7/15 Pyrex® joints. Total volume of the cell was 0.6 ml. The ruby was similiar to that described in part A of this section. However, the ruby in this cell was used horizontally rather than vertically.

Ag | AgCl on platinum electrodes were used.

E) FLOW STUDIES.

Flow studies were conducted by using the large cell as illustrated in Figure 6.6. A potentiometer (Rubicon Instruments Model 2704-G; Southhampton, Pa.) (via a 9.2 MΩ resistor) and a picoammeter (Keithley Model 414S; Cleveland Ohio.) were connected in parallel to the sensing electrodes of the cell (see Figure 6.8). The potentiometer and resistor were used as a variable current source to oppose the current generated in the cell. The picoammeter was used as a null meter to determine the current at which the potentiometer balanced the cell current. Values of opposing current and volume of solution were recorded.

Interelectrode DC voltages of the order of hundreds of microvolts could not be eliminated, so that the slopes of the plots of pressure head versus current were used to determine the electrokinetic coupling coefficient.

F) MATERIALS PREPARATION.

i) Liposome preparation.

Vesicles were prepared from soy lecithin (Sigma type 11-S ; commercial grade). Suspensions of 10 mg/ml lecithin in 0.149 M KCl were used. Thin-layer chromatography(*173*) of samples of the lecithin showed 3 - 5 % oxidation products. Weighed quantities of soy lecithin were added to a 12 ml centrifuge tube; 0.149 M KCl was then added. The tube was then alternately agitated (with a Vortex Genie ----- model K550G; Scientific Industries, Inc.; Springfield, Mass.) and warmed until all solid material disappeared. The agitation and warming procedure required 20 to 30 minutes and resulted in a cloudy white dispersion. The solution was then transferred to a 50 ml beaker, where it was sonicated (Sonifier Cell Disruptor; model W185; Heat Systems - Ultrasonics, Inc.; Plainview, N.Y.) for 10 minutes at 40 Watts. By this time the solution appeared to be clear; however, the solution scattered light when placed in a laser beam, confirming the presence of a colloid (i.e. the vesicles).

To size the vesicles and to remove dust, the solution was forced through a precleaned 0.3 μm Millipore® filter (Millipore Corp.). The Millipore® filters were precleaned for use by forcing 100 ml (in 3 ml portions) of deionized water through them. This was more than sufficient (*183*) to remove impurities and the residual detergent left in them during their manufacture. Afterwards, 15 ml (in 3 ml portions) of 0.149 M KCl was forced through them. A 3 ml syringe was used to force all solutions through the Millipore® filters.

Gramicidin D was obtained from P. L. Biochemicals (Milwaukee, Wis.). A standard 0.5 mg/ml gramicidin in methanol solution was used throughout. To observe the gramicidin relaxation, especially in liposome suspensions which had aged over one hour, the upper portion of the cell (containing the ruby aperture) was returned to a test tube containing the liposome preparation, which in turn was supported in an ultrasonic cleaner (Cole Parmer Model 8845-3). The ruby and solution were subjected to several minutes of sonication. This last sonication process was also required initially by all solutions to fill the ruby orifice with solution and to remove air bubbles.

The radii of similar vesicles (prepared from the same material by the same method) were also measured by dynamic light scattering(*174*). The radii in all cases were in the 50 - 60 nm range.

ii) Preparation of Ag | AgCl electrodes.

Platinum wires were used as cathodes in a silver plating solution consisting of 104 gms $AgNO_3$, 396 gms K_2CO_3, and 192 gms KCN dissolved in 2 liters of distilled H_2O was run at 5 ma/cm^2 for 20 minutes. The silver coated platinum electrodes were then used as anodes, at a current of $2ma/cm^2$ for 20 minutes, in concentrated HCL.

The Ag | AgCl electrodes were stored in 0.001 M KCL. The connector side of all the electrodes of a particular cell were connected to each other during periods of storage.

Legend for Figure 6.1

Schematic of Noise Measuring Apparatus and Measurement Cell.

A - Cell Partition Containing Noise Source of Interest
B - TP1321 Preamplifiers
C - HP400F Amplifier/Voltmeter
D - FFT Spectrum Analyzer
E - Oscilliscope
F - Battery Pack
G - Thermocouple
H - Keithley DVM, Reference Thermocouple, Ice-Water Reference Bath
I - Analog Plotter
J - Minicomputer
K - Digitizer Tablet
L - Digital Plotter
M - White Noise Generator
N - Shielded Box
R6 - Swamping Resistor

Not Shown:
1) Cell Heater and Piping
2) Shock Mounting

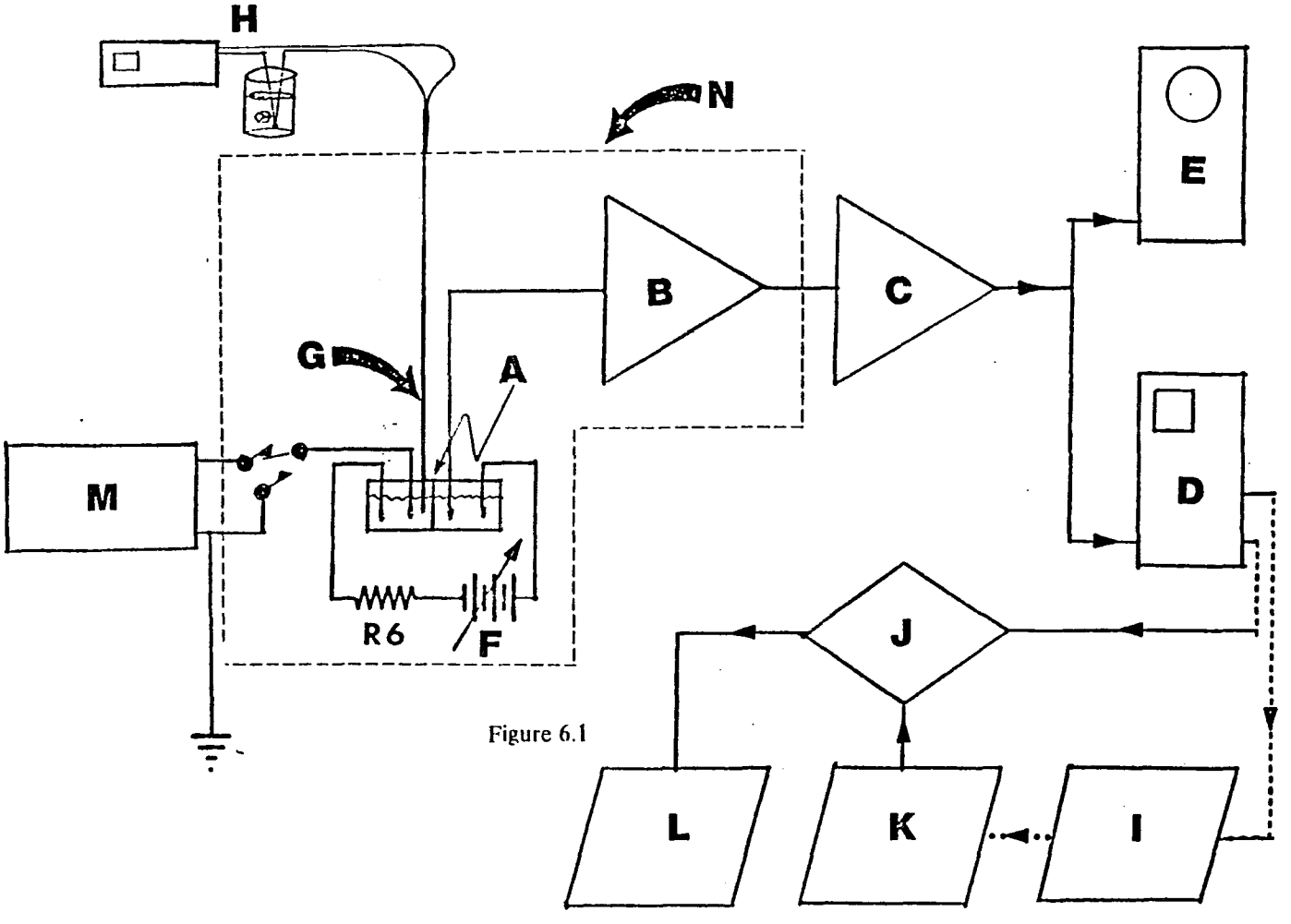

Figure 6.1

Legend for Figure 6.2

Enlarged View of Cell Schematic and Battery Pack.

A - Noise Source
u - Zero Current Socket
v - 22.5 Volt Socket
w - 31.5 volt socket
x - 54.0 Volt Socket
y - 76.5 Volt Socket
z - 99.0 Volt Socket
1 - Sense Electrodes
2 - Voltage Supply Electrodes
r - Pin-tip Plug
s - From Ground or White Noise Generator
t - To Input of TP1321's Preamplifiers
q - Aqueous Solution

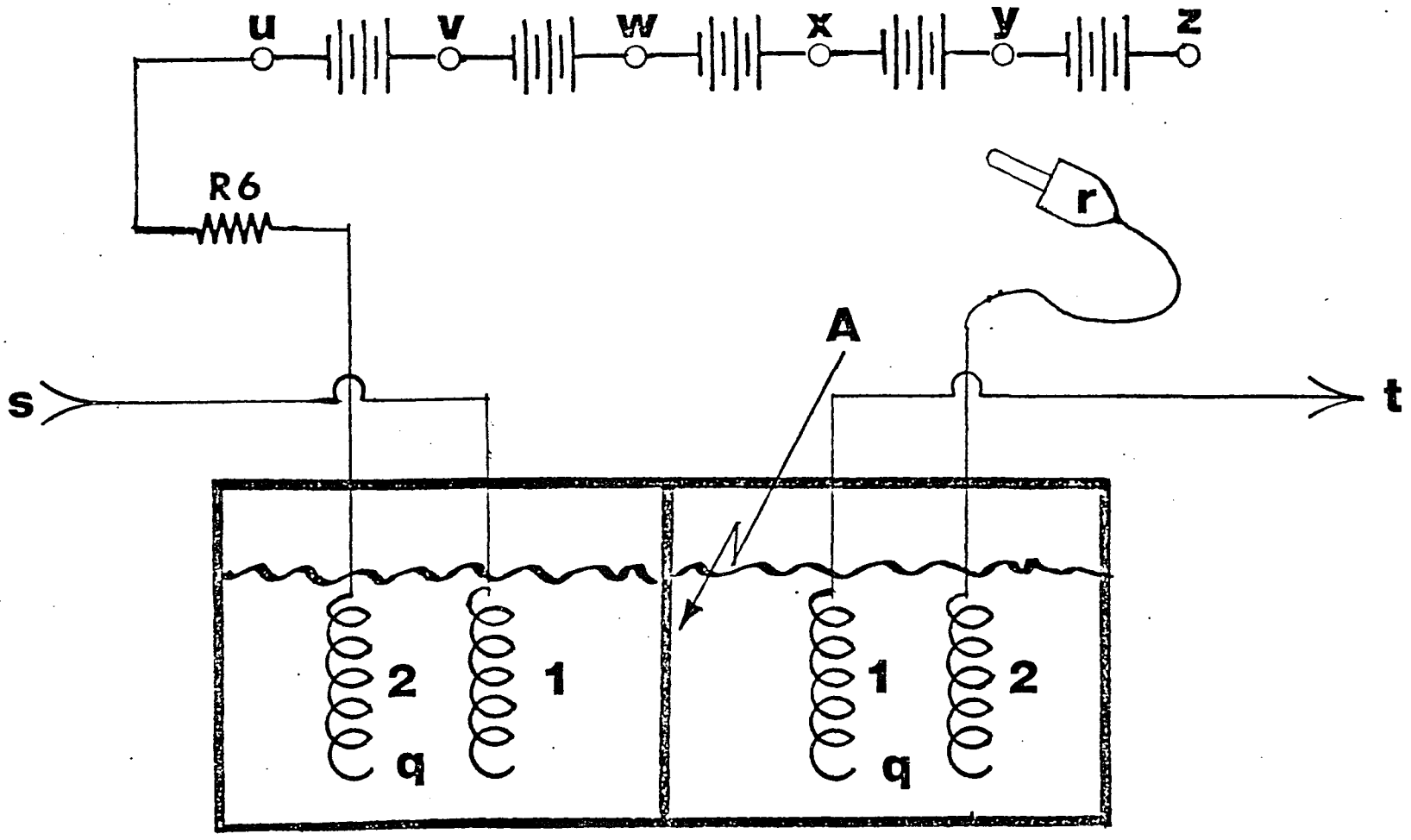

Figure 6.2

Legend for Figure 6.3

Preamplifier

1 - TP1321
2 - TP1321
R1 - 8 MΩ
R2 - 1 MΩ
R3 - 301 kΩ
R4 - 10 kΩ
R5 - 28.7 kΩ
C1 - 0.47 μF
C2 - 10 pF
C3 - 10 pF
t - Input from measurement cell
m - To input of HP400F Amplifier / Voltmeter

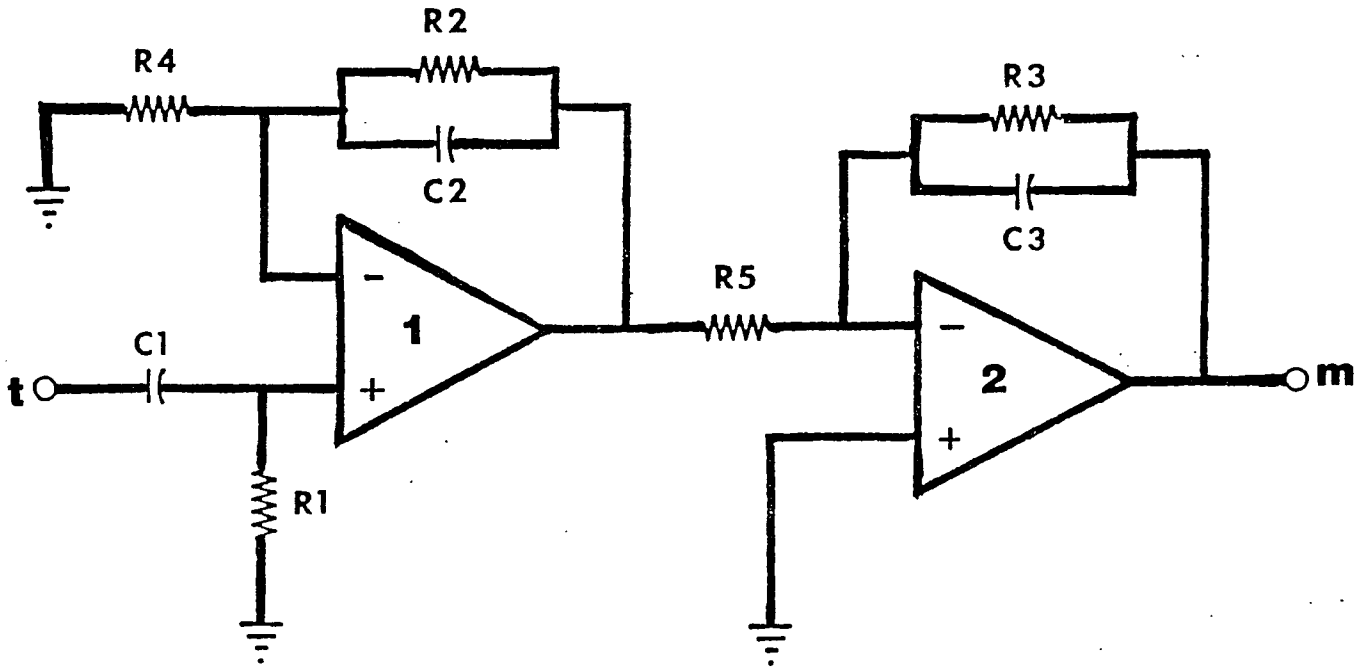

Figure 6.3

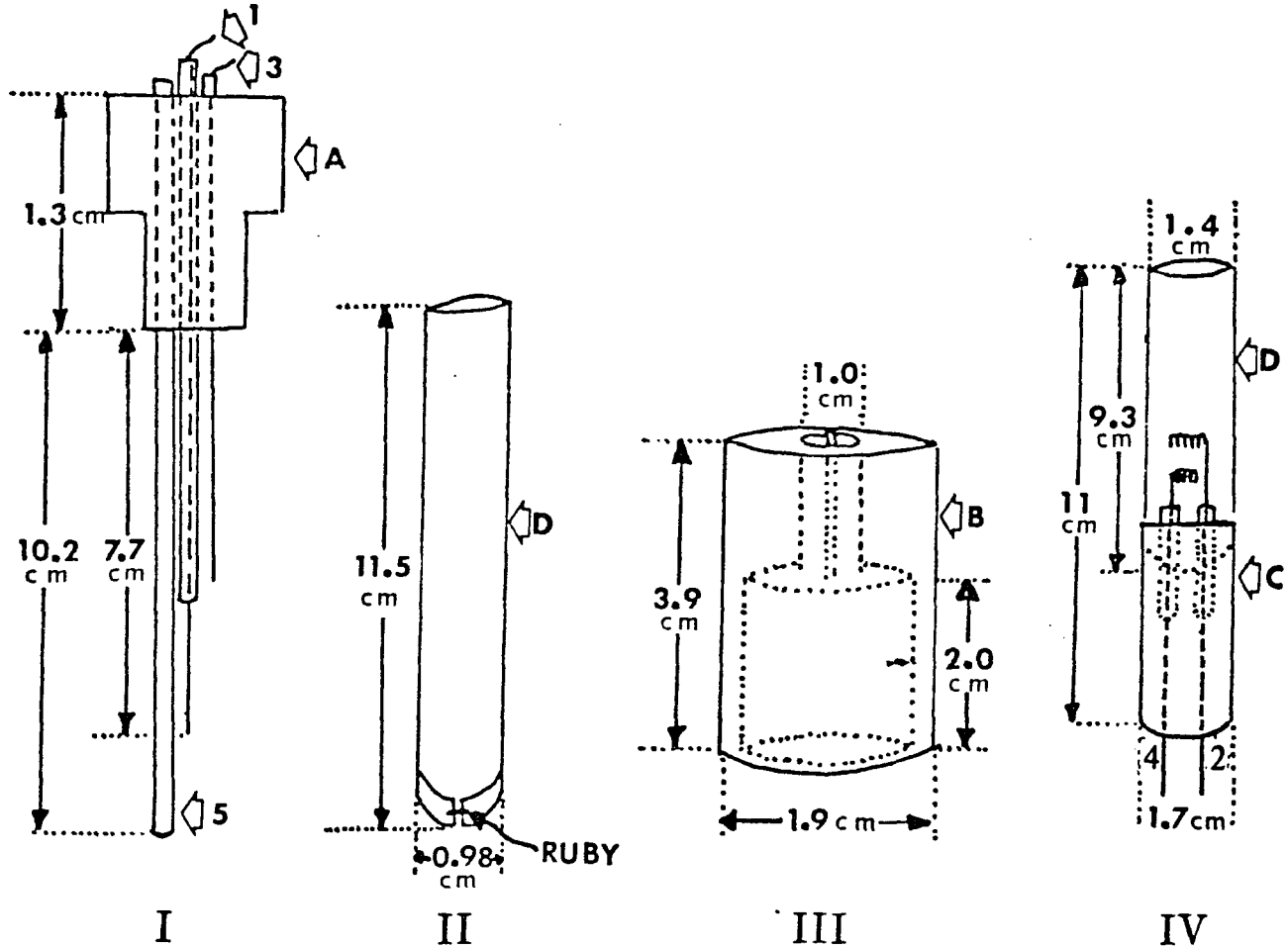

, Larger ruby cell used in measurements. Electrodes are Ag | AgCl: 1. to ground (and/or white noise generator for calibration); 2. to preamplifier; 3. and 4. to voltage supply; and 5. to thermocouple sleeve. A,B Teflon®, C electrodes encased in epoxy and glass jacket, 5, D glass. Assembly I is inserted into Tube II, which is connected to lower section IV via Teflon® coupler III.

Figure 6.4

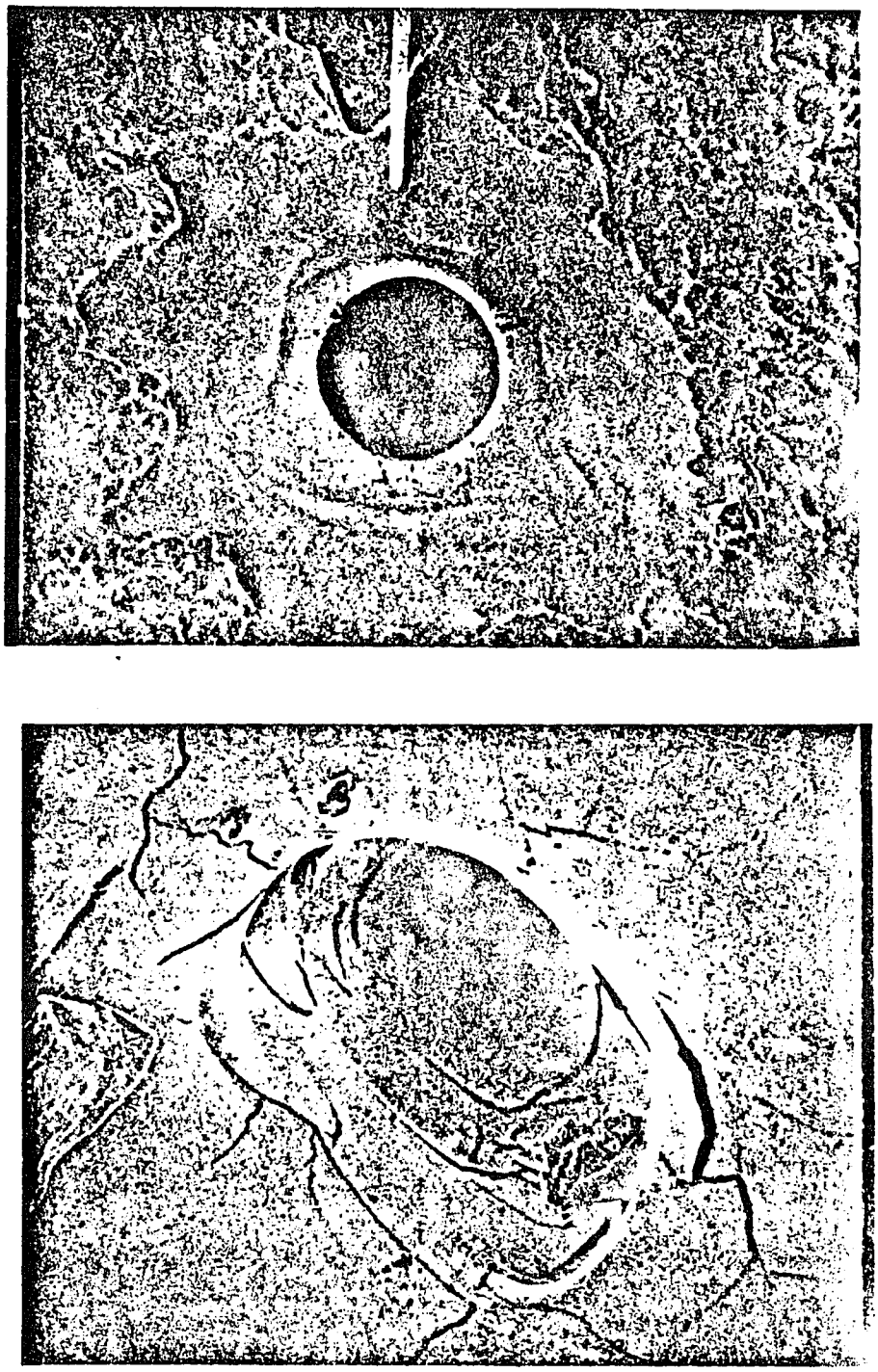

Figure 6.5

Scanning electron micrographs of ruby in larger cell.
(A) Small end (top) of pore x 1800.
(B) Large end (bottom) of pore x 900.

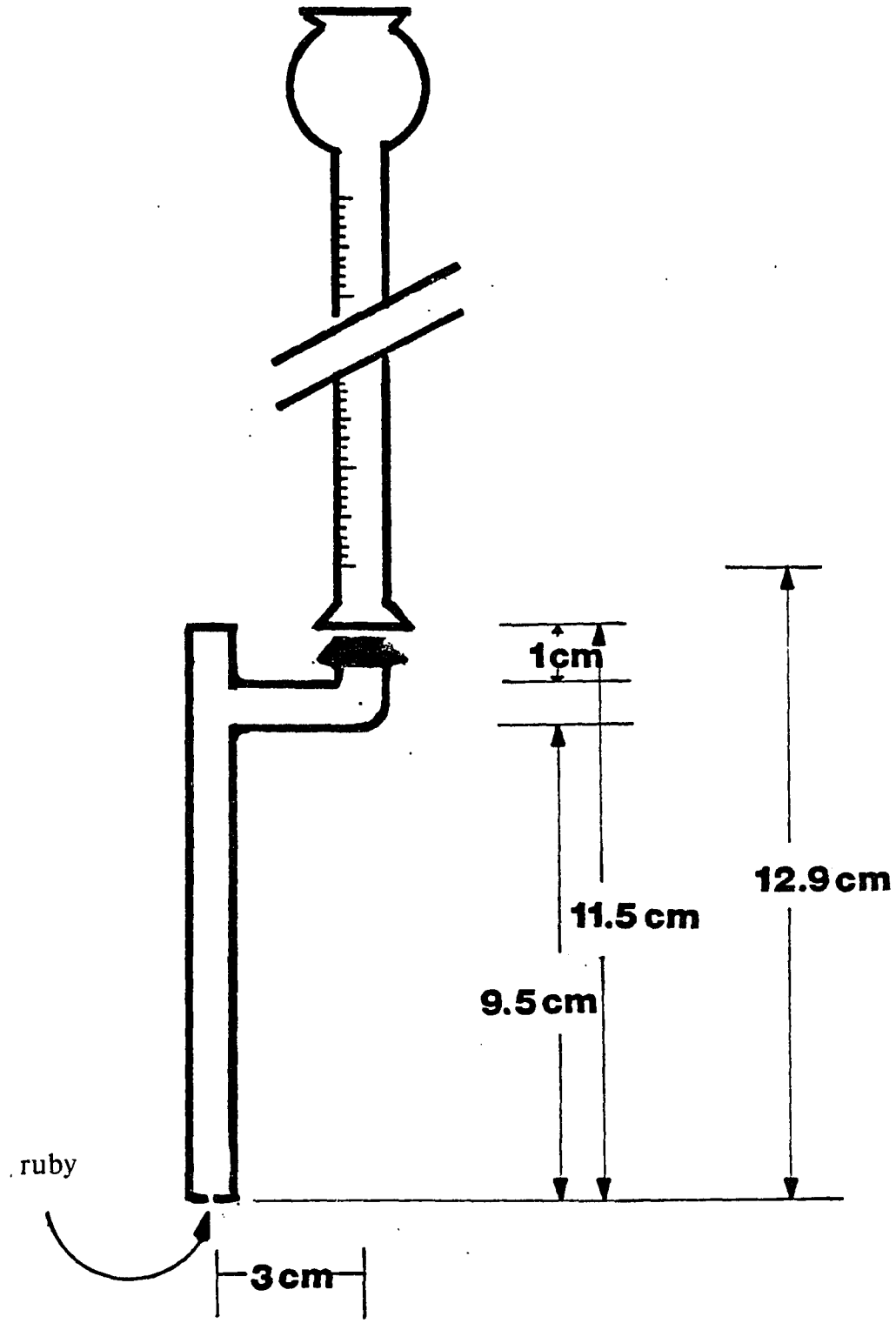

Figure 6.6

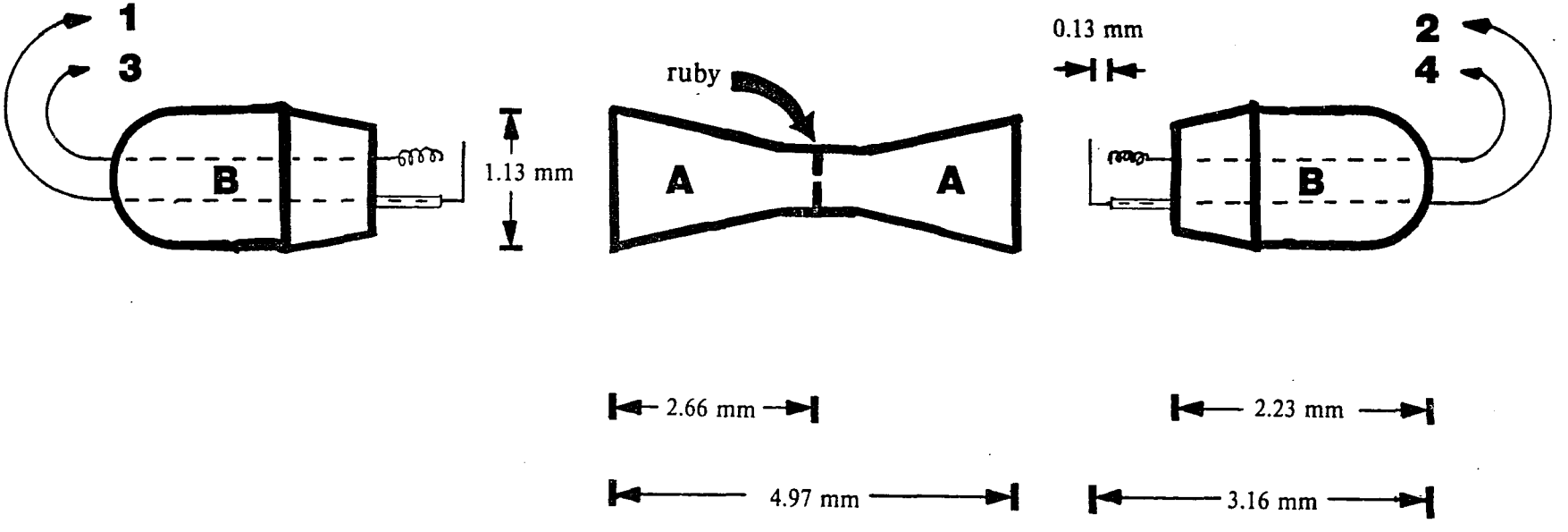

Smaller ruby cell used in measurements. Electrodes are Ag | AgCl: 1. to ground(and/or white noise generator for calibration); 2. to preamplifier; 3. and 4. to voltage supply. A. solution compartment; B. ground glass endpieces (removed from the cell).

Figure 6.7

Legend for Figure 6.8

Schematic of Flow Measurement Circuit.

A - Picoammeter
B - Potentiometer
R7 - Resistance between Inner Electrodes
(i.e. the resistance of
the electrolyte in the pore)
R8 - 9.2 MΩ Resistor

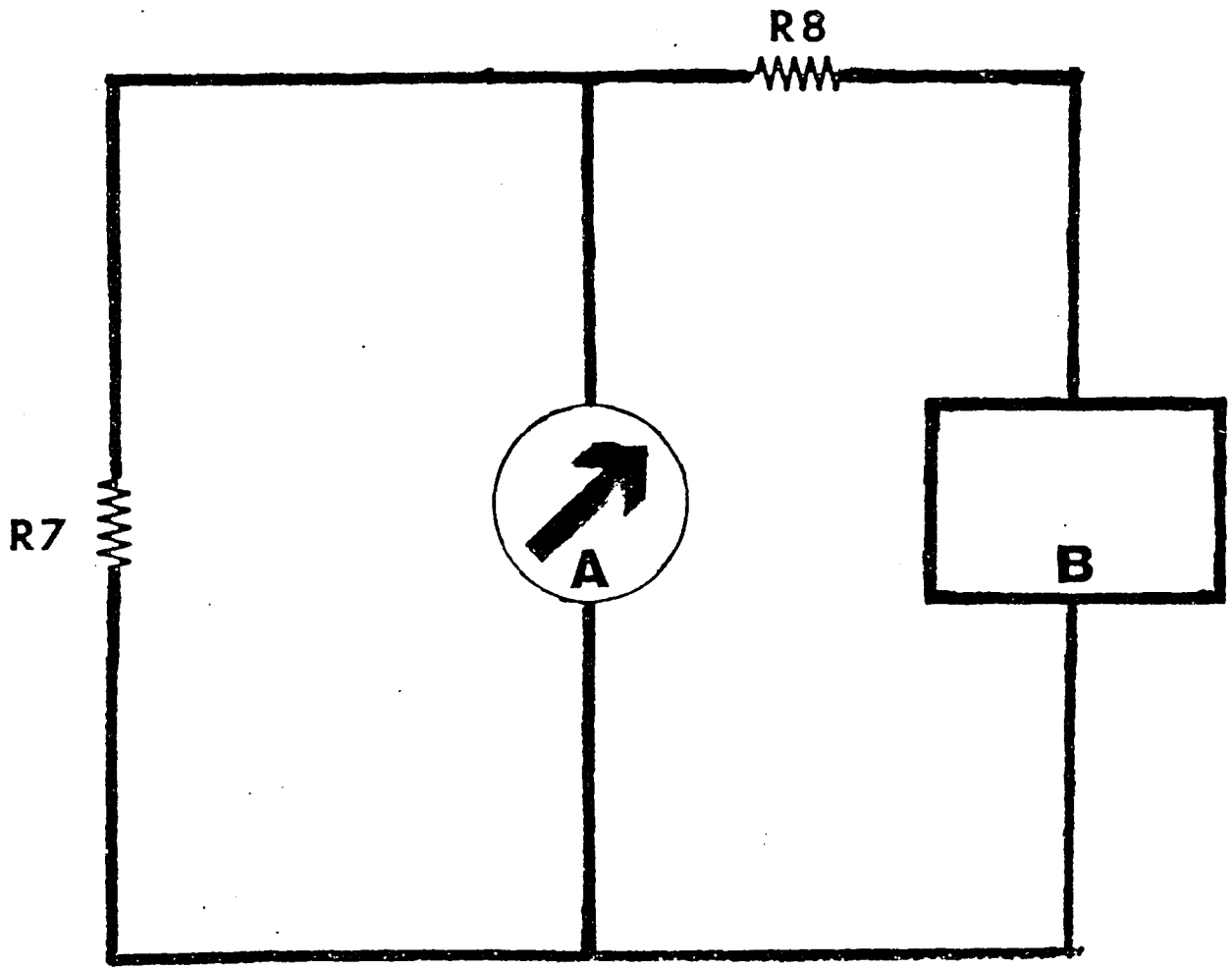

Figure 6.8

Chapter Seven

RESULTS AND DISCUSSION.

A) Results

(i) Vesicles containing Gramicidin: Spectra are shown in Figure 7.1, with upper frequency limit 1 kHz and 10 kHz. Within experimental error, there are two regions of -2 slope on the log-log plot, one of which begins at a frequency below the region measurable with the present apparatus. The first region is attributed to the known gramicidin relaxation; it was absent when gramicidin was not added, and disappeared if the liposomes were left to stand for a period of more than about one hour. It could be regenerated by again placing the suspension in a tube and sonicating in an ultrasonic cleaner.

The second apparent relaxation, at 152±46 Hz (one standard deviation), is attributed to the soy lecithin vesicles; a similiar relaxation was found without gramicidin.

Both relaxations were found, within experimental error, to be independent of the applied current. See Table 7.1

(ii) Vesicles without Gramicidin: Spectra are shown in Figure 7.2 . The approximately 150 Hz apparent relaxation remains (149±45 Hz (one standard deviation) measured on nine 1 kHz spectra). The frequency measurement was made by visual fit of a Lorentzian curve to the measured spectra. As with the spectra on the vesicles containing gramicidin, no current dependence of relaxation time could be observed within the limits of error. See Table 7.2 .

(iii) Solutions of NaCl and of KCl: For NaCl above 0.006 M, and for 0.149 M KCl, the spectra were 1/f in the frequency range 30 Hz to 10 kHz (which were the limits of accurate measurement) for (nominal) currents of 5

μa and 7 μa, and the intensity ratio was 2.14±0.33 (one standard deviation), it was thus approximately proportional to I^2. See Tables 7.3 and 7.4 .

For higher currents and lower concentrations, the spectra were often steeper than 1/f; these are excluded from consideration. See Figure 7.3 for typical KCl Spectra.

(iv) Flow Measurements: One possible source of noise was flow through an orifice due to coupling of electric current to bulk flow. The existence of flow could be indirectly demonstrated. A sidearm was attached to the upper chamber of the cell, as described in chapter 6 (section E), making it possible to impose a pressure head above the ruby. The current was determined to be $1.9 \cdot 10^{-9} \pm 0.3 \cdot 10^{-9}$ (one standard deviation) $A N^{-1} m^2$ for 0.01 M KCl. The flow experiments were originally carried out to correspond to another set of measurements so that a concentration other than 0.149 M KCl was used. Only the fact that the flow exists is used in this discussion; the actual value is thus not critical. The corresponding mass flow for the solution used, which had a resistance of 0.53 MΩ in the pore, (approximately 1/9 th of the 4.5 MΩ resistor which determined the current), and 22.5 volts applied, was approximately 10^{-2} ms^{-1} on the average. At the 10 μm diameter opening, the velocity reaches a maximum of approximately 0.5 ms^{-1}. As discussed below, it does not appear that flow alone determined the measured spectra.

B) Discussion.

i) Liposome Noise.

It is apparent that the capillary fluctuation spectroscopy method can be applied to liposome suspensions. It has proven possible to detect a relaxation which is associated with gramicidin channels; however, because of limits on the low frequency response of the present system caused by the electronics rather than by the method, it was not possible to determine the actual relaxation time. However, this is not a fundamental difficulty.

The origin of the second relaxation, associated with the vesicles alone, is less clear. It is known that two relaxations exist in solutions of micelles, one associated with nucleation and dissolution of a micelle, the other with exchange

of single molecules. The latter is more rapid than the former, but it is still difficult to believe that exchange of a phospholipid molecule could occur in times of the order of 1 m*s*. One possible explanation may involve exchange of impurities such as the oxidation products found in this sample of lecithin. Since the primary purpose of this work is to demonstrate the method, experimental attempts to further define the source of this relaxation have not yet been made. The source of noise being in any case ion concentration fluctuations, the process must involve either adsorption and desorption of ions from the liposome surface, or transport across the liposome membrane. (An ion in the interior of a liposome is electrically shielded from the exterior electrolytic solution and is thereby effectively removed from the population of charge carriers within the electrolytic solution contained within the pore.) While the oxidation products might produce either effect, the presence of hydroxyl or other oxidized groups in the lipid layer makes ion transport the more likely case, especially on a millisecond time scale. Additionally, transport of ions and non-electrolytes through vesicle bilayers has been demonstrated by radioactive labeling(*85*) and other(*176,177*) studies.

ii) Alternate Noise Sources.

(a) Thermal noise: The spectrum measured with no applied current should produce thermal noise. The RMS value of the noise was determined by the FFT Analyzer, with effective noise bandwidth equal to the full scale frequency. For the case of spectra with 10 kHz upper limit, essentially no correction for impedance was required. The cell resistance for 0.149 M KCl, determined experimentally, was 75 kΩ (independent of the presence or absence of liposomes). Predicted thermal noise (equation 1.1) for room temperature, 75 kΩ resistance, and 10 kHz bandwidth is 3.5 μV at input (to preamplifier). Measured values gave 3.63$\pm$0.25 μV (one standard deviation), in satisfactory agreement. The zero current spectra were measured for each spectrum and were subtracted by the analyzer. There was excess noise (above thermal) at zero current below 150 Hz. Analysis in all cases is based on the subtracted spectra.

(b) Diffusion noise: Diffusion noise through a pore in a salt solution (NaCl) has been shown to dominate the spectrum when the membrane is of the order of 10 μm thick(*41*), producing an $f^{-3/2}$ spectrum in the frequency region of interest here. In the same frequency region, the intensity of diffusion noise is inversely proportional to the thickness of the pore, leading to an approximate 14 dB decrease in diffusion noise intensity in the present case, compared with a 10 μm thick membrane.

1/f slopes rather than $f^{-3/2}$ slopes have been observed for KCl in this study. Green(*41*) showed that diffusion may lead to an f^{-1} spectrum, since the actual dependence is $f^{-1/2}$ at "low" frequency and $f^{-3/2}$ at "high" frequency. The cornering frequency, however, is $f_t \approx \frac{D}{\pi L^2}$, where D = diffusion coefficient, L = Thickness of the pore. For the case of the aperture in the ruby, L = 250 μm gives $f_t \approx 5 \cdot 10^{-3}$ Hz. To get the f^{-1} spectrum observed here, a distribution of path lengths down to 250 nm is required. Although the pore is not a perfect cylinder, this distribution is implausible. Both for the reasons of expected intensity and observed spectrum, diffusion appears unlikely to be a major contributor to the measured noise.

(c) Flow: The spectrum which would be produced by flow was calculated as follows: The correlation function for pure flow (no other important transport or relaxation process) may be written immediately as

$$C(\tau) = C_0 (1 - \frac{v\tau}{l}) \quad 0 \leqslant \tau \leqslant \frac{L}{v}$$

$$C(\tau) = 0 \qquad \tau > \frac{L}{v}$$

where v = flow rate, L = thickness of pore, and C_0 = proportionality constant (equal to the RMS value of the fluctuations). To understand this, consider fluctuations in a column of liquid being displaced at uniform velocity. The fraction $1 - \frac{v\tau}{L}$ of the original solution remains in the column at time τ, and is thus completely correlated with the time zero fluctuations; the remainder of the column has been filled from the external solution and thus has no correlation with the time zero fluctuations. The corresponding spectrum, for fixed v, is

$$G(\omega)=\left(\frac{2v}{\pi L\omega^2}\right)\left[1-\cos\left(\frac{L\omega}{v}\right)\right], \qquad (7.2)$$

and is illustrated in Figure 7.4 , upper curves; it bears no resemblance to measured spectra. However, Poiseuille's relation(*178*) requires a parabolic distribution of flow rates, so that the measured spectrum should be an average over a distribution of velocities. Such an averaging process was carried out numerically, by assuming a perfect cylinder, divided into annuli. The velocity of each annulus was taken to be that of the velocity at the average radius of the annulus, and the contribution to the overall spectrum, a spectrum of the form of equation (7.2), was weighted according to the area of the annulus. The results, for division into 10 and 100 annuli, are shown in Figure 7.4 , middle and lower curves. These do not resemble measured spectra; in particular, they produce f^{-2} rather than f^{-1} high frequency spectra, in contrast to the measured spectra, in addition to a set of "steps" including regions steeper than f^{-2}, at lower frequency. On the basis of these slope comparisons, it is concluded that the measured spectra do not arise from pure flow. (The computer program which evaluated equation (2) under the conditions mentioned in the foregoing paragraph may be found in appendix C.)

Aside from understanding what contribution flow may make to the measured noise spectra generated in the ruby, there exists another possible reason for interest in flow in a pore this size; while far too large for a nerve channel, the pore diameter is of the right order of size for a model of the entire axon. It is known that there are two types of mass fluxes along the long axis of the axon(*179*) (i.e. from the cell body towards the synaptic terminals); the fast flow also includes a retrograde component. The fast flow contains glycoproteins, phospholipids and synaptic terminal precursor materials. The fast flow has been associated with the maintenance of the axon's membrane and of the synaptic transmission mechanisms. The retrograde component of the fast flow has been associated with waste disposal and material recycling. The slow flow has been associated with the renewal of the soluble axoplasm and transport of mitochondria. The fast flow is of the order of 400 $\frac{mm}{day}$ (approximately 4.5 $\frac{\mu m}{sec}$) and the slow flow is typically of the order of 1 - 5 $\frac{mm}{day}$ in mammals.

Although the exact mechanisms of mass transport are in dispute, there is no question as to the existence of the two flows. Therefore, there should be an electrokinetic coupling in axon, as in any flow system, to the membrane zeta potential. While the present model does not lead to 1/f noise, possibly a refinement would.

(d) Flow plus diffusion: If laminar flow alone and diffusion alone do not produce the observed spectra (particularly the 1/f spectra), perhaps a combination of the two might. The equation for Poiseuille flow through a cylindrical pore, accompanied by diffusion, is well known. Unfortunately, the equation does not separate and only approximate solutions are known, most of which depend on some type of average over the pore. An attempt to solve an approximate version of this equation (see appendix D for the calculation and its associated computer program) yielded a spectrum far from 1/f. The spectrum was calculated over a limited frequency range using an eigenvalue expansion, as discussed by van Vliet and Fassett(*151*). While the solution is quite approximate, and the results preliminary (in particular, not all combinations of parameters have been tested), it does not now appear that any combination of laminar flow plus diffusion is a likely candidate as a source of 1/f noise, at least for relatively high flow rates.

(e) Turbulence: If neither diffusion nor laminar flow nor a combination of both leads to 1/f noise, it appears that turbulent flow emerges as the best explanation of the data. This has already been suggested in the context of similiar systems by Hooge(*107*), based on an earlier calculation by Handel(*29*). Turbulence may lead to 1/f spectra or to steeper spectra in small volumes in ionic solutions(*38*). Examination of spectra taken at high currents or low concentrations show steep slopes. Given the geometry of the ruby pore (see Figure 6.5), it would not be surprising to find eddy formation. However, the existence of turbulent flow remains to be demonstrated directly.

C) Conclusions and Summary:

A method has been developed for studying the relaxation associated with ion transport in liposome suspensions by studying fluctuations in a small orifice in a ruby. The spectra measured by this method make possible the determination of relaxation times in the 10 ms to 10 μs range, and the long time (low frequency) limit is set only by technical difficulties. The high frequency limit may be raised at higher salt concentrations, but is otherwise more fundamental. The vesicle experiments have been carried out with relatively crude preparations of soy lecithin, but more interesting (highly purified lipids) materials can be used. In the range of salt concentrations used, thermal noise can be corrected for, and diffusion and flow, which would be expected to be the main additional sources of noise, appear not to be important.

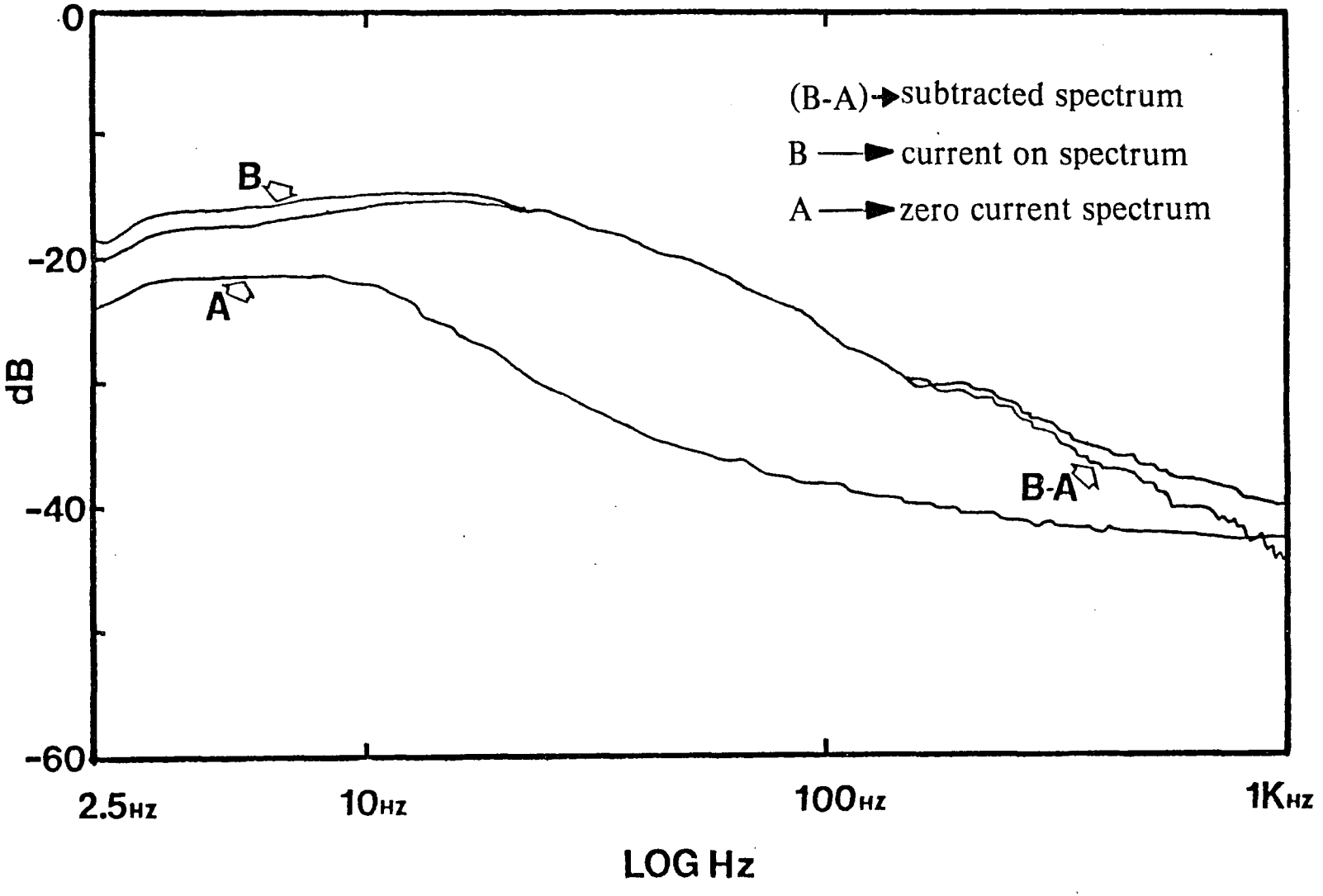
0
-20
-40
-60
dB
(B-A)→subtracted spectrum
B ——► current on spectrum
A ——► zero current spectrum
B
A
B-A
2.5Hz
10Hz
100Hz
1KHz
LOG Hz

Figure 7.1A

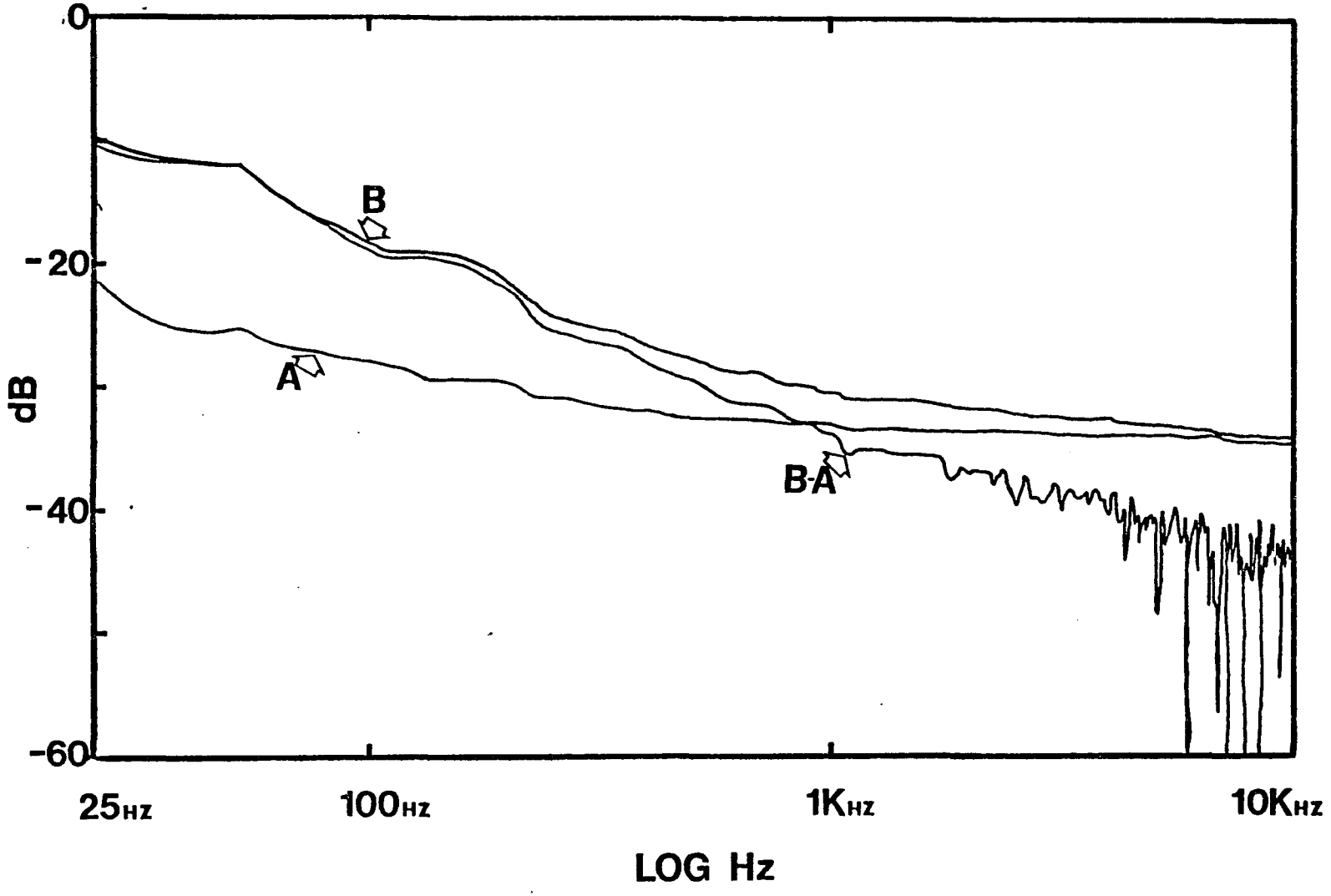

Figure 7.1B

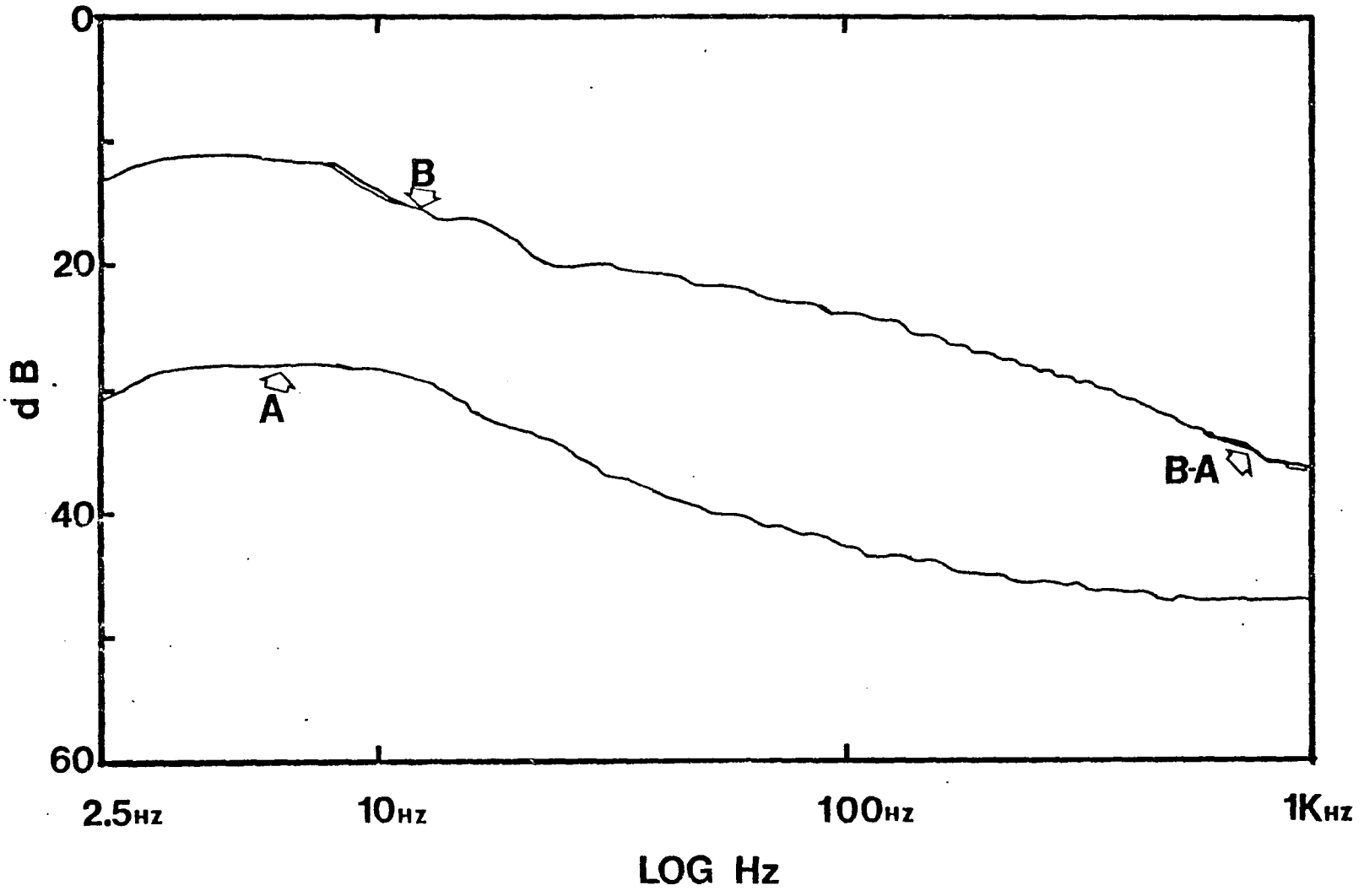

Figure 7.2A

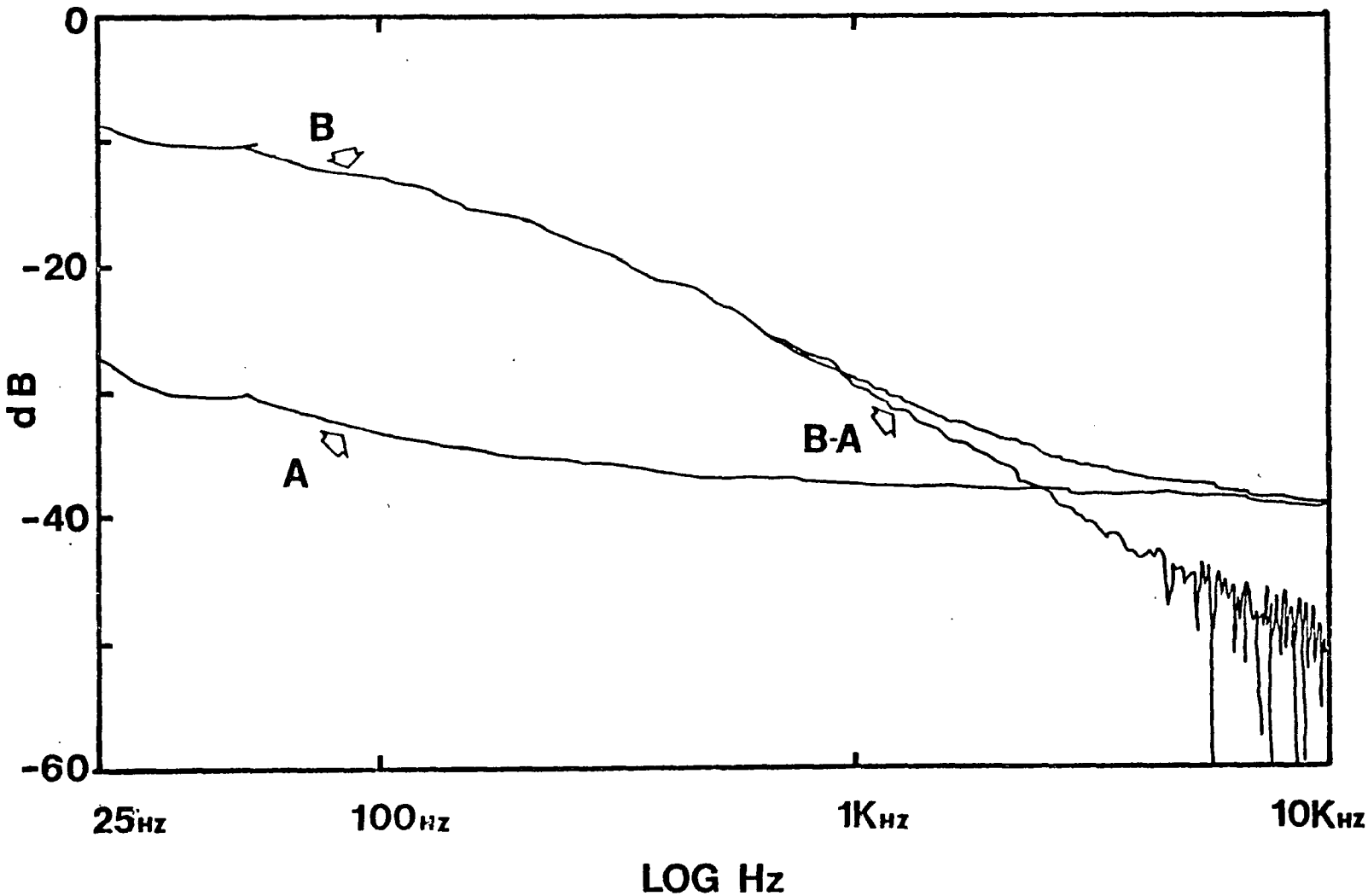

Figure 7.2B

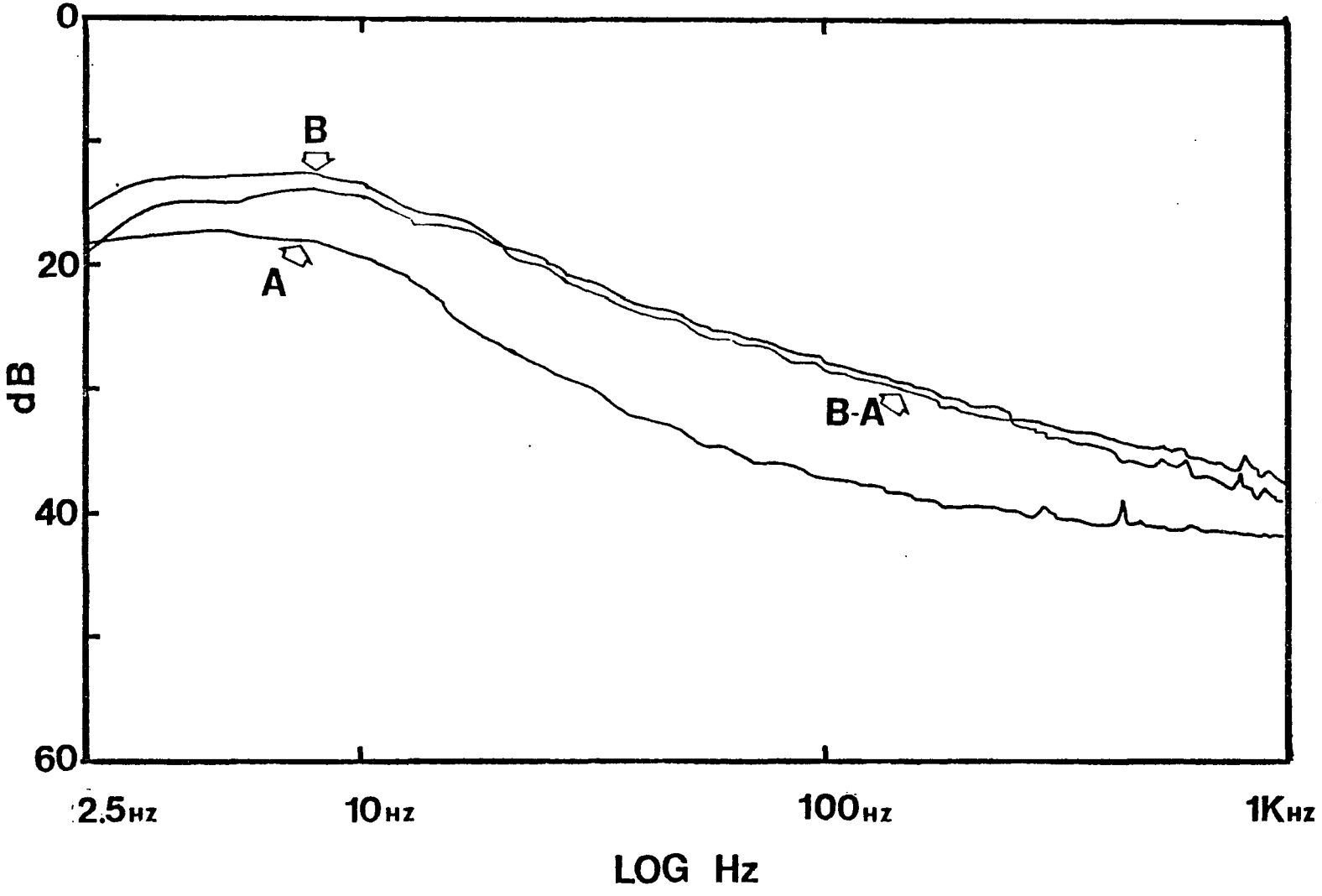

Figure 7.3A

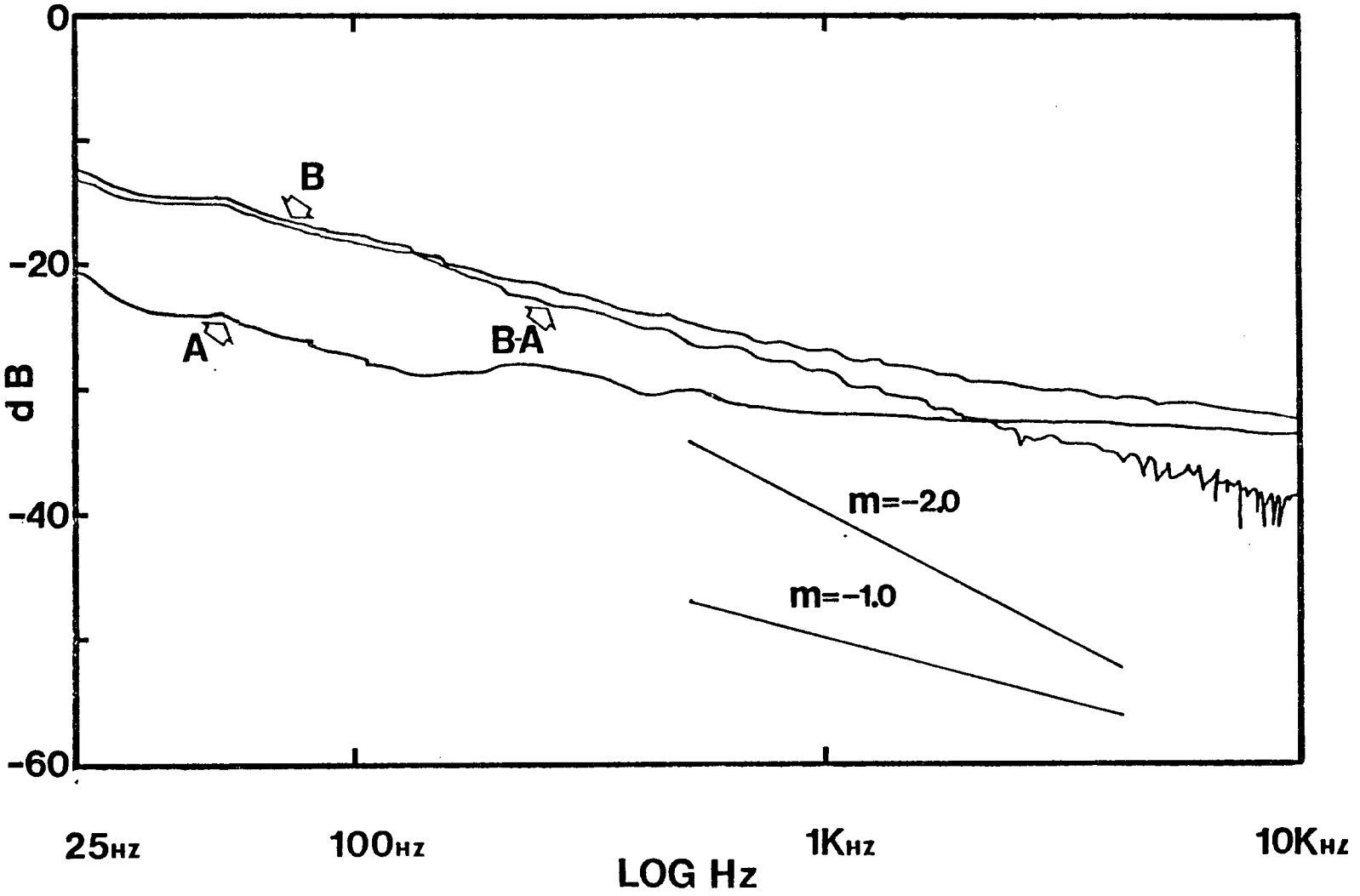

Figure 7.3B

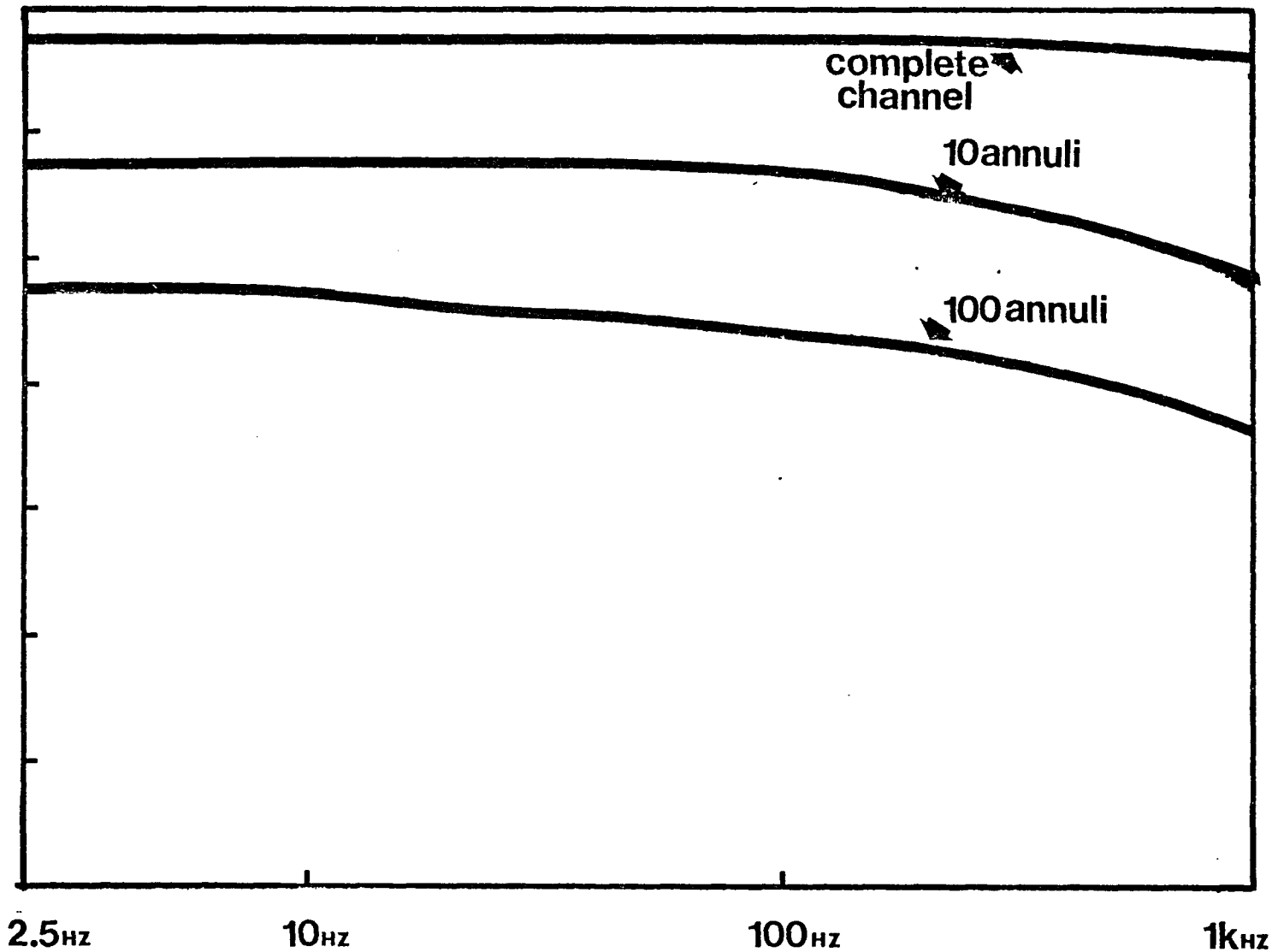

Figure 7.4A

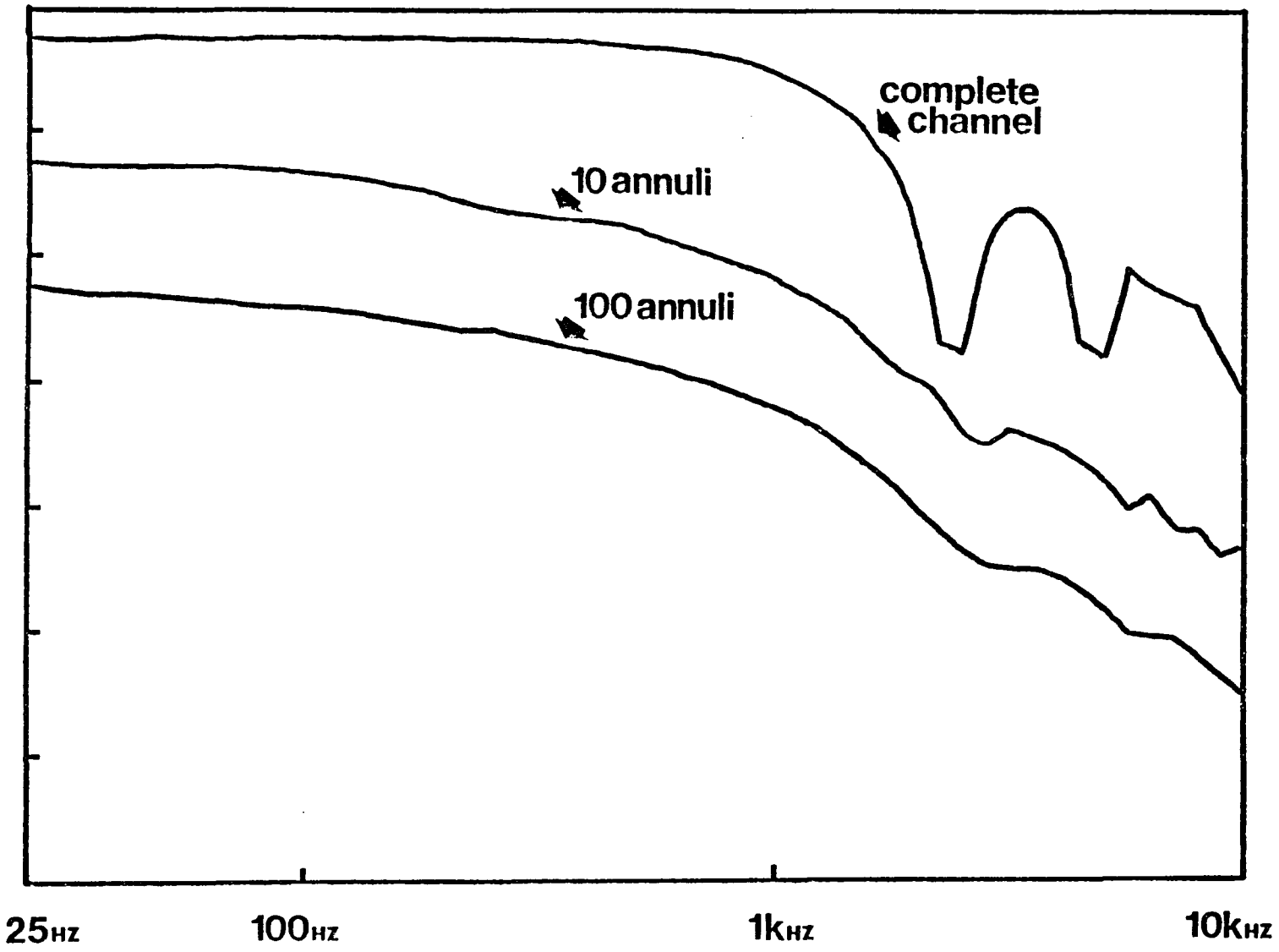
complete
channel
10 annuli
100 annuli
25Hz
100Hz
1kHz
10kHz

Figure 7.4B

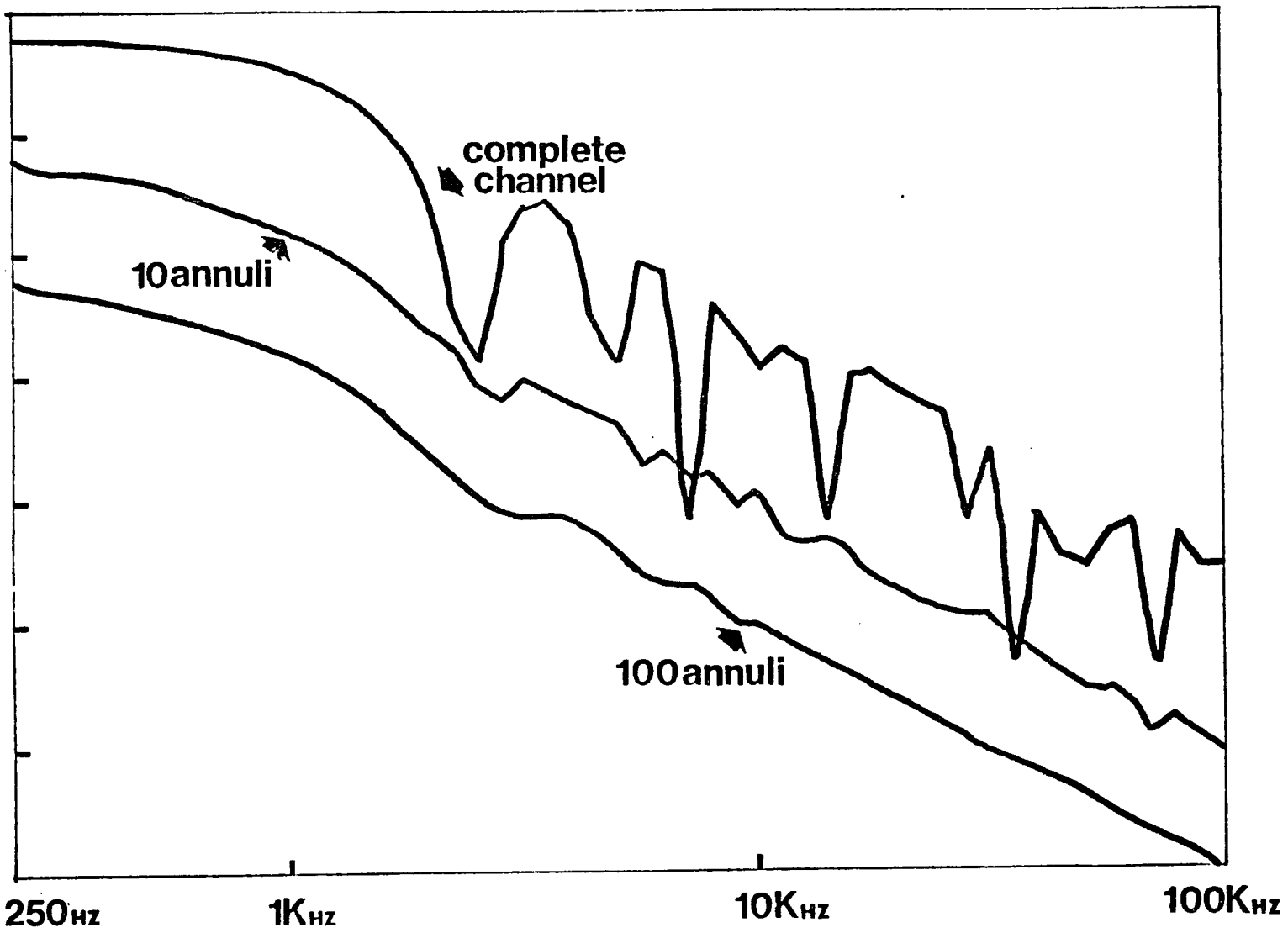
complete
channel
10annuli
100annuli
250HZ
1KHZ
10KHZ
100KHZ

Figure 7.4C

TABLE 7.1

Relaxation Times for Gramicidin Doped Soy Lecithin Vesicles from 1kHz Spectra with Negligible 1/f Correction.

Experiment #	Applied D.C. Volts	Relaxation Time (Hz)
R60	22.5	187
R61	31.5	113
R62	54.0	187
R104	22.5	152
R105	31.5	245
R106	54.0	127
R107	22.5	157
R111	22.5	408
R114	31.5	311
R117	54.0	182
R233	31.5	120
R243	22.5	89
R246	31.5	113

mean value = 152 Hz
standard deviation = 46 Hz
Excluding R114 and R111

mean value = 165 Hz
standard deviation = 63
Excluding R111

TABLE 7.2

Relaxation Times for Soy Lecithin Vesicles from 1kHz Spectra with Negligible 1/f Correction.

Experiment #	Applied D.C. Volts	Relaxation Time (Hz)
R48	22.5	123
R49	31.5	108
R92	22.5	219
R95	31.5	211
R98	54.0	125
R176	22.5	135
R256	22.5	171
R262	54.0	86
R280	22.5	160

mean value = 149 Hz
standard deviation = 45 Hz

TABLE 7.3

NaCl - 1/f Spectra
1 kHz Upper Frequency Range

Experiment Number	Concentration (mM)	D.C. Volts Applied	RMS Voltage† with Current On (mv.)	RMS Voltage† with Current Off (mv.)
M126	6.0	22.5	2.90	3.80
M129	6.0	31.5	4.76	3.80
M132	6.0	54.0	8.92‡	3.98‡
M27	9.5	22.5	1.85	- NA -
M30	9.5	31.5	2.92	3.11
M33	9.5	54.5	13.50	- NA -
M39	16.0	22.5	1.46	2.29
M40	16.0	31.5	2.09	2.42
M45	16.0	54.0	4.98	2.51
M52	22.0	22.5	1.24	2.20
M55	22.0	31.0	1.69	2.27
M58	22.0	54.0	3.42	2.00
M60	22.0	22.5	0.35	2.43
M64	31.6	22.5	0.80	1.61
M69	31.6	31.5	- NA -	4.61
M70	31.6	31.5	1.58	2.92
M73	31.6	54.0	2.75	3.18

M152	31.6	22.5	1.37	1.98
M155	31.6	31.5	1.52	2.20
M158	31.6	54.0	- NA -	- NA -
M160	31.6	31.5	1.38	2.28

† -- These voltages represent the RMS voltages at input to the TP1321 preamplifiers and have been calculated (see APPENDIX B) for the frequency range 500 Hz to 800 Hz (120 spectrum analyzer points).

‡ -- not 1/f in the 500 Hz to 800 Hz frequency region.

NA -- Not Available

TABLE 7.4

NaCl - 1/f Spectra
10 kHz Upper Frequency Range

Experiment Number	Concentration (mM)	D.C. Volts Applied	RMS Voltage† with Current On (mv.)	RMS Voltage† with Current Off (mv.)
M125	6.0	22.5	2.75	3.93
M128	6.0	31.5	3.87	4.11
M131	6.0	54.0	9.72	3.90
M26	9.5	22.5	2.04	2.85
M29	9.5	31.5	3.24	3.27
M32	9.5	54.0	12.3	3.41
M38	16.0	22.5	1.82	- NA -
M41	16.0	31.5	2.34	2.30
M44	16.0	54.0	5.21	2.46
M51	22.0	22.5	0.95	2.17
M54	22.0	31.5	1.51	2.19
M57	22.0	54.0	3.35	2.28
M59	22.0	22.5	1.22	2.07

† -- These voltages represent the RMS voltages at input to the TP1321 preamplifiers and have been calculated (see APPENDIX B)

for the frequency range 500 Hz to 800 Hz (12 spectrum analyzer points).
NA -- Not available

Appendix A

```
C      THIS PROGRAM HAS BEEN DESIGNED TO READ DATA FROM A
C      SUMMAGRAPHICS BIT PAD.
C
C      DEC RT-11 OPERATING SYSTEM.
C
C      THIS PROGRAM MUST BE LINKED TO:
C      CBDIG.OBJ   - INTERFACE MACRO TO DIGITIZER TABLET
C      PLOT55.OBJ  - DEC VT55 PLOT PACKAGE
C      VT52AD.OBJ  - VT55 TO VT105 INSTRUCTION  MACRO
C
C
C
C      THE FOLLOWING SUBROUTINES ARE REQUIRED TO DRIVE THE VT105 :
C
C                          CLEAR, INIT, GRID, GRAPH, SHADOW, BARS
C
C
C
C       THE LISTINGS OF THE LAST SEVEN SUBROUTINES MAY BE FOUND
C IN THE DEC VT55 PROGRAMING MANUAL
C
C
      DIMENSION IXVL(450),IYVL(450)
      DIMENSION XD(450),YD(450)
      REAL*4 LOWLMT,UPRLMT,INTRVL
      LOGICAL*1 ABC
      COMMON/STATUS/ISTAT(16)
C       ABC YIELDS TONE WHEN OUTPUTTED TO CONSOLE
      ABC='207
C      INITIALIZE PLOT ADJUST PARAMETERS
      CALL INIADJ(A3,B3,C3,A4,B4,C4,IV0,IU0,IU1)
C      SOUND TONE
   10  FORMAT(1X,' ','TOUCH THE STYLUS TO THE PAD'/
     1' MODE SWITCHES ARE  IN --- OUT  FOR STREAM MODE.',//)
C      READ DATA IN FROM THE DIGITIZER PAD
C
C
C
      IFLAG2=0
C     NLIM=202
      NLIM=402
      ALIM=NLIM
C       CALCULATE THE WIDTH OF THE SAMPLING INTERVALS.
C       X-DISTANCE/# OF POINTS TO BE TAKEN.
C     INTRVL=10
      INTRVL=(IU1-IU0)/(ALIM-2)
      TYPE 5,INTRVL,NLIM
5     FORMAT(1X,' SAMPLING INTERVAL = ',F10.2/
     1' THIS PROGRAM HAS BEEN SET TO DIGITIZE',I4,' POINTS')
      TYPE 10
      DO 15 I=1,NLIM
      IF (IFLAG2.EQ.1) GO TO 14
      M=I-1
12    CONTINUE
      CALL DINPUT(IXVL(I),IYVL(I),IBUTON)
C     TYPE 29,IXVL(I),IYVL(I),I
```

```
29 FORMAT(1X,I4,'    Y--Y      ',I4,'I =  ',I4)
C   IF(I.EQ.1) GO TO 15
    LOWLMT=IU0+INTRVL*M
    UPRLMT=LOWLMT+6.0
    IF (IYVL(I).GT.1650) GO TO 14
C   IF (IXVL(I).GE.IXVL(I)+2050) GO TO 15
    IF(IXVL(I).LT.LOWLMT) GO TO 12
    IF(IXVL(I).LT.UPRLMT) GO TO 15
     TYPE 34,ABC,IXVL(M),IYVL(M),I
34 FORMAT(1X,A1,'LAST X ACCEPTED = ',I4,'  Y =  ',
      I14,' I= ',I4)
C   PAUSE
35 CONTINUE
    CALL DINPUT(IXDUM,IYDUM,IBUTON)
    IF (IBUTON.NE.1) GO TO 35
    TYPE 88,ABC
88 FORMAT(1X,' DATA INPUT RESTARTED    ',A1)
    GO TO 15
CC34   FORMAT(1X,A1,24(/))
CC      LOAD REMAINING X'S WITH ZERO
14 CONTINUE
    IFLAG2=1
    IYVL(I)=IV0
  15   CONTINUE
20 CONTINUE
    TYPE 25,ABC,NLIM
  25   FORMAT(1X,A1,I4,'   POINTS ACCEPTED')
C     ADJUST FOR ROTATION AND TRANSLATION OF THE CHART AXES
C     RELATIVE TO THE DIGITIZER AXES.
    DO 100 K=1,NLIM
    CALL ADJUST(A3,B3,C3,A4,B4,C4,IXVL(K),IYVL(K),
     . IXD(K),YD(K))
  100 CONTINUE
    CALL DISPAS(NLIM,XD,YD)
    CALL FILNAM
    DO 40 J=1,NLIM
    WRITE(1,50) XD(J),YD(J)
   40   CONTINUE
50 FORMAT(1X,F10.2,' ',F10.2)
C   50 FORMAT(I4,' ',I4)
    CLOSE(UNIT=1)
    STOP
    END



    SUBROUTINE INIADJ(A3,B3,C3,A4,B4,C4,IV0,IU0,IU1)
C     THIS ROUTINE COMPUTES THE FACTORS NEEDED TO
C     ADJUST THE GRAPH AXES TO COINCIDE WITH THE DIGITIZER AXES.
C     CLEAR OUT THE INPUT BUFFER FROM THE DIGITIZER.
    LOGICAL*1 ABC
    ABC='207
    IU0=0
    IU1=0
    IU2=0
    IU3=0
    IV0=0
```

```
      IV1=0
      IV2=0
      IV3=0
C     CLOSE (UNIT=8,DISPOSE='DELETE')
      GO TO 4

      DO 12 I=1,50
    2   READ(8,20,END=4,ERR=4)IA,IB,IC
      TYPE 21, IA,IB,IC
     21   FORMAT(1X,2I5,I1)
     12   CONTINUE
      4   TYPE 5,ABC
      5   FORMAT(1X,'SET DIGIT PAD TO POINT MODE.',/,
     1'      BOTH MODE SWITCHES PRESSED IN. ',/,
     1' TYPE 1 FOR FOUR POINT CALIBRATION',/,
     1' TYPE 2 FOR 2 POINT CALIBRATION',A1)
      ISTOP=2
C     ACCEPT 6,ISTOP
      6   FORMAT(I1)
      IF (ISTOP.GT.2) STOP
      IF (ISTOP.EQ.1) GO TO 15
C       TWO POINT CALIBRATION SECTION.
      TYPE 10
      CALL DINPUT(IU0,IV0,IBUTON)
      TYPE 16, IU0,IV0,ABC
   16 FORMAT(1X,
     1' IU0 = ',I4,' IV0 = ',I4,//
     1' TOUCH UPPER LEFT CORNER/ FULL SCALE MARK ',A1)
      CALL DINPUT(IU2,IV2,IBUTON)
      TYPE 17, IU2,IV2,ABC,ABC
   17 FORMAT(1X,' IU2 = ',I4,' IV2 = ',I4,2A1)
      IU3=IU0
      IU1=IU2
      IV3=IV2
      IV1=IV0
      GO TO 70
   15 CONTINUE
C       FOUR POINT CALIBRATION
C
C
      TYPE 10
     10   FORMAT('  ','TOUCH LOWER LEFT CORNER')
      CALL DINPUT(IU0,IV0,IBUTON)
     20   FORMAT(2I5,I1)
      TYPE 30, IU0,IV0,ABC
     30   FORMAT(' U0=',I4,'V0=',I4,'  ',//'TOUCH
     1LR CORNER',A1)
      CALL DINPUT(IU1,IV1,IBUTON)
      TYPE 40, IU1,IV1,ABC,ABC
     40   FORMAT(' U1= ',I4,'V1=',I4,'    ',/,'TOUCH UR CORNER',2A1)
      CALL DINPUT(IU2,IV2,IBUTON)
      TYPE 50,  IU2,IV2,ABC,ABC,ABC
     50   FORMAT(' U2=',I4,'V2=',I4,'     ',/,'TOUCH UL CORNER',3A1)
      CALL DINPUT(IU3,IV3,IBUTON)
      TYPE 60, IU3,IV3,ABC,ABC,ABC,ABC
     60   FORMAT(' U3=',I4,'V3=',I4,' ',4A1)
   70 X7=IU0+IU1+IU2+IU3
      X8=-IU0+IU1+IU2-IU3
      X9=-IU0-IU1+IU2+IU3
      Y7=IV0+IV1+IV2+IV3
```

```
      Y8=-IV0+IV1+IV2-IV3
      Y9=-IV0-IV1+IV2+IV3
C       SPECTRUM ANALYZER PLOT IS 10 BY 6 INCHES.
C     DIGITIZER HAS 200 POINTS PER INCH --- RESOLUTION = 0.005 INCHES.
      IXX0=0
      IXX1=2000
      IYY0=0
      IYY1=1200
      D3=IXX1-IXX0
      D4=IYY1-IYY0
      M3=(IXX1+IXX0)/2
      M4=(IYY1+IYY0)/2
      D6=(X8*Y9-X9*Y8)/2
      A3=D3*Y9/D6
      B3=-D3*X9/D6
      C3=M3-(A3*X7+B3*Y7)/4
      A4=-D4*Y8/D6
      B4=D4*X8/D6
      C4=M4-(A4*X7+B4*Y7)/4
      TYPE 90,A3,A4,B3,B4,C3,C4
      90 FORMAT(1X,'A3= ',F12.1,'A4= ',F12.1,'B3= ',F12.1,'B4= ',F12.1,
        1'C3= ',F12.1,'C4= ',F12.1)
      RETURN
      END

      SUBROUTINE ADJUST(A3,B3,C3,A4,B4,C4,IX,IY,XD,YD)
C       THIS SUBROUTINE COMPENSATES FOR TRANSLATION AND ROTATION
C       OF THE GRAPH RELATIVE TO THE DIGITIZER AXES.
C       X,Y COORDINATES ARE ADJUSTED USING FACTORS DETERMINED
C       EARLIER IN THE MAIN PROGRAM.
      X=IX
      Y=IY
      XD=(A3*X)+(B3*Y)+C3
      YD=(A4*X)+(B4*Y)+C4
      RETURN
      END



C
C       THIS SUBROUTINE DRIVES THE HEWLETT-PACKARD DIGITAL PLOTTER.
C
      SUBROUTINE HPADJ(XD,YD,IX,IY)
      IX=5.0*XD
      IY=8.333*YD
      TYPE 10,XD,IX,YD,IY
   10   FORMAT(1X,'XD= ',G,'IX= ',I8,'YD= ',G,'IY= ',I8)
      RETURN
      END
C
C
C
C
C
C       THIS SUBROUTINE PERFORMS I/O TO THE DIGITIZER TABLET.
C
C
C       SUBROUTINE DINPUT REQUIRES THAT CBDIG.OBJ BE LINKED TO THE
C       MAIN PROGRAM!
```

```
C*************************************************************
C*************************************************************
      SUBROUTINE DINPUT(IXCRD,IYCRD,IBUTON)
      LOGICAL*1 ABC
      LOGICAL*1 BYTE(13)
      ABC='207
70    CONTINUE
C          BYTES  1 THROUGH 4  CONTAIN X-COORDINATE
C          BYTES  5 THROUGH 9 CONTAIN Y-COORDINATE
C          BYTES 5 AND 10 CONTAIN COMMAS
C          BYTE 11 CONTAINS CURSOR FLAG
C          BYTE 12 CONTAINS <LF>
C          BYTE 13 CONTAINS <CR>
      CALL START(NDUMMY,BYTE(1),BYTE(2),BYTE(3),BYTE(4),BYTE(5),
     1BYTE(6),BYTE(7),BYTE(8)
     2,BYTE(9),BYTE(10),BYTE(11),BYTE(12),
     2BYTE(13))
      DECODE(13,150,BYTE,ERR=200) IXCRD,IYCRD,IBUTON
      GO TO 180
200   CONTINUE
      TYPE 90,ABC,ABC,ABC
90    FORMAT(1X,' INPUT ERROR',3A1)
C     PAUSE
      GO TO 70
180   CONTINUE
150   FORMAT(I4,1X,I4,1X,I1)
      RETURN
      END
C          3-AUG-79
C           M.J.S.
C
C
C          CLOSE UNIT 1 BEFORE EXITING THE CALLING PROGRAM!!!!!
C
C
C
C
      SUBROUTINE FILNAM
      LOGICAL*1 NAME(10),ABC
      DOUBLE PRECISION FILNAM
      ABC='207
      TYPE 200,ABC,ABC,ABC,ABC
200   FORMAT(1X,'ENTER FILE NAME FOR THIS PLOT.',4A1)
      ACCEPT 201,(NAME(I),I=1,10)
201   FORMAT(10A1)
      TYPE 202, (NAME(I),I=1,10)
202   FORMAT(1X,10A1,'  WAS THE FILE NAME ENTERED. ')
      ENCODE(10,203,FILNAM) NAME
203   FORMAT(10A1)
C     TYPE 204,FILNAM
204   FORMAT(1X,' MESSAGE :',A12)
      OPEN(UNIT=1,TYPE='NEW',NAME=FILNAM)
      WRITE (1,206) (NAME(I),I=1,10)
C        WRITE 'BOF' AS A HEADER ON THE DISK FILE
206   FORMAT(1X,'BOF',/1X,10A1)
      RETURN
      END
```

```
C   3-AUG-79
C   M.J.S.
C
C
C   THIS SUBROUTINE IS REQUIRED FOR OUTPUTTING
C   DIGITIZED DATA TO TERMINAL DISPLAY AND HP DISPLAY.
C
C
    SUBROUTINE DISPAS(N,XD,YD)
    DIMENSION XD(512),YD(512),IX(512),IY(512)
    COMMON/STATUS/ISTAT(16)
    LOGICAL*1 ANSWER
    CALL VT52
    CALL INIT
    CALL GRID(157,235)
C
C     SET UP DATA FOR CONSOLE DISPLAY.
C       SET SCOPE LIMITS
    XMAX=2000.
    XMIN=0.
    YMAX=1200.
    YMIN=0.
    DO 30 JK=1,N
    IX(JK)=IFIX((470./(XMAX-XMIN))*(XD(JK)-XMIN))
    IY(JK)=IFIX((235./(YMAX-YMIN))*(YD(JK)-YMIN))
30  CONTINUE
C
C     PLOT DATA ON CONSOLE
    CALL GRAPH(N,IX,IY)
    PAUSE
    CALL SHADOW
    CALL ANSI


C       THIS SECTION WILL PRODUCE HARD COPY ON HP PLOTTER,
C       IF REQUESTED.
    ABC="207
    TYPE 5,ABC
5   FORMAT(1X,A1,'DO YOU WISH A HARD COPY PLOT?')
    ACCEPT 6,ANSWER
6   FORMAT(A1)
    IF (ANSWER.NE."131) GO TO 99
C       INITIALIZE PLOTTER
    WRITE (6,45)
    DO 50 I=1,N
C       ADJUST FOR HP PLOTTER LIMITS
    CALL HPADJ(XD(I),YD(I),IXXX,IYYY)
    WRITE (6,40) IXXX,IYYY
40  FORMAT(21)
50  CONTINUE
C       MUTE PLOTTER
    WRITE (6,46)
80  CONTINUE
    CLOSE(UNIT=6)
45  FORMAT(1X,'PLTL')
46  FORMAT(1X,'PLTT')
99  CONTINUE
    RETURN
    END
```

Appendix B

```
C      NOV 18,1979
C
C      M.J.S.
C
C     DEC RT-11 OPERATING SYSTEM USED.
C
C      THIS PROGRAM READS NICOLET ASCII AND/OR DIGITIZED FILES.
C
C
C   THIS PROGRAM WILL READ TWO PLOTS AND SUBTRACT
C        FROM THE OTHER.
C   SCOPE PLOT AND HARDCOPY WILL BE AVAILABLE.
C   SUBTRACTED SPECTRA WILL BE SAVED ON THE DISKETTE.
C
C        THIS PROGRAM MUST BE LINKED TO PLOT55.OBJ AND VT52AD.OBJ.

C                    PLOT55.OBJ - VT55 PLOT PACKAGE
C                    VT52AD.OBJ - VT55 TO VT105 INSTRUCTION  MACRO
C                    THE FOLLOWING SUBROUTINES ARE ALSO REQUIRED:
C
C                        CLEAR, INIT, GRID, GRAPH, SHADOW, BARS, LABEL
C
C          DOCUMENTATION FOR THE LAST SEVEN ROUTINES MAY BE
C          FOUND IN THE DEC PLOT55 PROGRAMING MANUAL.
C

    DOUBLE PRECISION FSTFIL,SECFIL,THRFIL
    DOUBLE PRECISION FILNAM
    DIMENSION FSTARX(500),SECARX(500),THRARX(500)
    DIMENSION FSTARY(500),SECARY(500),THRARY(500)
    INTEGER POINTR,ANSWR2
    LOGICAL*1 ANSWR5
    COMMON /IFLAG5/IFLAG5
    COMMON /DBGAIN/DBGAIN
    COMMON /IFLAG6/IFLAG6
    COMMON /IFLG10/IFLG10
3   CONTINUE
C      CLEAR DISPLAY
    CALL VT52
    CALL INIT
    CALL ANSI
    IFLAG5=0
    IFLAG6=0
    IFLG10=0
    NLIM=400
    COEFF=1.
    DBGAIN=0.0
    TYPE 2,NLIM
2   FORMAT(1X,'PROGRAM HAS BEEN SET TO ACCEPT ',I4,' DATA POINTS.'/
      1'      NICOLET ASCII FILES ARE REQUIRED FOR INPUT!!!!')
1   CONTINUE
C   NLIM=202
    TYPE 5
5   FORMAT(1X,'TYPE           IF YOU DESIRE DISPLAY OF: '//
      14X,'1',13X,'A FILE ON DISK DK.'/
      24X,'2',13X,'SUBTRACTION OF 2 LOG FILES ON DISK DK.'/
```

```
     319X,' ------ I.E. CURRENT ON MINUS CURRENT OFF.'/
     44X,'4',13X,'SUBTRACTION ---- COMPENSATE FOR WHITE NOISE.'/
     54X,'5',13X,'SET PROGRAM TO INCLUDE AN INTERMEDIATE RMS '/
     5,19X,'VOLTAGE CALCULATION.'/
     74X,'7',13X,'SUBTRACT OFF 1/F NOISE FROM A FILE ON THE DISK.'/
     9'   ?')
   ACCEPT 6,POINTR
6  FORMAT(I1)
   IF (POINTR.EQ.5) IFLG10=1
C  IF (POINTR.EQ.5) GO TO 1
   IF (POINTR.EQ.2) IFLAG5=1
   TYPE 10
10 FORMAT(1X,'    ENTER FIRST FILENAME.      ') "
   CALL FILNAM(FSTFIL,0)
   CALL RDFIL(FSTFIL,FSTARX,FSTARY,NLIM)
   GO TO (80,15,100,120,80,100,200),POINTR
15 CONTINUE
   TYPE 30
30 FORMAT(1X,'    ENTER SECOND FILE NAME      --
     1    NORMALLY THE B-FILE.')
   CALL FILNAM(SECFIL,0)
   CALL RDFIL(SECFIL,SECARX,SECARY,NLIM)
C
C
C
C       1) SUBTRACT THE VALUES
C       2) TAKE THE LOG OF THE RESULT
C
   DO 40 I=1,NLIM
   TEMP=SECARY(I)-FSTARY(I)
   IF(TEMP.LE.0.0) TEMP=10.
   THRARY(I)=(COEFF)*10.0*ALOG10(TEMP)+60.0+DBGAIN
C  WRITE (6,39) SECARX(I),THRARY(I),SECARY(I),FSTARY(I)
39 FORMAT(1X,4(E10.4,1X))
40 CONTINUE
   CALL GAIN(NLIM,SECARX,THRARY,0)
   CALL WRFIL(FILNAM,SECARX,THRARY,NLIM)
   GO TO 90
75 CONTINUE
C     THIS SECTION WILL DISPLAY DATA FILE FOUND ON DISK.
80 CALL GAIN(NLIM,FSTARX,FSTARY,0)
   GO TO 90
100   CONTINUE
   GO TO 1
120   CONTINUE
   TYPE 130
130   FORMAT(1X,/1X,'  ENTER NAME OF WHITE NOISE FILE.   ')
   CALL FILNAM(SECFIL,0)
   CALL RDFIL(SECFIL,SECARX,SECARY,NLIM)
   DO 140 KL=1,NLIM
   THRARY(KL)=FSTARY(KL)-SECARY(KL)
140   CONTINUE
   CALL GAIN(NLIM,SECARX,THRARY,1)
   TYPE 145,FSTFIL,SECFIL
145   FORMAT(1X,A10,'DIVIDED BY',A10/)
   TYPE 143
143   FORMAT(1X,' WOULD YOU LIKE THE DISPLAYED FILE TO BE SAVED AS
     1A DISK FILE(Y OR N)?')
   ACCEPT 144,ANSWR5
144   FORMAT(A1)
```

```
      IF (ANSWR5.NE."131) GO TO 158
      TYPE 150
150   FORMAT(1X,'ADJUSTED FILE IS TO BE NAMED?')
      CALL WRFIL(FILNAM,SECARX,THRARY,NLIM)
158   CONTINUE
      GO TO 90
200   CONTINUE
C     TYPE OUT THE VALUE OF Y, IN INCHES, CORRESPONDING TO
C     3 INCHES FROM THE RIGHT LIMIT OF THE PLOT.
      TYPE 221,FSTARY(141)/200.
221   FORMAT(1X,'Y( 7 INCHES FROM THE LEFT) =',F10.2,' INCHES.'/)
      TYPE 201
201   FORMAT(1X,'ENTER THE Y-VALUE, IN INCHES (6 INCHES = 1200
     1 DIGITIZER UNITS), CORRESPONDING TO 3 INCHES FROM THE RIGHT LIMIT
       2OF THE PLOT.'/)
      ACCEPT 202,REFPNT
202   FORMAT(F10.2)
C     CONVERT INCHES TO DIGITIZER UNITS.
      REFPNT=200.*REFPNT
      TYPE 203
203   FORMAT(1X,'WHAT IS THE FREQUENCY RANGE OF THE PLOT IN UNITS OF
       1KHZ?')
      ACCEPT 204,FRANGE
204   FORMAT(F3.0)
      ENDPNT=ALOG10(FRANGE)+3
      F0=10.**(ENDPNT-0.78)
      AREFPT=10.**(REFPNT*COEFF)
      DO 210 KA=1,NLIM
      IF (FSTARX(KA).LE. 0.0) FSTARX(KA)=KA*10.0-10.
      IF (FSTARY(KA).LE. 0.0) FSTARY(KA)=1200.
      FREQF=10.**((ENDPNT-2.6)+0.0013*FSTARX(KA))
      HOLD=(10.**(FSTARY(KA)*COEFF))-(AREFPT*(F0/FREQF))
C     TYPE 219,FREQF,HOLD
219   FORMAT(1X,'FREQ =',F10.2,'SUB =    ',F10.2)
      IF (HOLD.LE.0) HOLD=10.
      FSTARY(KA)=COEFF*ALOG10(HOLD)
C     TYPE 218,KA,HOLD,FSTARY(KA)
218   FORMAT(1X,I4,4X,F10.2,4X,F10.2)
209   CONTINUE
210   CONTINUE
      CALL GAIN(NLIM,FSTARX,FSTARY,1)
      TYPE 211
211   FORMAT(1X,'FILE WITH 1/F NOISE REMOVED IS TO BE CALLED?')
      CALL WRFIL(FILNAM,FSTARX,FSTARB)
***y
      GO TO 90
90 CONTINUE
      TYPE 230
230   FORMAT(1X,'WOULD YOU LIKE TO RUN THIS PROGRAM AGAIN (Y OR N) ?')
      ACCEPT 144,ANSWR5
      IF (ANSWR5.EQ."131) GO TO 3
      STOP
      END



      SUBROUTINE RDFIL(FILNAM,ARRAX,ARRAY,NLIM)
      DOUBLE PRECISION FILNAM,TSTNAM
```

```
      DIMENSION ARRAX(1),ARRAY(1)
      COMMON /IFLAG5/IFLAG5
      COMMON /IFLAG6/IFLAG6
      COMMON /IFLG10/IFLG10
      TYPE 20
   20 FORMAT(1X,'TYPE 0 TO INPUT ASCII FILE.'/1X,
        1'       1 TO INPUT DIGITIZED FILE.'/
        2'       2 TO INPUT PROCESSED FILE (I.E. FILE SCALED TO 60DB
        3).'///)
      ACCEPT 25,IFLAG6
   25 FORMAT(I1)
      OPEN (UNIT=1,TYPE='OLD',NAME=FILNAM)
C        TEST HEADER ON FILE FOR NAME.
C     READ (1,50) TSTNAM
   50 FORMAT(/1X,10A1)
C     IF (TSTNAM.NE.FILNAM) GO TO 70
      GO TO (55,58,45) IFLAG6+1
   55 CONTINUE
      CALL FFTFRD(NLIM,ARRAX,ARRAY)
      TYPE 56,FILNAM
   56 FORMAT(1X,' FFT ASCII FILE NAMED',A10,'HAS BEEN
        1 READ IN.')
      GO TO 90
   58 CONTINUE
      TYPE 57,FILNAM
   57 FORMAT(1X,' A DIGITIZED FILE NAMED ',A10,
        1' HAS BEEN READ IN.')
      READ (1,50) TSTNAM
      READ(1,60,END=85,ERR=85) (ARRAX(I),ARRAY(I),I=1,NLIM)
      DO 40 J=1,NLIM
      ARRAX(J)=ARRAX(J)*(2.60206/2000.)
      ARRAY(J)=ARRAY(J)*(60.0/1200.0)
C        CONVERT TO VOLTS SQUARED, FOR SUBTRACTION OF FILES.
      IF (IFLAG5.EQ.1) ARRAY(J)=10.0**(ARRAY(J)/10.0)
   40 CONTINUE
      GO TO 90
   45 CONTINUE
C        FILE WAS SCALED TO 60DB -- NO ADJUSTMENT IS REQUIRED.
      TYPE 99,FILNAM
   99 FORMAT(1X,' A PROCESSED FILE NAMED ',A10,' HAS BEEN READ
        1 IN.')
      READ (1,50) TSTNAM
      READ(1,60,END=85,ERR=85) (ARRAX(JJ),ARRAY(JJ),JJ=1,NLIM)
      IF (IFLAG5.NE.1) GO TO 90
C        CONVERT TO VOLTS SQUARED, FOR SUBTRACTION OF FILES.
      DO 100 KK=1,NLIM
      ARRAY(KK)=10.0**(ARRAY(KK)/10.0)
  100    CONTINUE
      GO TO 90
   60 FORMAT(1X,F10.4,1X,F10.4)
   70 TYPE 80,TSTNAM,FILNAM
   80 FORMAT(1X,10A1,'  DOES NOT MATCH',10A1)
      STOP
   85 CONTINUE
      TYPE 86
   86 FORMAT(1X,' READ ERROR ********************')
   90 CONTINUE
      CLOSE(UNIT=1)
      RETURN
      END
```

```
      SUBROUTINE WRFIL(FILNAM,ARRAX,ARRAY,NLIM)
      DIMENSION ARRAX(1),ARRAY(1)
      DOUBLE PRECISION FILNAM
C        WRITE HEADER AND ACCEPT NAME.
      TYPE 10
10    FORMAT(1X,' ENTER OUTPUT FILE NAME')
      CALL FILNAM(FILNAM,1)
      DO 20 J=1,NLIM
      WRITE (1,50,ERR=75,END=75) ARRAX(J),ARRAY(J)
20    CONTINUE
50    FORMAT(1X,F10.4,1X,F10.4)
      CLOSE(UNIT=1)
      RETURN
75       CONTINUE
      TYPE 80,NLIM
      WRITE(6,80) NLIM
80    FORMAT(1X,'WRITE ERROR HAS OCCURRED ***************
     1'/15,' POINTS WRITTEN ONTO DISK FILE.')
      CLOSE(UNIT=1)
      RETURN
      END



C
C
C
C
C        3-AUG-79
C         M.J.S.
C
C
C         CLOSE UNIT 1 BEFORE EXITING THE CALLING PROGRAM!!!!!!
C
C
C
C
      SUBROUTINE FILNAM(FILNAM,IFLAG1)
C        IFLAG=1 OPENS A NEW FILE.
      LOGICAL*1 NAME(10)
      DOUBLE PRECISION FILNAM
C     TYPE 200
200      FORMAT(1X,'ENTER FILE NAME FOR NEXT PLOT.')
      ACCEPT 201,(NAME(I),I=1,10)
201      FORMAT(10A1)
      TYPE 202, (NAME(I),I=1,10)
202      FORMAT(1X,10A1,'  WAS THE FILE NAME ENTERED. '/)
      ENCODE(10,203,FILNAM) NAME
203      FORMAT(10A1)
C     TYPE 204,FILNAM
204      FORMAT(1X,' MESSAGE ',A12)
      IF (IFLAG1.NE.1) GO TO 207
      OPEN(UNIT=1,TYPE='NEW',NAME=FILNAM)
      WRITE (1,206) (NAME(I),I=1,10)
C        WRITE 'BOF' AS A HEADER ON THE DISK FILE
206      FORMAT(1X,'BOF',/1X,10A1)
207      CONTINUE
      RETURN
      END
```

```
C
C   THIS SUBROUTINE IS REQUIRED FOR OUTPUTTING
C   DIGITIZED DATA TO TERMINAL DISPLAY AND HP DISPLAY.
C
C
    SUBROUTINE DISPAS(N,XD,YD)
    DIMENSION XD(512),YD(512),IX(512),IY(512)
    COMMON/STATUS/ISTAT(16)
    LOGICAL*1 ANSWER
    FACTOR=0.0
    INTEGER ANSWR2
10  CONTINUE
    CALL VT52
    CALL INIT
    CALL GRID(157,235)
C
C     SET UP DATA FOR CONSOLE DISPLAY.
C       SET SCOPE LIMITS
    XMAX=2.6
    XMIN=0.
    YMAX=60.
    YMIN=0.
    DO 30 JK=1,N
    IX(JK)=IFIX((470./(XMAX-XMIN))*(XD(JK)-XMIN))
    IY(JK)=IFIX((235./(YMAX-YMIN)))E!JK)-YMIN))+IFIX(39.17*FACTOR)
30  CONTINUE
C
C     PLOT DATA ON CONSOLE
    CALL GRAPH(N,IX,IY)
    PAUSE
    CALL SHADOW
    CALL ANSI


C       THIS SECTION WILL PRODUCE HARD COPY ON HP PLOTTER,
C       IF REQUESTED.
    ABC="207
    TYPE 5,ABC
5   FORMAT(1X,A1,'DO YOU WISH A HARD COPY PLOT?')
    ACCEPT 6,ANSWER
6   FORMAT(A1)
    IF (ANSWER.NE."131) GO TO 99
C       INITIALIZE PLOTTER
    WRITE (6,45)
    DO 50 I=1,N
C       ADJUST FOR HP PLOTTER LIMITS
    IXXX=IFIX((9999./(XMAX-XMIN))*(XD(I)-XMIN))
    IYYY=IFIX((9999./(YMAX-YMIN))*(YD(I)-YMIN))+IFIX(1666.5*FACTOR)
    WRITE (6,40) IXXX,IYYY
40  FORMAT(21)
50  CONTINUE
C       MUTE PLOTTER
    WRITE (6,46)
80  CONTINUE
    CLOSE(UNIT=6)
45  FORMAT(1X,'PLTL')
46  FORMAT(1X,'PLTT')
99  CONTINUE
    GO TO 148
```

```
      TYPE 145
  145 FORMAT(1X,'ARE YOU SATISFIED WITH THE DISPLAY?'/
     1 1X,' IF NOT, SHALL I MULTIPLY BY -6,-5,...0...5,6 ?')
      ACCEPT 146,ANSWR2
  146 FORMAT(I2)
      FACTOR=FLOAT(ANSWR2)
      IF (ANSWR2.EQ.0) GO TO 148
      DO 147 M=1,NLIM
      YD(M)=1666.5*FACTOR+YD(M)
  147 CONTINUE
      GO TO 10
  148 CONTINUE
      RETURN
      END
      SUBROUTINE GAIN(NLIM,ARRAY1,ARRAY2,IAUTO)
      DIMENSION ARRAY1(1),ARRAY2(1)
      LOGICAL*1 ABC
      ABC='207
      FACTOR=0.0
      IF (IAUTO.NE.0) GO TO 160
  143 CONTINUE
      CALL DISPAS(NLIM,ARRAY1,ARRAY2)
      TYPE 145
  145 FORMAT(1X,'ARE YOU SATISFIED WITH THE DISPLAY?'/
     1 1X,' IF NOT, SHALL I MULTIPLY BY -6,-5,...0...5,6 ?')
      ACCEPT 146,IFACT
  146 FORMAT(I2)
      IF (IFACT.EQ.0) GO TO 148
      FACTOR=FLOAT(IFACT)
      DO 147 M=1,NLIM
      ARRAY2(M)=FACTOR*10.0+ARRAY2(M)
  147 CONTINUE
      GO TO 143
      GO TO 148
  160 CONTINUE
      TYPE 161
  161 FORMAT(1X,'WHAT IS THE Y-AXIS LABELED AS --- IN DB')
      ACCEPT 162,NDB
  162 FORMAT(I2)
      IFACT=-(NDB/10)
      GO TO 143
  148 CONTINUE
      RETURN
      END
C
C
C
      SUBROUTINE FFTFRD(NLIM,XCD,YCD)
C       NOVEMBER 15,1979
C         M.J.S.
C
C         THIS SUBROUTINE TRANSLATES THE NICOLET ANALYZER ASCII FILES.
C
C         THIS PROGRAM MUST BE LINKED TO PLOT55.OBJ AND VT52AD.OBJ.
C
C
C
      DIMENSION INFO(5),XCD(4112),YCD(4112),ORYCD(4112),SENSIT(8)
      DOUBLE PRECISION FREQ(2),AMP(2),AVGMDE(4),NUMBER(11),
     1 VOLTS(7),RANGE(21),INPUT(4),WEIGHT(4),REFERE(4),UNITS(4),
```

```
      IRZLUTN(4),INWT(4)
      COMMON /IFLAG5/IFLAG5
      COMMON /DBGAIN/DBGAIN
      INTEGER CHAR1,PARIDX
      INTEGER BITS(20)
      REAL LNGAIN
      LOGICAL*1 ABC
      LOGICAL DISPA(14)
      ABC='207
      DATA FREQ/'HZ','LOG HZ'/
      DATA AMP/'LINEAR Y','LOG Y'/
      DATA AVGMDE/'SUM','DIFF','EXPON','PEAK'/
      DATA NUMBER/'1','2','4','8','16','32','64','128','256',
     1'512','CONT'/
      DATA RANGE/'1','2','5','RERR','10',
     1'20','50','RERR','100',
     1'200','500','RERR','1000',
     1'2,000','5,000','RERR','10,000',
     1'20,000','50,000','RERR','100,000'/
      DATA REFERE/'IV','R','RERR','SET R'/
      DATA UNITS/'VOLTS','VOLTS**2','UERR','DB'/
      DATA VOLTS/'100 MVS','200 MVS','500 MVS','1 VOLT'
     1,'2 VOLTS','5 VOLTS',
     1'10 VOLTS'/
C       EIGHTH VALUE IS AN ERROR CONDITION.
      DATA SENSIT/.1,.2,.5,1.,2.,5.,10.,-1./
      DATA INPUT/'DC','AC','IERR','TEST'/
      DATA WEIGHT/'FLAT','HANNING','WERR','AUTO'/
      DATA RZLUTN/'400 PNTS','ERROR','ERROR','ERROR'/
      DATA INWT/'OFF','A WGHTNG','ERROR','ERROR'/
      COMMON/STATUS/ISTAT(16)
      COMMON /IFLG10/IFLG10
C     TYPE 18,ABC
18    FORMAT(1X,A1,'ENTER NAME OF DATA FILE TO BE PROCCESSED.')
      IDBLIN=0
      SUM=0.0
      PARIDX=0
      IFLG11=0
      IRMSDN=0
5     CONTINUE
C       AVOID READING CONTROL-C ON DATA FILE
      IF (PARIDX.GE.401) GO TO 1901
      READ (1,20,END=1901,ERR=1901) (INFO(I),I=1,5)
      DO 15 I=1,5
C       TEST FOR CONTROL-C
      IF (INFO(I).EQ.'203) GO TO 1901
C       CHECK FOR EMPTY LINE.
C       CHECK FOR A SPACE.
      IF (INFO(I).EQ.'240) GO TO 5
      IF (INFO(I).EQ.0) GO TO 5
15    CONTINUE
20    FORMAT(5A1)
      IHEX=0
      DO 70 J=1,5
      CALL HEXBIN(INFO(6-J),BITS(4+(J-1)*4),BITS(3+(J-1)*4),
     1BITS(2+(J-1)*4),BITS(1+(J-1)*4),IHEXER)
      IHEX=IHEX+IHEXER
70    CONTINUE
      IF (IHEX.GE.1) GO TO 5
C     TYPE 80,(INFO(I),I=1,5)
```

```
80 FORMAT(1X,'DECIMAL VALUES ARE =',I6)
C  TYPE,90,(BITS(21-K),K=1,20)
90 FORMAT(1X,2011)
   GO TO (200,301,402,503,604,705,806,907,1008,
     11109,1210,1311,1412,1513,1614,1715),INFO(5)+1
200   CONTINUE
   ICHAR=BITS(8)*8+BITS(7)*4+BITS(6)*2+BITS(5)*1+1
   WRITE (6,246) NUMBER(ICHAR)
246   FORMAT(1X,'NUMBER OF SUMMATIONS = ',A8)
C     SENSE 0 - UPPER PANEL.
C     DISPLAY MODE.
C
   DATA DISPA/'TIME','INST','A','B','IN&A','IN&B',
     1'A&B','AERR','A+B','A-B','B-A','AERR','A/B','B/A'/
   ICHAR=BITS(18)*8+BITS(17)*4+BITS(16)*2+BITS(15)*1+1
   TYPE 210,DISPA(ICHAR)
   WRITE(6,210) DISPA(ICHAR)
210   FORMAT(1X,' DISPLAY MODE : ',A4)
   ICHAR=BITS(20)*2+BITS(19)*1+1
   WRITE (6,215) RZLUTN(ICHAR)
215   FORMAT(1X,'RESOLUTION OF X - AXIS : ',A8)
   ICHAR=BITS(14)*1+1
   WRITE (6,240) FREQ(ICHAR)
240   FORMAT(1X,'FREQUENCY - ',A8)
   IDBLIN=BITS(13)*1+1
   WRITE (6,242) AMP(IDBLIN)
242   FORMAT(1X,'POWER - ',A8)
   ICHAR=BITS(10)*2+BITS(9)*1+1
   WRITE (6,244) AVGMDE(ICHAR)
244   FORMAT(1X,'AVERAGER MODE :',A8)
   GO TO 5
301   CONTINUE
   ICHAR=BITS(20)*4+BITS(19)*2+BITS(18)*1+1
   IRMSDN=ICHAR
   WRITE (6,310) VOLTS(ICHAR)
310   FORMAT(1X,'INPUT SENSITIVITY = ',A8)
   ICHAR=BITS(17)*16+BITS(16)*8+BITS(15)*4+
     1BITS(14)*2+BITS(13)*1+1
   WRITE (6,315) RANGE(ICHAR)
315   FORMAT(1X,'SPECTRUM RANGE ',A8,'HZ')
   ICHAR=BITS(9)*2+BITS(8)*1+1
   WRITE (6,317) INPUT(ICHAR)
317   FORMAT(1X, 'INPUT COUPLING: ',A8)
   ICHAR=BITS(6)*2+BITS(5)*1+1
   WRITE (6,328) WEIGHT(ICHAR)
328   FORMAT(1X,'INPUT WEIGHTING -- ',A8)
   GO TO 5
402   CONTINUE
   ICHAR=BITS(11)*2+BITS(10)*1+1
   WRITE (6,410) REFERE(ICHAR)
410   FORMAT(1X,'REFERENCE LEVEL = ',A8)
   ICHAR=BITS(9)*2+BITS(8)*1+1
   WRITE (6,420) UNITS(ICHAR)
420   FORMAT(1X,'UNITS = ',A8)
   GO TO 5
503   CONTINUE
   ICHAR=BITS(20)*2+BITS(19)*1+1
   WRITE (6,510) INWI(ICHAR)
510   FORMAT(1X,'INPUT WEIGHTING WAS SET TO : ',A8)
   GO TO 5
```

```
604    CONTINUE
C      SPECTRUM OUTPUT - FLOATING POINT
C      COUNT COORDINATE SETS
   PARIDX=PARIDX+1
   IF(BITS(20).EQ.1) GO TO 610
C      CHARACTERISTIC HAS A POSITIVE SIGN.
   CHARS=BITS(19)*16.+BITS(18)*8.+
     1BITS(17)*4.+BITS(16)*2.+BITS(15)*1.
   GO TO 630
610    CONTINUE
C      CHARACTERISTIC WAS NEGATIVE.
C      PERFORM ONE'S COMPLEMENT.
   DO 625 KK=15,20
   BITS(KK)=BITS(KK).XOR.*1
625    CONTINUE
C      PERFORM TWO'S COMPLEMENT
   IF (BITS(15).EQ.0) GO TO 650
C      OTHERWISE
   BITS(15)=0
   CARRY=1
   DO 675 N=16,20
   BITS(N)=BITS(N)+CARRY
   IF (BITS(N).LE.1) CARRY=0
   IF (BITS(N).EQ.2) GO TO 670
   GO TO 675
670    CARRY=1
   BITS(N)=0
675    CONTINUE
   GO TO 655
C      TWO'S COMPLEMENT COMPLETE
650    BITS(15)=1
655    CONTINUE
   CHARS=BITS(19)*16.+BITS(18)*8.+
     1BITS(17)*4.+BITS(16)*2.+BITS(15)*1.
   CHARS=CHARS*(-1.0)
   GO TO 630
630    IF (BITS(14).EQ.1) GO TO 633
C      MANTISSA WAS POSITIVE.
   AMANT=BITS(13)*0.5+
     1      BITS(12)*0.25+
     2     BITS(11)*0.125+
     3     BITS(10)*0.0625+
     4     BITS(9)*0.03125+
     5     BITS(8)*0.015625+
     6     BITS(7)*0.0078125+
     7     BITS(6)*0.00390625
   GO TO 690
633    CONTINUE
C      CHARACTERISTIC WAS NEGATIVE.
C      PERFORM ONE'S COMPLEMENT.
   DO 635 KK=6,14
   BITS(KK)=BITS(KK).XOR.*1
635    CONTINUE
C      PERFORM TWO'S COMPLEMENT
   IF (BITS(6).EQ.0) GO TO 640
C      OTHERWISE
   BITS(6)=0
   CARRY=1
   DO 676 N=7,14
   BITS(N)=BITS(N)+CARRY
```

```
      IF (BITS(N).LE.1) CARRY=0
      IF (BITS(N).EQ.2) GO TO 671
      GO TO 676
671   CARRY=1
      BITS(N)=0
676   CONTINUE
      GO TO 656
C     TWO'S COMPLEMENT COMPLETE
640   BITS(6)=1
656   CONTINUE
      AMANT=BITS(13)*0.5+
     1     BITS(12)*0.25+
     2     BITS(11)*0.125+
     3     BITS(10)*0.0625+
     4     BITS(9)*0.03125+
     5     BITS(8)*0.015625+
     6     BITS(7)*0.0078125+
     7     BITS(6)*0.00390625
      AMANT=(-1)*AMANT
690   CONTINUE
      CHARI=IFIX(CHARS)
C     WRITE (6,688) AMANT,CHARI
C     TYPE 688,AMANT,CHARI
688   FORMAT(1X,'MANTISSA= ',F10.3,'CHARI',I8)
C     SKIP SPURIOUS FIRST POINT.
      IF (PARIDX.EQ.1) GO TO 5
      YCD(PARIDX-1)=AMANT*(2.0**CHARI)
      IF((IRMSDN.LT.1).OR.(IRMSDN.GT.7)) GO TO 4000
4003  CONTINUE
      ORYCD(PARIDX-1)=(YCD(PARIDX-1)*(SENSIT(IRMSDN)**2.))/(1.5)
      SUM=SUM+ORYCD(PARIDX-1)
C     JUMP FOR B MINUS A.
      IF (IFLAG5.EQ.1) GO TO 691
      IF (YCD(PARIDX-1).LE.0.0) YCD(PARIDX-1)=10.0
      YCD(PARIDX-1)=10.*ALOG10(YCD(PARIDX-1))
      YCD(PARIDX-1)=YCD(PARIDX-1)+60.+DBGAIN
C     WRITE (6,689) YCD(PARIDX-1)
C     TYPE 689,YCD(PARIDX-1)
689   FORMAT(1X,'YVALUE = ',E12.4)
691   CONTINUE
      GO TO 5
705   CONTINUE
      GO TO 5
806   CONTINUE
      GO TO 5
907   CONTINUE
      GO TO 5
1008  CONTINUE
      IVAL=(15-INFO(1))*1000+(15-INFO(2))*100+(15-INFO(3))*10+
     1(15-INFO(4))*1
      WRITE (6,1100) IVAL
1100  FORMAT(1X,'EXPERIMENT NUMBER = ',I5)
      GO TO 5
1109  CONTINUE
      GO TO 5
1210  CONTINUE
      GAIN=BITS(20)
      MLTPLR=INFO(2)
      IF (IDBLIN.EQ.0) GO TO 1250
C     DISPLAY WAS LOGARITHMIC
```

```
      IF ((INFO(2).GT.5).OR.(INFO(2).LT.(-5))) GO TO 1275
      DBGAIN=MLTPLR*10.
      IF (GAIN.EQ.1)  DBGAIN=DBGAIN*(-1.)
      WRITE (6,1225) DBGAIN
1225  FORMAT(1X,'DISPLAY GAIN = ',F10.1,'DB')
      GO TO 5
C       DISPLAY WAS LINEAR.
1250  IF ((MLTPLR.GT.8).OR.(MLTPLR.LT.(-8))) GO TO 1275
      LNGAIN=2.**MLTPLR
      IF (GAIN.EQ.1.)  LNGAIN=1/LNGAIN
      WRITE(6,1235) LNGAIN
1235  FORMAT(1X,'DISPLAY GAIN = ',F15.8)
      GO TO 5
1275  CONTINUE
      WRITE(6,1280)
1280  FORMAT(1X,'GAIN ERROR')
      GO TO 5
1311  GO TO 2000
1412  CONTINUE
1513  CONTINUE
1614  GO TO 2000
1715  GO TO 2000
      GO TO 1900
2000  CONTINUE
      GO TO 5
1900  CONTINUE
1901  CONTINUE
      TOTRMS=1.0*SQRT(SUM)
      WRITE (6,1906) TOTRMS
      TYPE 1906,TOTRMS
1906  FORMAT(1X,'TOTAL RMS VALUE = ',F12.4)
2990

      DO 1902 IG=1,400
698     FORMAT(1X,I3,G,2G)
      XCD(IG)=ALOG10(2.5*(IG))-ALOG10(2.5)
C     TYPE 698,IG,IG*2.5,XCD(IG),YCD(IG)
1902  CONUJ*
C       CHECK IF IFLAG10 WAS SET.
      TYPE 1979,IFLG10
1979  FORMAT(1X,'FLAG 10 =',I3)
      IF (IFLG10.EQ.0) GO TO 1950
      TYPE 1940
1940  FORMAT(1X,'ENTER LOWER CELL LIMIT <CR><LF>'/
     1  11X,'       UPPER CELL LIMIT <CR><LF>'/
     2  21X,'        TYPE ZERO FOR DEFAULT VALUES'/)
      ACCEPT 1941,LOWLMT
1941  FORMAT(I3)
      IF(LOWLMT.EQ.0) GO TO 1945
      ACCEPT 1941,IPRLMT
      GO TO 1946
1945  CONTINUE
      TYPE 1943
1943  FORMAT(1X,'DEFAULT FOR CELL LIMITS IN EFFECT!')
      LOWLMT=200
      IPRLMT=320
1946  CONTINUE
      ACCUM1=0.0
      DO 1947 IT=LOWLMT,IPRLMT
      ACCUM1=ACCUM1+ORYCD(IT)
```

```
1947  CONTINUE
      WRITE (6,1948) LOWLMT,IPRLMT,
     1(LOWLMT*2.5),(IPRLMT*2.5)
     2,SQRT(ACCUM1)
1948  FORMAT(1X,'RMS VOLTAGE FOR CELL LIMITS',I3,
     1'TO',I3,' I.E. - ',F10.2,' HZ TO ',
     2F10.2,' HZ IS :',F12.4)
      PAUSE
1950  CONTINUE
C     PAUSE
C     CLOSE(UNIT=1)
      WRITE(6,699) PARIDX
      TYPE 699,PARIDX
699     FORMAT(1X,'NUMBER OF POINTS READ IN = ',I5)
      IF (PARIDX.NE.400) TYPE 3000,ABC,ABC
      IF (PARIDX.NE.400) WRITE (6,3000) ABC,ABC
3000  FORMAT(1X,2A1,'INPUT FILE HAS INCORRECT NUMBER OF DATA POINTS'/
     1'**************************************************'//)
      GO TO 4010
4000  CONTINUE
      IF (IFLG11.EQ.1) GO TO 4003
      TYPE 4001
4001  FORMAT(1X,'MANUAL ENTRY OF THE
     1 INPUT SENSITIVITY( VOLTS ) OF THE FFT REQUIRED!')
      IRMSDN=8
      ACCEPT 4002,SENSIT(IRMSDN)
4002  FORMAT(F8.1)
      IFLG11=1
      GO TO 4003
4010  CONTINUE
      RETURN
      END
      SUBROUTINE HEXBIN(IASCH,B3,B2,B1,B0,IHEXER)
      LOGICAL*1 ITEST
      IHEXER=0
      ITEST=IASCH
      INTEGER B0,B1,B2,B3
      DATA IA/'A'/,I0/'0'/,I9/'9'/
      IF (IASCH.LE.I9) GO TO 40
15    IASCH=IASCH-IA+10
      GO TO 10
40    IASCH=IASCH-I0
10    CONTINUE
      IF((IASCH.GT.15).OR.(IASCH.LT.0)) GO TO 20
      CALL BTSTRP(IASCH,B3,B2,B1,B0)
      RETURN
C       SET ERROR FLAG.
20    IHEXER=1
      TYPE 30,ITEST
30    FORMAT(1X,' NON  - HEXADECIMAL CHARACTER ENCOUNTERED
     1IN INPUT FILE:',A1)
      RETURN
      END

C       THIS SUBROUTINE STRIPS BITS OFF.

      SUBROUTINE BTSTRP(IASCH,B3,B2,B1,B0)
      INTEGER B0,B1,B2,B3
      B0=IASCH.AND.'1
      B1=(IASCH/2).AND.'1
```

```
      B2=(IASCII/4).AND.'1
      B3=(IASCII/8).AND.'1
C     TYPE 60,IASCII,B3,B2,B1,B0
60    FORMAT(1X,'CHAR =',I6,'BITS = ',4I1)
      RETURN
      END
```

APPENDIX C

Calculation of the Spectrum from Pure Poiseuille Flow in a Cylinder.

The Correlation function is, as discussed (Chapter 7 - section (c)):

$$C(\tau)=C_0(1-\frac{\nu\tau}{l}) \quad 0\leqslant\tau\leqslant\frac{l}{\nu} \tag{C.1}$$

$$C(\tau)=0 \qquad \frac{l}{\nu}<\tau \tag{C.2}$$

where,

ν = velocity of flow
l = length of the cylinder
τ = transit time through the cylinder
C_0 = constant

The corresponding power spectrum is given by

$$G(\omega)=C_0\int_0^{\frac{l}{\nu}}(1-\frac{\nu\tau}{l})\cos\omega\tau\,d\tau \tag{C.3}$$

$$G(\omega)=\frac{\nu}{l\omega^2}(1-\cos(\frac{\omega l}{\nu})) \tag{C.4}$$

if the radius of the cylinder is a, and A is a constant, the velocity at the radius r is:

$$\nu(r)=A(a^2-r^2) \tag{C.5}$$

The average velocity is then given by:

$$\bar{\nu}=\int_0^a \nu(r)\frac{2\pi r}{\pi r^2}dr \tag{C.6}$$

$$=\frac{Aa^2}{2}$$

solving for A

$$A=\frac{2\bar{\nu}}{a^2} \tag{C.7}$$

Next, consider the cylinder as divided into annuli of mean radius r_j for the j^{th} annulus. The power spectrum produced in the j^{th} annulus is

$$G_{rj}(\omega)=\frac{\nu(r_j)}{l\omega^2}(1-\cos(\frac{\omega l}{\nu(r_j)})) \tag{C.8}$$

where,

$$\nu(r_j)=2\frac{\bar{\nu}}{a^2}(a^2-r_j^2) \tag{C.9}$$

so that

$$G(\omega)=\sum_{j=1}^{j_{max}} G_{rj}(\omega)\pi(r_{0j}^2-r_{ij}^2) \tag{C.10}$$

For computational purposes, variables were defined as follows:

$$r_{0j}=r_{i(j+1)} \tag{C.11}$$

and take (for 10 annuli)

$$j_{max}=10 \tag{C.12}$$

$$r_{0(jmax)}=a$$

$$r_{i(j=1)}=0$$

$$r_{0(j)}=r_{i(j)}+\frac{a}{j_{max}}$$

$$r_j=\frac{r_{0j}+r_{ij}}{2}$$

The program that follows computes the spectum $G_{rj}(\omega)$. The results are plotted in Figure 7.4.

Flow Program

```
C       FLOW CALCULATION - ANNULI
      DIMENSION P(7),TGRAL(60),GTGRA(60),IDISPX(60)
     1,IDISPY(60),SUM(60)
      DIMENSION FLOGOF(60)
      REAL*4 OMEGA(60),L,JMAX
      INTEGER POINTS
      COMMON/STATUS/ISTAT(16)
      CALL VT52
      CALL INIT
      CALL GRID(100,235)
C       INITIALIZE SUM
      POINTS=53
      DO 5 IK=1,POINTS
      SUM(IK)=0.
5     CONTINUE
C     JMAX=10.
      TYPE 30
30    FORMAT(1X,' ENTER THE NUMBER OF ANNULI TO BE
     1AVERAGED OVER.')
      ACCEPT 31,JMAX
31    FORMAT(F5.0)
      TYPE 32
32    FORMAT(1X,' ENTER THE UPPER LIMIT OF THE PLOT IN UNITS OF KHZ.')
      ACCEPT 33,UPRLMT
33    FORMAT(F5.2)
      A=10.**(-5.)
      VBAR=0.4
      COEFFA=2*(VBAR/(A**2))
      L=2.5*10.**(-4.)
      LANULI=JMAX
      DO 58 JINDEX=1,LANULI
      ROJ=JINDEX*A/JMAX
      RIJ=(JINDEX-1)*A/JMAX
      RT2=2.**(1./6.)
      OMEGA(1)=6.28*((UPRLMT*1000.)/400)
 6    DO 11 J=1,POINTS
      IF(J.EQ.1) GO TO 7
      JJ=J-1
      OMEGA(J)=OMEGA(JJ)*RT2
      OMEGA(53)=(UPRLMT*1000.*6.28)
7     RSUBJ=RIJ+(A/(2*JMAX))
      VSUBRJ=COEFFA*(A**2-RSUBJ**2)
      TGRAL(J)=(VSUBRJ/(L*OMEGA(J)**2))
     1*(1-COS((OMEGA(J)*L)/VSUBRJ))
      SUM(J)=SUM(J)+TGRAL(J)*3.14
     1*((ROJ**2)-((RIJ)**2))
11    CONTINUE
58    CONTINUE
      DO 65 IP=1,POINTS
      IF (SUM(IP).LE.0)    WRITE(6,67) IP
      IF (SUM(IP).LE.0)    SUM(IP)=1.0
67    FORMAT(1X,'  Y-VALUE EQUAL TO OR LESS THAN ZERO ENCOUNTERED --
     1CHECK DATA PAIR NUMBERED: ',I1)
      GTGRA(IP)=ALOG10(SUM(IP))
      FLOGOF(IP)=ALOG10(OMEGA(IP)/6.28)
65    CONTINUE
```

```
      CALL SCALE(POINTS,FLOGOF,GTGRA,IDISPX,IDISPY)
      CALL GRAPH(POINTS,IDISPX,IDISPY)
      WRITE (6,20) POINTS,LANULI,
     1(OMEGA(IL)/6.28,FLOGOF(IL),GTGRA(IL),IL=1,POINTS)
   20 FORMAT(1X,'POINTS = ',I5/,1X,'NUMBER OF ANNULI = ',I5/
     1(5X,F10.2,5X,F10.2,5X,F10.2))
      PAUSE
      CALL SHADOW
   60 CONTINUE
      CALL ANSI
      STOP
      END
      SUBROUTINE SCALE(N,ARRX,ARRY,ITJEJ%MAe%
C
C
C
C
C
C
C
C
C
C
C     THE FOLLOWING SUBROUTINE IS USEFUL FOR
C     PLOTTING SIMULATED DATA.
C
C
      DIMENSION ARRX(512),ARRY(512),IDISPX(512),IDISPY(512)
      LOGICAL*1 ANSWER
      XMAX=ARRX(1)
      XMIN=ARRX(1)
      YMAX=ARRY(1)
      YMIN=ARRY(1)
      DO 10 I=2,N
      IF(ARRX(I).GE.XMAX)   XMAX=ARRX(I)
      IF(ARRX(I).LE.XMIN)   XMIN=ARRX(I)
   10 CONTINUE
      DO 20 IK=2,N
      IF (ARRY(IK).GE.YMAX)   YMAX=ARRY(IK)
      IF (ARRY(IK).LE.YMIN)   YMIN=ARRY(IK)
   20 CONTINUE
C
C
C     TEMPORARY FIX
      YMAX=-12.0
      YMIN=-18.0
      TYPE 55
   55 FORMAT(1X,'NOTE Y-LIMITS HAVE BEEN SET TO  -3<=Y<=-11')
C      TEMP FIX ----  ADJUSTS X-LIMITS TO FORM AN OVERLAY ON SPECTRUM
C                     PLOTS.
C     XMIN=1.4
C     XMAX=4.0
      TYPE 56
   56 FORMAT(1X,'SET HP PLOTTER FOR A 7 BY 10 INCH PLOT.')
C       SCALE DATA TO FIT SCOPE LIMITS.
      DO 30 IL=1,N
      IDISPX(IL)=IFIX((500./(XMAX-XMIN))*(ARRX(IL)-XMIN))
      IDISPY(IL)=IFIX((200./(YMAX-YMIN))*(ARRY(IL)-YMIN))
   30 CONTINUE
C        PLOT DATA ON CONSOLE
      CALL GRAPH(N,IDISPX,IDISPY)
```

```
C
C
C
C       THIS SECTION PRODUCES HARD COPY.
C      SET PLOTTER X INCHES = PLOTTER Y INCHES
      TYPE 5
5     FORMAT(1X,' DO YOU WISH A HARD COPY PLOT? ')
      ACCEPT 6,ANSWER
6     FORMAT(A1)
      IF(ANSWER.NE.'131') GO TO 88
C     OPEN(UNIT=6)
      WRITE (6,45)
      DO 50 J=1,N
      IHPX=IFIX((9999./(XMAX-XMIN))*(ARRX(J)-XMIN))
      IHPY=IFIX((9999./(YMAX-YMIN))*(ARRY(J)-YMIN))
      WRITE(6,40) IHPX,IHPY
40    FORMAT(2I)
45    FORMAT(1X,' PLTL')
50    CONTINUE
C       PLOTTER:       STOP MONITORING DATA
      WRITE (6,46)
46    FORMAT(1X,'PLTT')
88    CONTINUE
      CLOSE (UNIT=6)
      RETURN
      END
```

APPENDIX D

Noise in Cylinder with Flow and Diffusion

The equation for flow with diffusion is (*91*):

$$\frac{\partial C}{\partial t}=D\left(\frac{\partial^2 C}{\partial r^2}+\frac{1}{r}\frac{\partial C}{\partial r}+\frac{\partial^2 C}{\partial z^2}+u_0\left(1-\frac{r^2}{a^2}\right)\frac{\partial C}{\partial z}\right) \qquad \text{(D.1)}$$

Boundary conditions are: (1) at $r=a$, $\frac{\partial C}{\partial r}=0$; (2) at $r=0$, C is finite; (3) $\frac{\partial C}{\partial z}+qC|_{z=0}=\frac{\partial C}{\partial z}+qC|_{z=L'}$ The last condition states that there is no net gain or loss at the ends of the cylinder.

where:

C = concentration fluctuation
r = distance from center of cylinder
a = radius of cylinder
D = diffusion coefficient
(of the ionic species)
u_0 = velocity of flow in
z direction at $r=0$
t = time
z = distance along cylinder axis
($z=0$ at one boundary and $z=L'$ at the other)

Define:

Ignoring diffusion in the direction of flow (assume that the flow is rapid compared to diffusion). First, treat the case of uniform flow (velocity = u_0 everywhere).

The resulting dimensionless equation is of the form

$$\frac{\partial^2 C}{\partial \rho^2}+\frac{1}{\rho}\frac{\partial C}{\partial \rho}+\frac{au_0}{D}\frac{\partial C}{\partial \xi}=-\lambda C \tag{D.2}$$

This equation separates as

$$C(\rho,\xi)=R(\rho)X(\xi)$$

$$\frac{1}{R}\frac{d^2R}{d\rho^2}+\frac{1}{\rho R}\frac{dR}{d\rho}=-\kappa q \tag{D.3}$$

$$\frac{q}{x}\frac{dx}{d\rho}-\lambda=-\kappa$$

The R equation is the zeroth order Bessel equation

$$R=\alpha J_0(\sqrt{\kappa_n q_i}\rho)+\beta Y_0(\sqrt{\kappa_n q_i}\rho) \tag{D.4}$$

To keep R finite at $\rho=0$, $\beta=0$ the boundary conditions at $r=a$ requires that the κ_n be the zeroes of $J_1(\sqrt{\kappa_n q_i}\rho)$.

So

$$R_n=\alpha_n J_0(\sqrt{\kappa_n q_i}\rho) \tag{D.5}$$

The X equation gives

$$X=\gamma_n e^{-(\frac{\lambda-\kappa_n}{q})\xi} \tag{D.6}$$

applying the boundary condition at $z=0$ and $z=L'$, either $\lambda_n=\kappa_n$ or $\lambda_n=\kappa_n-q^2$; choose $\lambda_n=\kappa_n$ on physical grounds: This choice provides positive eigenvalues, and no average variation in concentration along the axis (such an average variation would not be possible, as it would lead to a concentration discontinuity at the end of the cylinder).

Then

$$C(\rho,\xi)=\sum_n \zeta_n J_0(\sqrt{\kappa_n q_i}\rho) \tag{D.7}$$

where ζ_n is the normalization constant for the n^{th} eigenvalue.

Performing the normalization,

$$\zeta_n=(\pi L J_0^2(\sqrt{\kappa_n q_i}))^{-0.5} \tag{D.8}$$

Then

$$C_n(\rho,\xi)=\frac{J_0(\sqrt{\kappa_n q_i}\rho)}{\sqrt{\pi L}J_0(\sqrt{\kappa_n q_i})} \tag{D.9}$$

Using the method of van Vliet and Fassett (*151*), the power spectrum of concentration fluctuations becomes

$$G_c(\omega)=\frac{4<C^2>}{V_s}\sum_n \frac{\lambda_n\left|\int_{V_s} C_n(\rho,\xi)\rho d\rho d\xi\right|^2}{\lambda_n^2+\omega^2} \tag{D.10}$$

where,

$<C^2>$ = mean square concentration
V_s = volume of the cylinder

If the integral is taken directly over volume at constant velocity, a zero spectrum results. However, the correct procedure requires that the spectrum is taken over a series of annuli of differing velocity. Now, the cylinder is divided into a number of annuli such that diffusion does not significantly mix regions separated by the differences in mean radii of the annuli. For the case considered here, three annuli will represent the system to a first approximation. Now, let $q_i=q_0(1-\rho_i^2)$ where $\rho_i=\frac{i-0.5}{3}$; $i=1,2,3$ and $q_0=\frac{au_0}{D}$.

The normalization integral becomes a sum

$$\zeta_n^2=\left(\sum_{i=1}^{3}\frac{2\pi L}{\kappa_n q_i}\int_{(i-1)\sqrt{\kappa_n q_i}}^{i\sqrt{\kappa_n q_i}} J_0^2(u_i)\cdot u_i du_i\right)^{-1} \tag{D.11}$$

The power spectrum is then:

$$G_c(\omega)=\frac{4<C^2>}{V_s}\sum_n\sum_i \frac{\kappa_n}{(\kappa_n^2+(2\pi\phi)^2)}\left|\frac{1}{\zeta_n^2}\int_{i-1}^{i}\int_0^L J_0(\rho_i\sqrt{\kappa_n q_i})\rho_i d\rho_i d\xi\right|^2 \tag{D.12}$$

$$G_c(\omega)=\frac{4<C^2>L}{\pi}\sum_n\frac{1}{\zeta_n^2}\sum_i\frac{\kappa_n}{(\kappa_n^2+(2\pi\phi)^2)}\left|\frac{i}{\kappa_n q_i}J_1(i\sqrt{\kappa_n q_i})-\frac{(i-1)}{\kappa_n q_{i-1}}J_1((i-1)\sqrt{\kappa_n q_{i-1}})\right|^2$$

where, $\phi=\frac{\omega a^2}{2\pi D}$ (numerically the cylinder considered here, $\phi\approx\frac{f}{40}$; where $f=\frac{\omega}{2\pi}$= frequency).

The calculation proceeds in two steps:

(1) Determination of the Eigenvalues $\sqrt{\kappa_n q_i}$.

For the Bessel functions, large eigenvalues are given asymptotically as $(n+\frac{1}{4})\pi$. However, the values were computed only for the first hundred eigenvalues.

(2) Determination of the spectrum given the eigenvalues.

Although not all possible parameters were tried, the requirement for an approximately $\frac{1}{n}$ distribution for κ_n, for f^{-1} noise, is not, nor is there any obvious way to meet it by this procedure. Although the calculation was carried out, the measured spectrum does not emerge as a result, nor can it be made to do so by any apparent change in parameters.

The program for the calculation follows:

Diffusion Plus Flow

```
C      PART I - CALCULATION OF THE EIGENVALUES.
C
C
C
      IJ=0
      J=1
      THN0=0.25
      DO 77 N=1,6000
      XINC=0.03
      XN=N
   81   THN0=THN0+XINC
      THN1=THN0*0.97222**0.5
      THN2=THN0*0.75**0.5
      THN3=THN0*0.30555**0.5
C       EVALUATE TERMS AT RHO EQUALS 1/3
      ARG=THN1/3.
      ARGS=(ARG/3.)*(ARG/3.)
      ARGB=3./ARG
      IF (ARG.LE.3.) GO TO 65
      U=F0(ARGB*1.0)
      V=T0(ARGB*1.0)
      W=F1(ARGB*1.0)
      X=T1(ARGB*1.0)
      XJ0112=XJ0B(ARGB*1.0,U*1.0,V*1.0)
      XJ1112=XJ1B(ARGB*1.0,W*1.0,X*1.0)
      Y0112=Y0B(ARGB*1.0,U*1.0,V*1.0)
      Y1112=Y1B(ARGB*1.0,W*1.0,X*1.0)
      GO TO 64
C   FOR SMALL ARGUMENTS
   65   XJ0112=XJ0S(ARGS*1.0)
      XJ1112=XJ1S(ARGS*1.0)
      Y0112=Y0S(ARGS*1.0,1.0*XJ0112)
      Y1112=Y1S(ARGS*1.0,1.0*XJ1112)
   64   ARG=THN2/3.
      ARGS=(ARG/3.)*(ARG/3.)
      ARGB=3./ARG
      IF (ARG.GT.3.)GO TO 63
      XJ0212=XJ0S(ARGS*1.0)
      XJ1212=XJ1S(ARGS*1.0)
      Y0212=Y0S(ARGS*1.0,1.0*XJ0212)
      Y1212=Y1S(ARGS*1.0,1.0*XJ1212)
      GO TO 62
   63   U=F0(ARGB*1.0)
      V=T0(ARGB*1.0)
      W=F1(ARGB*1.0)
      X=T1(ARGB*1.0)
      XJ0212=XJ0B(ARGB*1.0,U*1.0,V*1.0)
      XJ1212=XJ1B(ARGB*1.0,W*1.0,X*1.0)
      Y0212=Y0B(ARGB*1.0,U*1.0,V*1.0)
      Y1212=Y1B(ARGB*1.0,W*1.0,X*1.0)
C       EVALUATE FUNCTIONS AT OUTER RING
   62   ARG=THN2*2./3.
      ARGS=(ARG/3.)*(ARG/3.)
      ARGB=3./ARG
      IF (ARG.GT.3.) GO TO 61
```

```
      XJ0223=XJ0S(ARGS*1.0)
      XJ1223=XJ1S(ARGS*1.0)
      YJ0223=Y0S(ARGS*1.0,1.0*XJ0223)
      YJ1223=Y1S(ARGS*1.0,1.0*XJ1223)
      GO TO 60
   61 U=F0(ARGB*1.0)
      V=T0(ARGB*1.0)
      W=F1(ARGB*1.0)
      X=T1(ARGB*1.0)
      XJ0223=XJ0B(ARGB*1.0,U*1.0,V*1.0)
      XJ1223=XJ1B(ARGB*1.0,W*1.0,X*1.0)
      Y0223=Y0B(ARGB*1.0,U*1.0,V*1.0)
      Y1223=Y1B(ARGB*1.0,W*1.0,X*1.0)
   60 ARG=THN3*2./3.
      ARGS=(ARG/3.)**2.
      ARGB=3./ARG
      IF (ARG.GT.3.) GO TO 59
      XJ0323=XJ0S(ARGS*1.0)
      XJ1323=XJ1S(ARGS*1.0)
      Y0323=Y0S(ARGS*1.0,1.0*XJ0323)
      Y1323=Y1S(ARGS*1.0,1.0*XJ1323)
      GO TO 58
   59 U=F0(ARGB*1.0)
      V=T0(ARGB*1.0)
      W=F1(ARGB*1.0)
      X=T1(ARGB*1.0)
      XJ0323=XJ0B(ARGB*1.0,U*1.0,V*1.0)
      XJ1323=XJ1B(ARGB*1.0,W*1.0,X*1.0)
      Y0323=Y0B(ARGB*1.0,U*1.0,V*1.0)
      Y1323=Y1B(ARGB*1.0,W*1.0,X*1.0)
   58 IF (THN3.LE.3.) GO TO 57
      Q=3./THN3
      W=F1(Q*1.0)
      Z=T1(Q*1.0)
      XJ13=XJ1B(Q*1.0,W*1.0,Z*1.0)
      Y13=Y1B(Q*1.0,W*1.0,Z*1.0)
      GO TO 56
   57 QS=THN3/3.
      XJ13=XJ1S(1.0*QS)
      Y13=Y1S(1.0*QS,1.0*XJ13)
C     FIND DENOMINATORS AND NUMERATORS
   56 D1=XJ0323-XJ13*Y0323/Y13
      IF(ABS(D1).LT.0.0000001) GO TO 76
      D2=THN3*(XJ1323-XJ13*Y1323/Y13)
      IF (ABS(D2).LT.0.0000001) GO TO 76
      D3=XJ0112
      IF (ABS(D3).LT.0.0000001) GO TO 76
      D4=THN1*XJ1112
      IF (ABS(D4).LT.0.0000001) GO TO 76
      D21=D4*XJ0212-D3*THN2*XJ1223
      IF (ABS(D21).LT.0.0000001) GO TO 76
      D22=D4*Y0212-D3*THN2*Y1223
      IF(ABS(D22).LT.0.000001) GO TO 76
      XNL=D2*XJ0223-THN2*D1*XJ1223
      XNR=D2*Y0223+THN2*D1*Y1223
C     CALCULATE VALUE OF EXPRESSION.
      EXP=XNL/D21-XNR/D22
      IF  (IJ.GT.0) GO TO 751
      IF(N.EQ.1.OR.N.EQ.2) GO TO 80
      IF (J.EQ.2) PRINT 97,EXP
```

```
   80   IF (N.EQ.1) PV1=EXP
    IF (N.EQ.1) GO TO 77
    IF (N.EQ.2) PV=EXP
    IF (N.EQ.2) GO TO 77
C     TEST FOR SIGN CHANGE, TO FIND ZEROES.
    PV1=PV
    TST=EXP*PV
    IF (TST.LE.0.) GO TO 75
    J=1
    PV1=PV
    PV=EXP
    GO TO 77
   75   PRINT 99,THN0,PV,EXP,PV1
    GO TO 84
  751   PRINT 991,THN0,PV,EXP
  84    IF((ABS(EXP).LT.1..OR.ABS(PV).LT.1.).AND.IJ.LE.0) GO TO 82
    J=2
    PV1=PV
    PV=EXP
    IF (IJ.LE.0) GO TO 77
    IF (IJ.GT.0) GO TO 83
   82   IJ=24
    XINC=0.003
    THN0=THN0-0.033
  83    IJ=IJ-1
    GO TO 81
  991   FORMAT(///' THETA N0 = ',G,5X,' PREVIOUS VALUE ='
      1,G,5X,' PRESENT VALUE= ',G)
  76    PRINT 98,D1,D2,D3,D4,D21,D22,N
   77   CONTINUE
  97    FORMAT(1X,'VALUE FOLLOWING LAST ZERO CROSSING =',E12.5)
   99   FORMAT(///,' ROOT BEFORE',F6.2,'BETWEEN
      1VALUES ',E12.5,'AND',E12.5,5X,'PREVIOUS VALUE = ',E12.5)
   98   FORMAT(//,5X,'D1=',E12.5,2X,'D2=',E12.5,
      12X,'D3=',E12.5,2X,'D4=',E12.5,2X,'D21=',E12.5,2X,
      2'D22=',E12.5,2X,'N=',I4)
    STOP
    END



    FUNCTION T0(X)
    T0=3./X-0.78539816-0.04166397*X-0.00003954*X**2
      1+0.00262573*X**3-0.00054125*X**4-0.00029333*X**5
    RETURN
    END



    FUNCTION F0(X)
    F0=.79788456-0.00000077*X-0.0055274*X**2-
      10.00009512*X**3.+0.00137237*X**4
      2-0.00072805*X**5+0.00014476*X**6
    RETURN
    END
```

```
FUNCTION T1(X)
T1=3./X-2.35619449+0.12499612*X+0.0000565*X**2.0
  1-0.00637879*X**3.0+0.00074348*X**4.+0.00079824*X**5.0
  2-0.00029166*X**6.0
RETURN
END



FUNCTION F1(X)
F1=0.79788456+0.00000156*X+0.01659667*X**2.0
  1+0.00017105*X**3.0+0.00249511*X**4.0
  1+0.00113653*X**5.0-0.00020033*X**6.0
RETURN
END



FUNCTION XJ0S(X)
XJ0S=1-2.2499997*X+1.2656208*X**2.0-0.3163866*X**3.0
  1+0.0444479*X**4.-0.0039444*X**5.0+0.00021*X**6.0
RETURN
END



FUNCTION Y0S(X,Y)
Y0S=(2./3.1415926)*ALOG(1.5*(X**0.5))*Y+0.36746691+
  10.60559366*X-0.74350384*X**2.0+0.25300117*X**3.0
  2-0.04261214*X**4.0+0.00427916*X**5.0
  3-0.00024846*X**6.
RETURN
END



FUNCTION XJ0B(X,Y,Z)
XJ0B=(3./X)**(-0.5)*Y*COS(Z)
RETURN
END



FUNCTION Y0B(X,Y,Z)
Y0B=(3./X)**(-0.5)*Y*SIN(Z)
RETURN
END
```

```
FUNCTION XJ1S(X)
XJ1S=3.*(X)**0.5*(0.5-0.56249985*X+0.21093573*X**2.
  1-0.03954289*X**3.+0.00443319*X**4.-0.00031761*X**5.0)
RETURN
END



FUNCTION Y1S(X,Y)
Y1S=(2./3.1415926)*ALOG(1.5*(X**0.5))*Y+
  1(1/(3*X**0.5))*(-0.63662+0.221091*X+2.168271*X**2.0
  2-1.3164827*X**3.0+0.3123951*X**4.-0.04*X**5.0
  3+0.00279*X**6.0)
RETURN
END


FUNCTION XJ1B(X,Y,Z)
XJ1B=(3./X)**(-0.5)*Y*COS(Z)
RETURN
END



FUNCTION Y1B(X,Y,Z)
Y1B=(3./X)**(-0.5)*Y*SIN(Z)
RETURN
END
```

```
C      PART II
C     THIS PROGRAM CALCULATES THE
C     SPECTRUM GIVEN THE EIGENVALUES.
C
C
C
      DIMENSION THETAN(200),PARSUM(200)
      REAL OMEGA(200)
      DIMENSION GOFW(200),FREQ(200)
C     EXTERNAL P2,P3,P4
C     EXTERNAL XJONE,XJZERO,YONE,YZERO
C     EXTERNAL F0,F1,T0,T1,XJ0S,XJ0B,XJ1S,XJ1B,Y0S,Y0B,Y1S,Y1B
C     SET THE NUMBER OF X POINTS.
      GO TO 802
C       TEMPORARY FIX TO CHECK SERIES.
      TYPE 800
  800   FORMAT(1X,' ENTER TEST ARGUMENT')
      ACCEPT 801,ARGT
  801   FORMAT(G)
      ALPHA=YZERO(ARGT*1.0)
      BETA=YONE(ARGT*1.0)
      GAMMA=XJZERO(ARGT*1.0)
      DELTA=XJONE(ARGT**1.0)
      TYPE 802,ALPHA,BETA,GAMMA,DELTA
  802   FORMAT(1X,'YZERO= ',G,
     1'YONE =',G,'JZERO= ',G,'JONE = ',G)
      IX=54
C     ENTER THE NUMBER OF THETAS.
      TYPE 10
   10   FORMAT(1X,' ENTER THE NUMBER OF THETA S ')
      ACCEPT 20,N
   20   FORMAT(I3)
      TYPE 5
    5   FORMAT(1X,' ENTER Q')
      ACCEPT 6,Q
    6   FORMAT(G)
      PRINT 72,Q,N
   72   FORMAT(1X,' Q = ',G,10X,'TOTAL NUMBER OF THETA S
     1 SUMMED =  ',I3)
      OPEN( UNIT=22,FILE='STORAG.')
      READ (22,40) (THETAN(I),I=1,N)
   40   FORMAT(G)
C     INITIALIZE FREQUENCY PARAMETERS.
      RT2=2.0**(1./3.)
      FREQ(1)=0.25
C     LOOP FOR FREQUENCY.
      DO 30 K=1,IX
      GOFW(K)=0.0
      SUMI=0.
      SUMII=0.
      PARSUM(K)=0.
      IF (K.EQ.1) GO TO 7
      KK=K-1
      FREQ(K)=FREQ(KK)*RT2
    7   CONTINUE
      DO 90 L=1,N
      CALL POWER(THETAN(L),FREQ(K),SUMI,SUMII,Q,K)
      PARSUM(K)=PARSUM(K)+SUMII
      GOFW(K)=GOFW(K)+SUMI*SUMII
      IF (K.GT.1 ) GO TO 90
```

```
C   PRINT 8,L,THETAN(L),PARSUM(K),GOFW(K)
  8    FORMAT(1X,' N TH  THETA SUMMED =',I3,'VALUE OF NTH THETA',
     1G,'PARTIAL SUM =',G,'TOTAL SUM =',G)
 90    CONTINUE
C   PRINT 80,K,FREQ(K),GOFW(K)
 80    FORMAT(1X,I3,2X,G,2X,G)
  30   CONTINUE
     PRINT 111,(K,FREQ(K),PARSUM(K),GOFW(K),K=1,IX)
 111   FORMAT(1X,I3,G,3X,G,3X,G)
C   CALL SALVGE(IX,FREQ,GOFW)
     STOP
     END


     SUBROUTINE POWER(THN0,FREQ,SUMI,SUMII,Q,K)
C    EXTERNAL P2,P3,P4,XJZERO,XJONE,YZERO,YONE,F0,F1,T1,T0
     SUM=0.0
     PI=3.14159
     WOMEGA=2*PI*FREQ
     THN1=THN0*(0.97222)**0.5
     THN2=THN0*(0.75)**0.5
     THN3=THN0*0.552765773
C    PRINT 772,THN3
   772 FORMAT(1X,'THN3 = ',G)

     PTWO=P2(1.0*THN1,1.0*THN2)
     PTHREE=P3(PTWO*1.0,1.0*THN1,1.0*THN2)
     PFOUR=P4(PTWO*1.0,1.0*THN2,THN3*1.)
     TERM1=XJONE(THN1/3.)
     TERM2=XJONE(2.0*THN2/3.0)
     TERM3=XJONE(THN2/3.0)
     TERM4=YONE(2.0*THN2/3.0)
     TERM5=YONE(THN2/3.0)
     TERM6=XJONE(THN3*1.)
     TERM7=XJONE(2.0*THN3/3.0)
     TERM8=XJONE(THN3*1.)
     TERM9=YONE(THN3*1.0)
     TERM10=YONE(2.0*THN3/3.0)
     SUMI = ((THN0**2.0*Q)
       1/(THN0**4.0+Q**2.0*WOMEGA**2.0))
     SUMII= ABS(
       3             ((2.0*PI*PTHREE*
       4      XJONE(THN1/3.))/(3.0*THN1**2.0))
       5       +((2.0*PI)/(3.0*THN2**2.0))
       6      *   (PTWO*(2.0*XJONE(2.0*THN2/3.0)
       7            -XJONE(THN2/3.0))
       8              -2.0*YONE(2*THN2/3.0)  -  YONE(THN2/3.0))
       9   + ((2.0*PI)/(3.0*THN3**2.0))  *  PFOUR
       1          * (   3.0*XJONE(THN3*1.0)-2.0*XJONE(2.0*THN3/3.0)
       1           -      (XJONE(THN3*1.0)/YONE(THN3*1.0))  *
       2             (3.0*YONE(THN3*1.0)-2.0*YONE(2.0*THN3/3.0)))
       3                        )**2.0

     IF (K.GT.1) RETURN

     PRINT 777,TERM1,TERM2,TERM3,TERM4,TERM5,
       1TERM6,TERM7,TERM8,TERM9,TERM10
   777 FORMAT(1X,'TERMS 1 TO 10 FOLLOW'/10(4X,G/)///)
     PRINT 888,THN0,THN1,THN2,THN3,PTWO,PTHREE,PFOUR,SUMII
  888  FORMAT(1X,' 4 THETAS,P2,P3,P4 AND PASS SUM FOLLOW:'/
```

```
      18(2X,G/)///)


C     IF (SUMII.LT.0.00000001.OR.SUMII.GT.10.**38.) STOP
      RETURN
      END


      FUNCTION P2(THN1,THN2)
C     EXTERNAL YZERO,XJZERO,YONE,XJONE
      ARGP21=THN1/3.0
      ARGP22=THN2/3.0
      TOP=(YZERO(1.0*ARGP22)/XJZERO(1.0*ARGP21)) +
     1  (THN2/THN1)*(YONE(1.0*ARGP22)/XJONE(1.0*ARGP21))
      BOTTOM= (XJZERO(1.0*ARGP22)/XJZERO(1.0*ARGP21))-
     1(THN2/THN1)*(XJONE(1.0*ARGP22)/XJONE(1.0*ARGP21))
      P2=TOP/BOTTOM

      RETURN
      END




      FUNCTION P3(PTWO,THN1,THN2)
C     EXTERNAL XJONE,YONE
      ARGP31=THN1/3.
      ARGP32=THN2/3.0
      TOP = PTWO*XJONE(1.0*ARGP32) + THN2 * YONE(ARGP32)
      BOTTOM = THN1 * XJONE(1.0*ARGP31)
      P3 =  TOP/BOTTOM
      RETURN
      END



      FUNCTION P4(PTWO,THN2,THN3)
C     EXTERNAL XJONE,YONE
      ARGP42=THN2/3.0
      ARGP43=THN3/3.0
      TOP = (THN2/THN3)*(PTWO*XJONE(1.0*ARGP42)-YONE(2*ARGP42))
      BOTTOM = (XJONE(2.0*1.0*ARGP43)-
     1XJONE(THN3*1.0)*YONE(2*1.0*ARGP43)/YONE(THN3*1.0))
      P4 = TOP/BOTTOM
      RETURN
      END



      FUNCTION YZERO(ARG)
C     EXTERNAL Y0S,XJ0S,F0,T0,Y0B
      IF (ARG.GT.3) GO TO 10
```

```
      TARG=(ARG/3.0)**2.0
      Y=XJ0S(TARG*1.0)
      YZERO = Y0S(TARG*1.0,Y)
      RETURN
   10   TARG=3.0/ARG
      Y=F0(TARG*1.0)
      Z=T0(TARG*1.0)
      YZERO=Y0B(TARG*1.0,Y,Z)
      RETURN
      END


      FUNCTION YONE(ARG)
C     EXTERNAL Y1S,XJ1S,Y1B,F1,T1
      IF (ARG.GT.3.0) GO TO 10
      UARG=(ARG/3.0)**2.0
      Y=XJ1S(UARG*1.0)
      YONE=Y1S(UARG,Y)
      RETURN
   10   UARG=3.0/ARG
      Y=F1(UARG*1.0)
      Z=T1(UARG*1.0)
      YONE=Y1B(UARG*1.0,Y,Z)
      RETURN
      END



      FUNCTION XJZERO(ARG)
C     EXTERNAL XJ0S,XJ0B,F0,T0
      IF (ARG.GT.3.0) GO TO 10
      VARG=(ARG/3.0)**2.0
      XJZERO = XJ0S(VARG*1.0)
         RETURN
   10   VARG=3.0/ARG
      Y=F0(VARG*1.0)
      Z=T0(VARG*1.0)
      XJZERO = XJ0B(VARG*1.0,Y,Z)
      RETURN
      END



      FUNCTION XJONE(ARG)
C     EXTERNAL XJ1S,XJ1B,F1,T1
      IF (ARG.GT.3.0) GO TO 10
      WARG=(ARG/3.0)**2.0
      XJONE = XJ1S(WARG*1.0)
      RETURN
   10    WARG=3./ARG
      Y=F1(WARG*1.0)
      Z=T1(WARG*1.0)
      XJONE = XJ1B(WARG*1.0,Y,Z)
      RETURN
      END
```

```
FUNCTION T0(X)
T0=3./X-0.78539816-0.04166397*X-0.00003954*X**2
  1+0.00262573*X**3-0.00054125*X**4-0.00029333*X**5
RETURN
END



FUNCTION F0(X)
F0=.79788456-0.00000077*X-0.0055274*X**2-
  10.00009512*X**3.+0.00137237*X**4
  2-0.00072805*X**5+0.00014476*X**6
RETURN
END



FUNCTION T1(X)
T1=3./X-2.35619449+0.12499612*X+0.0000565*X**2.0
  1-0.00637879*X**3.0+0.00074348*X**4.+0.00079824*X**5.0
  2-0.00029166*X**6.0
RETURN
END



FUNCTION F1(X)
F1=0.79788456+0.00000156*X+0.01659667*X**2.0
  1+0.00017105*X**3.0+0.00249511*X**4.0
  1+0.00113653*X**5.0-0.00020033*X**6.0
RETURN
END



FUNCTION XJ0S(X)
XJ0S=1-2.2499997*X+1.2656208*X**2.0-0.3163866*X**3.0
  1+0.0444479*X**4.-0.0039444*X**5.0+0.00021*X**6.0
RETURN
END



FUNCTION Y0S(X,Y)
Y0S=(2./3.1415926)*ALOG(1.5*(X**0.5))*Y+0.36746691+
  10.60559366*X-0.74350384*X**2.0+0.25300117*X**3.0
  2-0.04261214*X**4.0+0.00427916*X**5.0
  3-0.00024846*X**6.
RETURN
END



FUNCTION XJ0B(X,Y,Z)
```

```
      XJ0B=(3./X)**(-0.5)*Y*COS(Z)
      RETURN
      END



      FUNCTION Y0B(X,Y,Z)
      Y0B=(3./X)**(-0.5)*Y*SIN(Z)
      RETURN
      END



      FUNCTION XJ1S(X)
      XJ1S=3.*(X)**0.5*(0.5-0.56249985*X+0.21093573*X**2.
     1-0.03954289*X**3.+0.00443319*X**4.-0.00031761*X**5.0)
      RETURN
      END



      FUNCTION Y1S(X,Y)
      Y1S=(2./3.1415926)*ALOG(1.5*(X**0.5))*Y+
     1(1/(3*X**0.5))*(-0.63662+0.221091*X+2.168271*X**2.0
     2-1.3164827*X**3.0+0.3123951*X**4.-0.04*X**5.0
     3+0.00279*X**6.0)
      RETURN
      END


      FUNCTION XJ1B(X,Y,Z)
      XJ1B=(3./X)**(-0.5)*Y*COS(Z)
      RETURN
      END



      FUNCTION Y1B(X,Y,Z)
      Y1B=(3./X)**(-0.5)*Y*SIN(Z)
      RETURN
      END
```

BIBLIOGRAPHY

1. Bentnear, R. *J. Am. Chem. Soc.* **1914**,*36*,2040.
2. Baur, M. *Z. Electrochem.* **1926**,*32*,547.
3. Michaelis, A.A.; Weech, L. *J. Gen. Physiol.* **1928**,*12*,55.
4. Teorell, T. *J. Gen. Physiol.* **1928**,*12*,55.
5. Mueller, P.; Rudin, D. O.; Tien, H. T.; Wescott, W. C. *Nature* **1962**,*194*,979.
6. Tien, H. T.; Diana, A.L. *Chem. Phys. Lipids* **1968**,*2*,55.
7. Feher, G.; Weissman, M. *Proc. Natl. Acad. Sci. U.S.A.***1973**,*70*,870.
8. Chessin, P. L. *IRE Trans. Inform. Theory* **1955**,*1T*,15.
9. Hull, A. W.; Williams, N. H. *Phys. Rev.* **1925**,*25*,147.
10. Johnson, J. B. *Phys. Rev.* **1928**,*32*,97.
11. Nyquist, H. *Phys. Rev.* **1928**,*32*,110.
12. MacDonald, A. "Noise and Fluctuations: An Introduction"; John Wiley and Sons, Inc.: New York, 1962.
13. Johnson, J. B. *Phys. Rev.* **1925**,*26*,71.
14. Schottky, W. *Phys. Rev.* **1926**,*28*,74.
15. Surdin, M. *Le Journal de Physique et La Radium* **1939**,*7*,10.
16. Surdin, M.,ibid., **1951**,*8*,777.
17. Racker, E. *Accounts of Chem. Res.* **1979**,*12*,338.
18. Kingston, R. H.; McWhorter, A. L. *Phys. Rev.* **1956**,*103*,534.
19. Hooge, F. N. *Phys. Lett.* **1969**,*29A*,139.
20. Hooge, F. N.; Van Dujk, H. J. A.; Hoppenbrouers, A. M. H. *Philips Research Reports* **1970**,*25*,81.
21. Hooge, F. N.; Gaal, J. L. M., op cit.,**1971**,*26*,345.
22. Hooge, F. N.; Hoppenbrouers, A. M. H. *Physica* **1969**,*45*,386.
23. Hooge, F. N.; Hoppenbrouers, A. M. H. *Phys. Lett.* **1969**,*29A*,642.
24. Hooge, F. N.; Gaal, J. L. M. *Philips Research Reports* **1971**,*26*,77.
25. DeFelice, L. J.; Firth, D. R. *IEEE - Transactions on Biomedical Engineering* **1971**,*BME - 18*,339.
26. Green, M. E.; Yafuso, M. *J. Phys. Chem.* **1968**,*72*,4072.; correction: *J. Phys. Chem.* **1969**,*73*,1626.
27. Hooge, F. N. *Physica* **1976**,*83B*,14.
28. Teitler, S.; Osborne, M. F. M. *Phys. Rev. Lett.* **1971**,*27*,912.
29. Handel, P. H. *Phys. Rev.* **1971**,*A3*,2066.
30. Tchen, C. M. *Phys. Fluids* **1973**,*16*,13.
31. Tchen, C. M. *Phys. Rev.* **1973**,*A8*,500.

32. Weissman, M. *Biophys. J.* **1978**,*2*,87.
33. Lax, M. *Revs. Mod. Phys.* **1960**,*32*,25.
34. Green, M. E. *J. Phys. Chem.* **1974**,*78*,761.
35. Van Vliet, K. M.; Blok, J.; Ris, C.; Stekete, J. *Physica* **1956**,*22*,723.
36. Weissman, M.; Schindler, H.; Feher, G. *Proc. Natl. Acad. Sci. U.S.A.* **1976**,*73*,2776.
37. Yafuso, M.; Green, M. E. *J. Phys. Chem.* **1971**,*75*,654.
38. Stern, S. H.; Green, M. E. *J. Phys. Chem.* **1973**,*77*,1567.
39. Sokol, B. Ph.D. Dissertation, The City University of New York, 1974.
40. Dorset, D. L.; Fishman, H. M. *J. Membr. Biol.* **1975**,*21*,291.
41. Green, M. E. *J. Membr. Biol.* **1976**,*28*,181.
42. Green, M. E. *J. Membr. Biol.* **1977**,*32*,197.
43. Overton, E. *Vjschr. Naturforsch. Ges. Zurich* **1896**,*41*,383.
44. Gorter, E.; Grendel, F. *J. Exptl. Med.* **1925**,*41*,439.
45. Danielli, J. F.; Davson, H. *J. Cell. Comp. Physiol.* **1935**,*5*,495.
46. Robertson, J. D. *Protoplasma* **1967**,*63*,218.
47. Branton, D. *Proc. Natl. Acad. Sci. U.S.A.* **1966**,*55*,1048.
48. Devaux, P.; McConnell, H. M. *J. Am. Chem. Soc.* **1972**,*94*,4475.
49. Cole, K. S. "Membranes, Ions, and Impulses"; University of California : 1968.
50. Jain, M. "The Bimolecular Lipid Membrane: A System"; Van Nostrand Rheinhold: London, 1972.
51. Young, J. Z. *Q. Jl. Microsc. Sci.* **1936**,*78*,367.
52. Cole, K. S.; Curtis, H. J. *J. Gen. Physiol.* **1939**,*22*,649.
53. Hodgkin, A. L.; Huxley, A. F. *J. Physiol.* **1952**,*116*,449.
54. Hodgkin, A. L.; Huxley, A. F. *J. Physiol.* **1952**,*116*,473.
55. Hodgkin, A. L.; Huxley, A. F. *J. Physiol.* **1952**,*116*,497.
56. Hodgkin, A. L.; Huxley, A. F. *J. Physiol.* **1952**,*117*,500.
57. Hodgkin, A. L.; Keynes, R. D. *J. Physiol.* **1955**,*128*,61.
58. Moore, J. W.; Narahashi, T. *Fed. Proc.* **1967**,*26*,1655.
59. Narahashi, T. *Physiol. Rev.* **1974**,*51*,199.
60. Hille, B. *J. Gen. Physiol.* **1968**,*51*,199.
61. Armstrong, C. M. *J. Gen. Physiol.* **1969**,*54*,553.
62. Stark, G.; Ketterer, B.; Benz, R.; Lauger, P. *Biophys. J.* **1971**,*11*,981.
63. Parsegian, A. *Nature* **1969**,*221*,884.
64. Frankenhaeuser, B.; Moore,L. E. *J. Physiol.* **1963**,*169*,431.
65. Bamberg, E.; Lauger, P. *J. Membr. Biol.* **1973**,*11*,177.
66. Bamberg, E.; Lauger, P. *Biochim. Biophys. Acta.* **1974**,*367*,127.
67. Hille, B. *J. Gen. Physiol.* **1971**,*58*,599.

68. Hille, B. *J. Gen. Physiol.* **1972**,*59*,637.
69. Woodhull, A. M. *J. Gen. Physiol.* **1973**,*61*,687.
70. Schrager, P.; Profera, C. *Biochim. Biophys. Acta.* **1973**,*318*,141.
71. Baker, P. F.; Rubinson, K. A. *Nature* **1975**,*257*,412.
72. Armstrong, C. M.; Benzanilla, F.; Rojas, E. *J. Gen. Physiol.* **1973**,*62*,375.
73. Rojas, E.; Armstrong, C. M. *Nature New Biol.* **1971**,*229*,177.
74. Hille, B. *J. Gen. Physiol.* **1973**,*61*,669.
75. Benzanilla, F.; Armstrong, C. M. *J. Gen. Physiol.* **1972**,*60*,588.
76. Cole, K. S. *Arch. Sci. Physiol.* **1949**,*3*,253.
77. Armstrong, C. M.; Benzanilla, F. *Nature (Lond.)* **1973**,*233*,28.
78. Keynes, R. D.; Rojas, E. *J. Physiol. (Lond.)* **1973**,*233*,28.
79. Singer, S. J.; Nicholson, G. L. *Science* **1972**,*175*,720.
80. Requena,J.; Haydon, D. A.; Hladky, S. B. *Biophys. J.* **1975**,*15*,77.
81. Benz, R.; Frolich, O.; Lauger, P.; Montal, M. *Biochim. Biophys. Acta.* **1975**,*394*,323.
82. Montal, M.; Mueller, P. V. *Proc. Natl. Acad. Sci. U.S.A.* **1972**,*69*,3561.
83. Rothman, J. E.; Lenard, J. *Science* **1977**,*195*,743.
84. Bangham, A.D. In "Progress in Biophysics and Molecular Biology"; Butler, A. J. V.; Noble, D.,Eds.; Pergammon Press: New York, 1968; Vol. 18, p 29.
85. Hendersen, P. J. F.; McGivan, J. D.; Chappell, J. B. *Biochem. J.* **1969**,*111*,521.
86. Hargreaves, W. R.; Deamer, D. W. In "Light Transducing Membranes"; Deamer, D.W., Ed.; Academic Press: New York, N.Y., 1978.
87. Haines, T. H. *Annu. Rev. Microbiol.* **1973**,*27*,403.
88. Chen, L. L.; Pousada, M.; Haines, T. H. *J. Biol. Chem.* **1976**,*251*,1835.
89. Hargreaves, W. R.; Deamer, D. W. *J. Biochem.* **1978**,*17*,3759.
90. Racker, E.; Knowles, A. F.; Eytan, E. *Ann. N. Y. Acad. Sci.* **1975**,*264*,17.
91. Oroveanu, T. *Rev. Roum. Sci. Techn.-Mec. Appl.* **1973**,*18*,449.
92. Schein, S. J.; Colombini, M.; Finkelstein, A. *J. Membr. Biol.* **1976**,*30*,99.
93. Colombini, M. *Nature (Lond.)* **1979**,*279*,643.
94. Villegas, R.; Villegas, G.; Condrescu-Guidi, M. "Abstracts of Papers",Second International Conference on Carriers and Channels in Biological Systems - Transport Proteins of the N.Y. Acad. Sci., New York, Feb. 1980; N.Y. Acad. Sci.: New York, N. Y., 1980.
95. Ehrenstein, G.; Lecar, H. *Quart. Revs. Biophys.* **1977**,*10*,1.
96. Alvarez, O.; Latorre, R.; Vergudo, P. *J. Gen. Physiol.* **1975**,*65*,421.
97. Mueller, P. *Ann. N.Y. Acad. Sci.* **1975**,*264*,247.
98. Eisenberg, M.; Hall, J.E.; Mead, C.A.; *J. Membr. Biol.* **1973**,*14*,143.
99. Bohiem, G. *J. Membr. Biol.* **1974**,*14*,277.
100. Urry, D. W.; Goodall, M. C.; Glickson, J. D.; Mayers, D. F. *Proc. Natl. Acad. Sci. U.S.A.* **1971**,*68*,1907.

101. Hladky, S. B.; Haydon, D. A. *Nature* **1970**,*225*,451.

102. Levitt, D. G.; Elias, S. R.; Hautman, J. M. *Biochim. Biophys. Acta.* **1978**,*512*,436.

103. Boehler,B. A.; DeGier, J.; Van Deenan, L. L. M. *Biochim Biophys. Acta.* **1978**,*512*,480.

104. Eisenmann, G.; Sandbloom, J.; Neher, E. *Biophys. J.* **1978**,*22*,307.

105. Szabo, G.; Urry, D.W. *Science* **1979**,*203*,55.

106. Kennedy, S. J.; Roeske, R. W.; Freeman, A. R.; Watanabe, A. M.; Besch, Jr., H. R. *Science* **1977**,*196*,1341.

107. Gordon, L. G. M.; Haydon, D. A. *Biochim. Biophys. Acta* **1972**,*255*,1014.

108. Hladky, S. B.; Haydon, D. A. *Biochim. Biophys. Acta.* **1972**,*274*,294.

109. Myers, V.B.; Haydon, D. A. *Biochim. Biophys. Acta.* **1972**,*274*,313.

110. McLaughlin, S.; Eisenberg, M. *Ann. Rev. Biophys. and Bioeng.* **1975**,*4*,335.

111. Pinkerton, M.; Steinrauf, L.; Dawkins, P. *Biochem. Biophys. Res. Commun.* **1969**,*35*,512.

112. Ciani, S.; Eisenman, G.; Laprade, R.; Szabo, G. In "Membranes: A Series of Advances"; Eisenman, G., Ed.; Dekker: New York, 1973; Vol. 2, p 61.

113. Ciani, S.; Laprade, R.; Eisenman, G.; Szabo, G. *J. Membr. Biol.* **1973**,*11*,255.

114. Eisenman, G.; Szabo, G.; Ciani, S.; McLaughlin, S.; Krasne, S. In "Progress in Surface and Membrane Science"; Danielli, J.; Rosenberg, M.; Cadenhead, D., Eds.; Academic Press: New York, 1973; Vol. 6, p 139.

115. Lauger, P. *Science* **1972**,*178*,24.

116. Benz, R.; Stark, G.; Janko, K.; Lauder, P. *J. Membr. Biol.* **1973**,*14*,339.

117. Szabo, G.; Eisenman, G.; Laprade, R.; Ciani, S.; Krasne, S. In "Membranes: A Series of Advances"; Eisenman, G., Ed.; Dekker: New York, 1973; Vol. 2, p 179.

118. Stevens, C. F. *Biophysical J.* **1972**,*12*,1028.

119. Veerven, A. A.; Derksen, H. E. *Proc. IEEE* **1968**,*56*,906.

120. Dirksen, H. E. *Acta. Physiol. Pharmacol. ne'erl.* **1965**,*13*,373.

121. Yafuso, M.; Kennedy, J; Freeman A. R. *J. Membr. Biol.* **1974**,*17*,201.

122. Conti, F.; Wanke, E. *Quart. Revs. Biophys.* **1975**,*8*,4.

123. Kolb, H. A.; Lauger, P. *J. Membr. Biol.* **1978**,*41*,167.

124. Strassfeld, M. J. "Noise Studies of Gramicidin Doped Diphythanoyl-lecithin BLM" -- Unpublished.

125. Kolb, H. A.; Lauger, P.; Bamberg, E. *J. Membr. Biol.* **1975**,*20*,133.

126. Bamberg. E.; Benz, R. *Biochem. Biophys. Acta.* **1976**,*426*,570.

127. Kolb, H. A.; Bamberg, E. *Biochem. Biophys. Acta.* **1977**,*464*,127.

128. Neher, E.; Zingsheim, H.P. *Pflugers* **1974**,*351*,61.

129. Sauve, R.; Bamberg, E. *J. Membr. Biol.* **1978**,*43*,317.

130. DeGoede, J.; Verveen, A. A. In "Electrical Phenomena at the Biological Membrane Level"; Elsevier Scientific Pub. Co.: Amsterdam, 1976.

131. Siebenga, E.; Verveen, A. A. In "Biomembranes"; Kreuzer, F.; Slegers, J. F. G., Eds.; Plenum Pub. Co.: New York, 1973; vol. 3, p 261.

132. Fishman, H. M.; Moore, L. E. *Ann. N.Y. Acad. Sci.* **1977**,*303*,399.
133. Siebenga, E.; deGoede, J.; Verveen, A. A. *Pflugers. Arch.* **1974**,*351*,25.
134. Derksen, H. E.; Verveen, A. A. *Science* **1966**,*151*,1388.
135. Conti, F.; DeFelice, L. J.; Wanke, E. *J. Physiol.* **1975**,*248*,45.
136. Fishman, H. M.; Moore, L. E.; Poussart, D. J. M. *J. Membr. Biol.* **1975**,*24*,281.
137. Fishman, H. M. *J. Gen. Physiol.* **1973**,*61*,267.(abstr.)
138. Fishman, H. M. *J. Membr. Biol.* **1975**,*24*,265.
139. Fishman, H. M. *Biophys. J.* **1972**,*12*,119.(abstr.)
140. Fishman, H. M. *Proc. Natl. Acad. Sci. U.S.A.* **1973**,*70*,876.
141. Poussart, D. J. M. *Proc. Natl. Acad. Sci. U.S.A.* **1969**,*64*,95.
142. Poussart, D. J. M. *Biophys. J.* **1971**,*11*,211.
143. Lindenmann, B; Van Driessche, W. *Science* **1977**,*195*,292.
144. Neher, E.; Sakmann, B. *J. Physiol.* **1976**,*258*,705.
145. Fishman, H. M.; Moore, L. E.; Poussart, D. J. M. *J. Membr. Biol.* **1975**,*24*,305.
146. Wanke, E.; DeFelice, L. J.; Conti, F. *Pflugers. Arch.* **1974**,*347*,63.
147. DeFelice, L. J.; Wanke, E.; Conti, F. *Fed. Proc.* **1975**,*34*,1338.
148. Siebenga, E.; Verveen, A. A.. "Proceedings", First Europ. Biophys. Congress; Verlag Wiener Midizinischen Akademia: Vienna, Austria, 1971; Vol. 5, p 219.
149. Siebenga, E; Verveen, A. A. *Pflugers. Arch.* **1973**,*341*,87.
150. Fishman, H. M. *Fed. Proc.* **1975**,*34*,1330.
151. Van Vliet, K. M.; Fasett, J. R. In "Fluctuation Phenomena in Solids"; Burgess, R. E., Ed.; Academic Press: New York,1965; Vol. 19, p 267.
152. Hill, T. L.; Chen, Y. *Biophys. J.* **1972**,*12*,948.
153. Szabo, G. *Ann. N.Y. Acad. Sci.* **1977**,*303*,266.
154. Zingsheim, H. P.; Neher, E. *Biophys. Chem.* **1974**,*2*,197.
155. Mikulinsky, M. A.; Mikulinsky-Fishman, S. N. *Phys. Lett.* **1976**,*58A*,46.
156. Neumcke, B. *Biophys. Struct. Mech.* **1978**,*4*,179.
157. Holden, A. V.; Rubio, J. E. *Biol. Cyber.* **1976**,*24*,227.
158. Pasechnik, V. I.; Gianik, T. *Biophys. (Engl. Transl.)* **1979**,*23*,939; *Biofizika* **1978**,*23*,926.
159. Moore, L. E.; Tufts, M.; Soroka, M. *Biochim Biophys. Acta.* **1975**,*382*,286.
160. Moore, L. E.; Fishman, H. M.; Poussart, D. J. M. *J. Membr. Biol.* **1979**,*47*,99.
161. Fishman, H. M.; Moore, L. E.; Poussart, D. J. M. *Biol. Bull.* **1976**,*151*,408.
162. Mueller, P. V.; Rudin, D. O. *J. Theo. Biol.* **1968**,*18*,222.
163. Cole, K. S.; Moore, J. W. *J. Gen. Physiol.* **1960**,*44*,123.
164. Montal, M.; Mueller, P. V. *Proc. Natl. Acad. Sci. U.S.A.* **1972**,*69*,3561.
165. Heer, C. V. "Statistical Mechanics, Kinetic Theory, and Stochastic Processes"; Academic Press: New York, 1972.

166. Laidler, K. J. "Reaction Kinetics"; Pergammon Press: New York, 1966; Vol. 1.

167. White, S. H.; Petersen, D. C.; Simon, S.; Yafuso, M. ***Biophys. J.*** **1976**,*16*,481.

168. Moore, W. J. "Physical Chemistry", 4th ed.; Prentice Hall, Inc.: Englewood Cliffs, N.J., 1972: Chapter 10.

169. Sokol, B.; Green, M. E. ***Electroanal. Chem. and Interfac. Chem.*** **1973**,*41*,27.

170. Strassfeld, M. J. "Noise Studies of Micellar Solutions in Pores of various Diameters and Lengths" -- Unpublished.

171. Prigogine, I. "Introduction to Thermodynamics of Irreversible Processes", 3rd ed.; John Wiley and Sons, Inc.: New York, 1967.

172. Miller, D. G. *Chem. Rev.* **1960**,*60*,15.

173. Haines, T. H.; Drobenko, J., Personal communication, Dept. of Chem., The City College of New York, 1979.

174. Cummins, H., Personal communication, Dept. of Physics, The City College of New York, 1979.

175. Verveen, A. A.; DeFelice, D. J. In "Progress in Biophysics and Molecular Biology"; Butler, A. J. V.; Noble, D., Eds.; Pergammon Press: Oxford; New York, 1974; Vol. 28, p 189.

176. Lawaczek, R; ***J. Membr. Biol.*** **1979**,*51*,229.

177. DeGier, J.; Mandersloot, J.G.; Van Deenan, L.L.M. ***Biochim. Biophys. Acta.*****1968**,*150*,166.

178. Castellan, G. W. "Physical Chemistry", 2nd ed.; Addison-Wesley, Inc.: Reading, Mass., 1971; p 701.

179. Grafstein, B. In "Handbook of Physiology", 2nd ed.; Kandel, E., Ed.: American Physiological Society: place, 1977: Vol 1.

180. Hooge, F. N. ***Physica*** **1972**,*60*,130.

181. Howard, R.E.; Burton, R.M. *J. Am. Oil Chem. Soc.* **1968**,*45*,202.

182. Danielli, J. F.; Harvey, E.N. ***J.Cell Comp. Physiol.***,**1935**,*5*,483.